

Approaches for improving the rheological characterization of fermented dairy products

DEPARTMENT OF FOOD TECHNOLOGY, ENGINEERING AND NUTRITION | LUND UNIVERSITY
ABDULRAHMAN MUHAMMAD | MASTER OF SCIENCE THESIS IN FOOD ENGINEERING 2020



Approaches for improving the rheological characterization of fermented dairy products

ABDULRAHMAN MUHAMMAD

SUPERVISOR: FREDRIK INNINGS

CO-SUPERVISOR: ANDREAS HÅKANSSON



Copyright © 2020 Abdulrahman Muhammad

Published by

Department of Food Engineering
Faculty of Engineering LTH, Lund University
P.O. Box 118, SE-221 00 Lund, Sweden

Abstract

Fermented dairy products are widely consumable products in today societies, and these products are known for their unique rheological properties due to the complex structural systems they possess. The simplest rheological model for describing yogurt behavior is the Power Law model, but this model parameters are not sufficient for describing the complex behavior during flow and filling. Therefore, it is important to utilize more sophisticated models that can capture other properties of the products such as the yield stress and the time dependency.

Another challenge is to define a standard measuring protocol that can produce reliable and repeatable results, and at the same time can overcome the challenges associated with the thixotropic and viscoelastic behavior of the samples.

This investigation includes a review of the possible regression methods that can be utilized using EXCEL sheets, and recommend the more suitable method for analyzing rheological measurements. This study also compares the behavior of several yogurt products (Vanilla, Naturell and Långfil) using different models with and without including the yield stress. The investigation includes an attempt to measure the zero- shear viscosity and infinite- shear viscosity which are important parameters for further CFD simulations.

The thixotropic behavior of the three products was also described qualitatively and improved the understanding of the break down and build- up of the studied samples, and to what extent thixotropy can affect the rheological measurements. The study also recommends several methods for eliminating the time effect to improve the measurements of the studied products, which can also be applied to other types of samples.

Elongation tests were performed using two different methods, and even though the results are difficult to interrupt, it was possible to qualitatively estimate the elasticity difference between the studied samples.

Acknowledgment

This work would have not been done without the support and guidance of the supervisors of this project; Fredrik Innings and Andreas Håkansson.

I would also want to thank Jenny Jonsson for her support and her continuous and valuable inputs. I would also like to thank the experts at Tetra Pak, Dragana Arlov, Jannika Timander and Sofia Klasen for their valuable tips and feedbacks and providing their knowledge at my disposal during the project.

I would like to thank Roland Kadar, Associate Professor at Chalmers university for his help with the high-pressure capillary rheometer measurements.

And finally, my family, Raneem, Annabella and my unborn child. Without your support and patience, none of this would be possible. My father and mother, I can finally tell you that I am an Engineer, and for that I would like to thank you. I love you all!

Contents

1. Introduction	3
1.1. Background and motivation	3
1.2. Objectives	4
2. Background and theory	4
2.1. Rheology	4
2.1.1. Yield stress	7
2.1.2. Power law model.....	7
2.1.3. Herschel- Bulkley model	8
2.1.4. Cross model.....	8
2.1.5. Zero shear viscosity η_0	9
2.1.6. Infinite shear viscosity η_∞	10
2.2. Rotational rheometer	10
2.3. Capillary rheometer	11
2.4. Thixotropy.....	13
2.4.1. The relation between Thixotropy and viscoelasticity	13
2.4.2. Eliminating the time- effect (Pre- Shear).....	15
2.5. Elongation	15
2.6. Different regression methods for the prediction of data	16
2.6.1. Evaluation the goodness of the regression.....	19
2.6.2. Evaluating the propagated uncertainty produced by the regression.....	20
3. Methodology.....	20
3.1. Samples handling and loading.....	20
3.2. Flow curve measurement	22
3.3. Assessment of Regression methods used in curve fitting	23
3.4. Batches variation	24
3.5. Measurements using different geometries.....	25
3.6. Static yield stress measurement.....	25
3.6.1. The tangent method.....	26
3.6.2. The bayod method	26
3.7. Zero shear viscosity measurement	27
3.8. Infinite shear viscosity measurement.....	27
3.9. Thixotropy measurements	28

3.9.1.	Break down test	28
3.9.2.	Build up test	29
3.9.3.	Varied shear rate step test	30
3.10.	Pre- shearing	31
3.10.1.	Pre- shearing using constant shear rate.....	31
3.10.2.	Multiple hysteresis loops test	32
3.11.	Elongation (Tack test)	32
4.	Results and discussion	33
4.1.	Regression method evaluation.....	33
4.1.1.	Evaluating the tightness of the fit for the regression methods	35
4.1.2.	Evaluating the propagated uncertainty of the regression methods	37
4.2.	Rheological modelling results	40
4.2.1.	Power Law model	40
4.2.2.	Herschel- Bulkley model	42
4.3.	Batch variation.....	46
4.4.	Measuring using different geometries	47
4.5.	Yield stress	50
4.6.	Zero shear viscosity	50
4.7.	Infinite shear viscosity.....	52
4.8.	Cross model.....	56
4.9.	Thixotropy.....	57
4.9.1.	Break down test	58
4.9.2.	Build up test	60
4.9.3.	Varied shear rate steps test.....	62
4.9.4.	Investigating the effect of pre- shearing	64
4.10.	Elongation	70
5.	Conclusion and remarks	71
5.1.	General remarks	71
5.2.	Suggestions for future work.....	73
6.	Appendices	74
6.1.	Kinexus rheometer use instructions.....	74
6.2.	Kinexus rheometer range and limitations	75
6.3.	Applying the OLS regression method using EXCEL sheets.....	75
6.4.	Applying the WLS regression method using EXCEL sheets.....	76
6.5.	The methodology for the Monte- Carlo simulation	77
6.6.	The results of the curve fitting for Naturell and Långfil using different regression methods...	79

6.7. Evaluating the goodness of the fits for Naturell and Långfil.....	82
6.8. The uncertainty analysis for the Power Law viscosity equation when regressed using different curve fitting methods.....	84

1. Introduction

1.1. Background and motivation

One of the most consumed products in the world are fermented dairy products, these products have been developed through time, and the most popular one these days is yogurt with its different forms (stirred, set, drinking, and frozen types). The quality, texture and composition of yogurt products varies depending on where it is produced, and the processes needed for production¹.

Tetra Pak is manufacturing and developing yogurt processing lines and packages and filling machines, but the challenges that comes with this complex line of products need to be understood, because of the problems caused often by the complex behavior they possess, which is caused by their gel structures and anisotropic composition which can be different from product to product based on how it was made and the bacterial culture used².

These issues can appear all over the production line, from an unpredicted pressure drop over the heat exchangers to dripping and splashing (causing a need for more frequent cleaning) during filling under given conditions.

In order to anticipate these issues and understand the reason behind them, a better understanding of the rheology of yogurt products must be developed. To achieve that, it is important to define and measure the relevant properties and it is suspected that the rheological models available now are not enough to give a clear picture of the yogurt properties.

This study is a completion of previous work³, and is a part of a bigger project at Tetra Pak aimed to measure the right fluid properties that can best describe yogurt behavior during flow and filling, and to present the required data and parameters for applying Computational Fluid Dynamics (CFD), which is used to present a model for yogurt behavior during different flow conditions. This is done to correlate the validation data to predict yogurt behavior during flow and filling.

¹ Bylund, G. (2015) ‘Rheology’, in Dairy Processing Handbook. 2nd edn. Lund: Tetra Pak

² Rohm, H. and Jaros, D. (2010) ‘The rheology and textural properties of yoghurt’, in *Texture in Food*. DOI: 10.1201/9780203501276.ch13.

³ H. Williamson and R. Osterus. “Characterising the rheology of fermented dairy products during filling”. MA thesis. Sweden: Lund University, 2019.

1.2. Objectives

- I. Provide a review of different rheological characterization methods for different yogurt products.**
 - This is important for characterizing different dairy products using different methods and compare these methods in order to achieve a better level of accuracy.
- II. Develop a method for measuring zero- and infinite- shear rate viscosities of different yogurt products.**
 - These parameters are important for a valid CFD modelling.
- III. Describe the effect of thixotropy on the rheology of different yogurt products.**
 - This is important to understand the properties of structural decomposition and regeneration as a function of time which will contribute to the quality of the process and the end product.
- IV. Develop a method for eliminating or minimizing the thixotropic properties by using pre-shearing techniques when measuring yogurt rheology**
 - This will be done by investigating different techniques in order to optimize the most time-saving and efficient one.
- V. Measuring the elongation rheology of three dairy products and compare to qualitative and quantitative results.**
 - This will help get a better understanding on how the rheological properties differ between different yogurt products.

2. Background and theory

This section will be concerned of the theoretical aspect of the study. A literature overview regarding rheology measurements, modelling methods, thixotropy and predicting the pressure drop during flow will be presented. The literature overview will be supplemented with the numerical techniques for the data analysis.

2.1. Rheology

The word “Rheology” is derived from the Greek word “Rheo” which means flow, and “Logia” which means “the study of”. Therefore, Rheology is the study of the materials flow behavior under applied deformation forces or stress⁴.

There are four essential elements that must be taken under consideration when a material flows or is deformed, the first of which is the material inner structure and how the material is built and what molecular make up does it have. The second essential element revolves around morphology, and this is related to the resulting shape and size when molecules associate and bond with each other, morphology can range from a needle- like structure to a bulky- cotton like structures. The third element is concerned with the outside forces that stress the material and cause it to deform or flow, materials can be pulled apart, compressed or sheared, and in each case the material will behave differently. The fourth element is the ambient conditions, and it means the environment that the material in, such as temperature⁵.

⁴ W. R. Schowalter (1978) Mechanics of Non-Newtonian Fluids Pergamon. ISBN 0-08-021778-8

⁵ R.Moreno (2001) Encyclopedia of Materials: Science and Technology (Second Edition). ISBN: 978-0-08-043152-9

Fluids can be grouped into two basic flow profiles:

1- Newtonian fluids:

These fluids do not change their viscosity with shear rate. when plotting viscosity against shear rate, the flow profile of these fluids exhibits no change in viscosity with increasing shear rate and no change also when the shear rate is reduced or removed (e.g. water) (Figure 2.1)

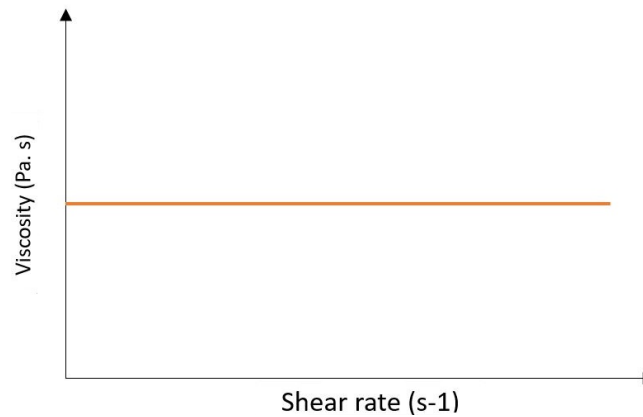


Figure 2.1: Example of flow profile of a Newtonian fluid

2- Non- Newtonian fluids

In contrast to Newtonian fluids, non- Newtonian fluids change their viscosity with shear rate⁶, and they can be categorized into different groups, among those groups -but not limited to- are the following:

a) Pseudoplastic (Shear thinning)

These fluids are shear thinning, and their viscosity decreases by increasing shear rate, and recovers along the same path when the shear rate decreases. This type of fluids is the most common among non-Newtonian fluids, and the reason for their behavior is that Pseudoplastic systems contain polymers, which are coiled up at rest due to stabilizing molecular forces. When applying shear, the polymer chains begin to untangle, and with the increase of shear, the polymer chains will be aligned in the direction of the flow and the internal resistance will decrease, and therefore the viscosity will decrease with the increased shear⁷.

b) Dilatant (Shear thickening)

These fluids are shear thickening, where the viscosity increases with increased shear rate and also recovers with the same path when the shear rate is decreased. The flow profile is called dilatant, because the system increases its volume with increasing shear rate. The system is often made up of a high percentage of deep flocculated particles, and a small percentage of the continuous phase to allow the particles to move over one another at rest or with very little shear. With applying a high shear, the

⁶ Chhabra R.P. (2010) Non-Newtonian Fluids: An Introduction. In: Krishnan J., Deshpande A., Kumar P. (eds) Rheology of Complex Fluids. Springer, New York, NY. ISBN: 978-1-4419-6493-9

⁷ G. L. Wilkes. An overview of the basic rheological behavior of polymer fluids with an emphasis on polymer melts. Journal of Chemical Education 1981 58 (11), 880. DOI: 10.1021/ed058p880

flocculation effect decreases and the void between the particles increases along with air and space, and this allow the system to start taking a stronger and firmer structure.

c) Thixotropic

These fluids are time dependant. Therefore, the viscosity of these fluids is dependent on shear rate and more importantly, the time that it takes for the viscosity to recover. This time effect appears for shear thinning fluids with thixotropic behavior as follows; increasing shear rate results in decreasing viscosity, however, reducing the shear rate will result in a slower path or a longer time to reform the structure and achieve full viscosity recovery (figure 2.2). The difference between the upward and downward curves in thixotropic systems is known as the degree of hysteresis. Since systems with high molecular weight particles take longer time to recover, their degree of hysteresis will be larger than systems with low molecular weight particles⁸.

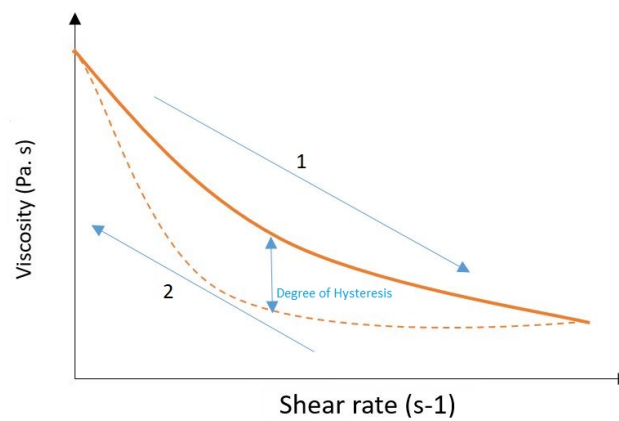


Figure 2.2: Example of a thixotropic fluid with the viscosity decreases with increased shear rate (1), and increasing with decreasing the shear rate

Yogurt is generally considered a thixotropic fluid⁹, which will be discussed in further details in section (§ 2.4).

Some complex fluids show another type of behavior called; elasto- viscoplasticity (EVP). This behavior manifest with a yield-like transition when the stress applied on a material exceeds a critical value. The material behaves as an elastic solid below the yield stress value, whereas above the yield stress the material flows as a liquid¹⁰. This behavior coupled with the thixotropic behavior of some fluids leas to a thixotropic elasto- viscoplasticity behavior (TEVP). The use of this behavior in the characterization of yogurt products, will not be the main focus of this study.

⁸ Dealy, John M, Wissbrun, K.F. Melt Rheology and Its Role in Plastics Processing. Springer. ISBN: 978-0792358862

⁹ T.BenezechJ, F.Maingonnat. Characterization of the rheological properties of yoghurt—A review. Journal of Food Engineering, Volume 21, Issue 4, 1994, Pages 447-472. DOI: 10.1016/0260-8774(94)90066-3

¹⁰ Ch. J. Dimitriou, G. H. McKinley. A canonical framework for modeling elasto- viscoplasticity in complex fluids. Journal of Non-Newtonian Fluid Mechanics Volume 265, March 2019, Pages 116-132. DOI: 10.1016/j.jnnfm.2018.10.004

2.1.1. Yield stress

The yield stress property —that several complex fluids express — is the stress value, at which the material does not flow unless the applied stress increases over the yield stress value.

It should be in mind that the yield stress value resulting from the curve fitting of the Herschel-Bulkley model is the dynamic yield stress, which can be different from the static yield stress. The definition of the dynamic yield stress is the minimum stress required to maintain the flow, and it can be strongly influenced by the data-range of shear rates used and the model used for fitting the data. On the other hand, the static yield stress is the stress required to initiate the flow. The importance of the static yield stress comes from its use in investigating the stress needed to initiate the flow (e.g. pumping), while the dynamic yield stress is more relevant for the application of maintaining or stopping the flow¹¹.

Mathematical models are great tools for describing the rheological behavior of non-Newtonian fluids. Among these models but not limited to are the Power Law model and the Herschel-Bulkley model. Choosing the right model that can accurately predict the real values in a shear stress- shear rate analysis or (viscosity- shear rate) is essential for achieving a proper characterization of the fluid flow and getting accurate results for hydraulic calculations (i.e. pressure drops predictions).

2.1.2. Power law model

The Power Law model is the most common model used to describe non-Newtonian fluids, especially food products¹². In addition to that, the Power Law model can describe both shear thinning and shear thickening fluids. The equation representing this model has two constants, K (Pa· sⁿ) and n (-), these two constants describe the consistency and the flow respectively:

$$\tau = K\dot{\gamma}^n \quad (2.1)$$

where τ is the shear stress (Pa) and $\dot{\gamma}$ is the shear rate (s⁻¹). The flow behavior index (n) indicates to the type of the fluid, where $n < 1$ in the case of Pseudoplastic fluids, $n > 1$ for Dilatant fluids and $n=1$ for Newtonian fluids (figure 2.3).

Since $\mu = \frac{\tau}{\dot{\gamma}}$ where μ is the viscosity (Pa. s), it is possible to write the Power Law- viscosity equation as follow:

$$\mu = K\dot{\gamma}^{(n-1)} ; \dot{\gamma} \neq 0 \quad (2.2)$$

The use of the Power Law- viscosity equation is possible with the condition of $\dot{\gamma} \neq 0$.

¹¹ F.J. Galindo-Rosales, F. J. Rubio-Hernandez. Static and Dynamic Yield Stresses of Aerosil® 200 Suspensions in Polypropylene Glycol. Applied Rheology 20(2). January 2010. DOI: 10.3933/ApplRheol-20-22787

¹² Mokhtari, M. (2011) 'Thixotropic and Rheopectic Modeling of Xanthan-Borate Gel System', in American Association of Drilling Engineers National Technical Conference and Exhibition. Houston, TX.

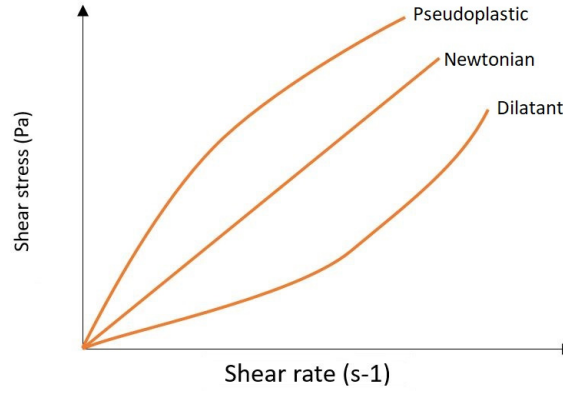


Figure 2.3: Power law fluid behavior dependence on the flow index.

2.1.3. Herschel- Bulkley model

Viscoplastic fluids exhibit a property called the yield stress, these fluids do not deform neither flow below a certain critical shear stress (yield stress) and behaves as a solid, but when that yield stress (τ_0) value is exceeded, the material flows as a fluid. Many models have been developed to integrate the concept of the yield stress into the shear stress and the viscosity functions. One of these models is the Herschel- Bulkley model which has the ability to produce a very high viscosity value at low shear rates to resemble the approximate plastic state of the fluids at low shear rates. The equation of the Herschel- Bulkley model is commonly written as:

$$\tau = \tau_0 + A\dot{\gamma}^b \quad (2.3)$$

Where τ_0 (Pa) is the yield stress and the constants A (Pa. s^b) describes the consistency of the fluid and b (-) describe the fluid flow. The flow behavior index (b) indicates to the type of the fluid, where $b < 1$ in the case of Pseudoplastic fluids, $b > 1$ for Dilatant fluids and $b=1$ for Bingham fluids.

The Herschel- Bulkley model- viscosity equation can be written as follow:

$$\mu = \frac{\tau_0}{\dot{\gamma}} + A\dot{\gamma}^{(b-1)}; \dot{\gamma} \neq 0 \quad (2.4)$$

τ_0 determines the flowing and non-flowing region of the fluid (equation 2.5)

$$\mu = \begin{cases} \frac{\tau_0}{\dot{\gamma}} + A\dot{\gamma}^{(b-1)} & ; \text{if: } \tau > \tau_0 \\ \mu_\infty & ; \text{if: } \tau < \tau_0 \end{cases} \quad (2.5)$$

2.1.4. Cross model

The cross model (equation 2.6), which is a variation of the Power Law model. was developed to account for these limitations by utilizing the viscosity values at very high and very low shear rates (figure 2.4)

$$\eta = \eta_\infty + \frac{(\eta_0 - \eta_\infty)}{1 + (C\dot{\gamma})^{-m}} \quad (2.6)$$

where η_0 is the maximum viscosity as the shear rate approaches zero (zero-shear viscosity) in Pa·s, η_∞ is the limiting viscosity as the shear rate approaches infinity (viscosity at infinite shear rate) in Pa·s,

and m is the Rate Constant, which is dimensionless and represents the degree of the viscosity dependency on the shear rate in the shear-thinning region. When $m=0$, the model indicates to a Newtonian behavior for the studied fluid, and with m value closer to 1 the model indicates to increasingly shear thinning behavior. C is the Cross Time Constant and has dimensions of time.

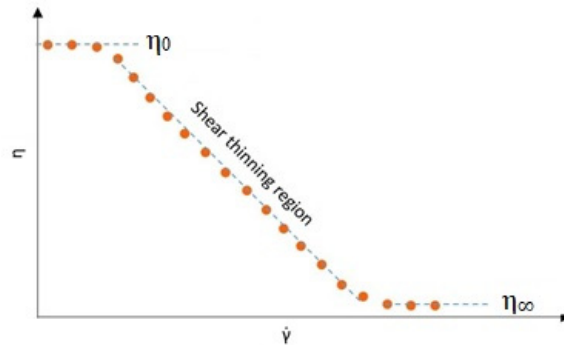


Figure 2.4: Determining Cross model constants (C & m) utilizing η_0 and η_∞

The limiting viscosity plateaus at very high and very low shear rates are required as inputs when performing CFD simulations.

2.1.5. Zero shear viscosity η_0

The zero- shear viscosity (η_0) is the apparent viscosity plateau of the measured sample in the viscoelastic region (LVER) which appears at very low shear values below the yield stress value (figure 2.5). Viscoelasticity is a property that some materials exhibit with both viscous and elastic behaviors when these materials are subjected to deformation.

The viscosity plateau at η_0 can be observed for polymers and suspensions while some fluids don't have this viscosity plateau. The polymer chains move so slowly that entanglement of these chains would not be affected by shear flow, until a certain shear value that cause the polymer chains to be free and align in the direction of the flow.

Extrapolation is used to determine (η_0), and the value determined by extrapolation depends heavily on the model used, and the range and quality of the data used for the extrapolation. Therefore, the margin of error can be very large¹³. Several methods were suggested for measuring (η_0) such as a performing a shear stress ramp at values well below the yield stress value.

¹³ Montgomery T. Shaw. On estimating the zero-shear-rate viscosity: Tests with PIB and PDMS. 31 October 2016. AIP Conference Proceedings 1779, 070011 (2016); DOI: 10.1063/1.4965543

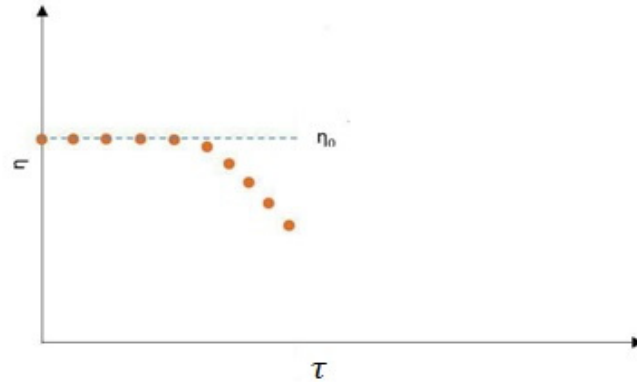


Figure 2.5: Determining η_0 using the apparent viscosity plateau analysis on controlled shear rate test data

2.1.6. Infinite shear viscosity η_∞

The infinite- shear viscosity (η_∞) represents the limiting value of the viscosity (a viscosity plateau) at very high shear rates or frequencies¹⁴.

Since stirred yogurt contains ~80% water, which is a Newtonian fluid that has a viscosity unrelated to shear rates and has a viscosity of 8.9×10^{-4} Pa. s, it makes sense to assume that the viscosity of yogurt at a shear rate value approaching infinite value would not drop below the viscosity of water (figure 2.6).

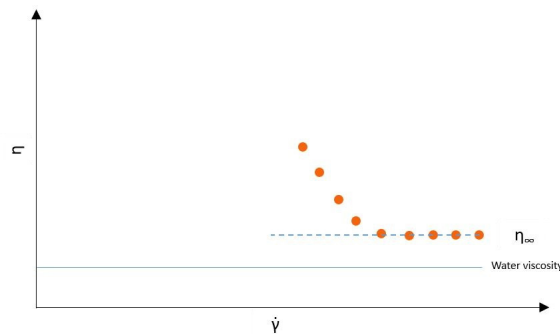


Figure 2.6: η_∞ determination using plateau analysis on constant shear rate measurement conducted at the highest applicable shear rate, compared to water viscosity

2.2. Rotational rheometer

A rotational rheometer is an instrument used to determine the flow of fluids (figure 2.7). The working principle of a rotational rheometer includes one of two operating modes, the first one including setting up the rotational speed (shear rate) simulating processes that are dependent on flow velocity. The second operating mode includes setting the driving force using torque (shear stress) in order to simulate the conditions of applications that are dependent on force. The rheometer converts the measured

¹⁴ Cross, M. M. (1965) 'Rheology of Non-Newtonian Fluids: A New Flow Equation for Pseudoplastic Systems', Journal of Colloid Science, 20, pp. 417–437. DOI: 10.1016/0095-8522(65)90022-X

torque into the shear stress and the rotational speed into the shear rate, and vice versa, this is done by pre- installed conversion factors into the system¹⁵.

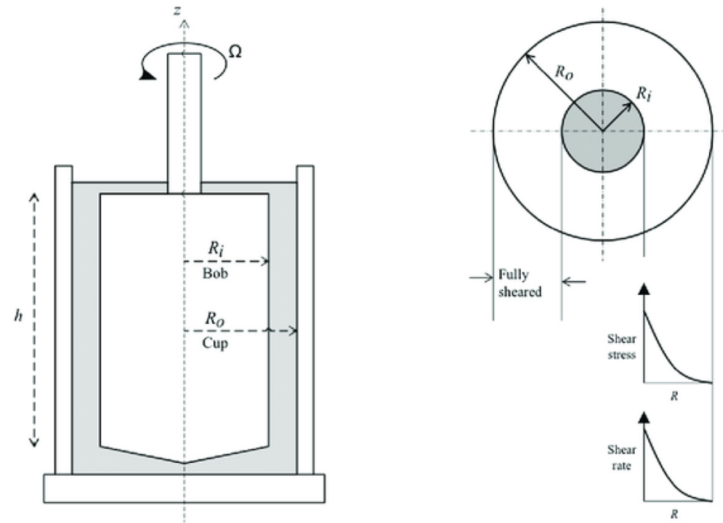


Figure 2.7: Schematic of the cup-and-bob geometry in a rotational rheometer

2.3. Capillary rheometer

It is difficult to measure η_{∞} using a rotational rheometer, due to the development of turbulent flow in the geometry used. The preferred rheometer for measurements at high shear rates is the high- pressure capillary rheometer that can operate using shear rate values that are not applicable using rotational rheometers (figure 2.8). Compressed gas and a piston are used to generate a certain amount of pressure on the fluid in the reservoir to flow in a tube connected to the reservoir with a known radius R and length L , the pressure drop and the flow rate through this tube are used to determine viscosity¹⁶.

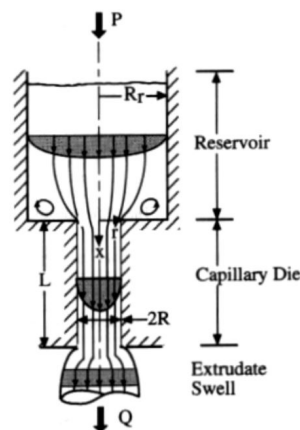


Figure 2.8: High pressure capillary viscometer

¹⁵ Anton Paar GmbH (2019) Basics of rheology. Available at: <https://wiki.anton-paar.com/en/basics-of-rheology/> [Accessed: 21 January 2020].

¹⁶ James F. Steffe. Rheological methods in food process engineering. Second edition. published by Freeman Press. ISBN: 0-9632936 1 4

For the capillary rheometer measurements, the pressure drop (ΔP) and the flow (Q) are recorded.

The shear stress inside the tube is written as follow:

$$\tau = \frac{r}{2} \left(\frac{\Delta P}{L} \right), \text{ At the wall (r=R) and that gives } \tau = \frac{R}{2} \left(\frac{\Delta P}{L} \right) \quad (2.7)$$

The velocity profile inside the tube:

$$u(r) = \frac{\Delta P R^2}{2\mu L} \left[1 - \left(\frac{r}{R} \right)^2 \right] \quad (2.8)$$

The Hagan- Poiseuille law for pressure driven flow of Newtonian fluids inside the tube is given:

$$\Delta P = \mu L \cdot \frac{8Q}{\pi} R^{-4} \quad (2.9)$$

And the shear rate is:

$$\dot{\gamma} = \frac{du}{dr} = \frac{\Delta P}{2\mu L} R = \frac{4Q}{\pi R^3} = \dot{\gamma}_{apparent} \quad (2.10)$$

The $\dot{\gamma}$ in (equation 2.10) refers to Newtonian fluids, and the $\dot{\gamma}_{apparent}$ refers to non- Newtonian fluids.

For non-Newtonian fluids, the use of the apparent shear rate provides the ability to calculate the Apparent viscosity as follow:

$$\eta_{app} = \frac{\tau_w}{\dot{\gamma}_{app}} \quad (2.11)$$

For non- Newtonian fluids, the Rabinowitch analysis is done as the following:

$$Q = 2\pi \int_0^R r u(r) dr \xrightarrow{\text{integrating by parts}} Q = 2\pi r^2 u \Big|_0^R - \int_0^R \pi r^2 \left(\frac{du}{dr} \right) dr \quad (2.12)$$

By applying the “no- slip” boundary condition, and eliminating r with the aid of (equation 2.7):

$$\frac{\tau_w^3 Q}{\pi R^3} = \int_0^{\tau_w} \tau^2 \left(\frac{du}{d\tau} \right) d\tau \quad (2.13)$$

After several manipulations, the Rabinowitch equation is obtained:

$$\dot{\gamma} = \frac{4Q}{\pi R^3} \left(\frac{3}{4} + \frac{1}{4} \frac{d \ln Q}{d \ln \tau_w} \right) = \dot{\gamma}_w \left(\frac{3}{4} + \frac{1}{4} \frac{d \ln Q}{d \ln \tau_w} \right) \quad (2.14)$$

And the actual viscosity of the fluid is:

$$\eta = \frac{\tau_w}{\dot{\gamma}_w} \quad (2.15)$$

To obtain the true shear rate, an evaluation of the derivative $\frac{d \ln Q}{d \ln \tau_w}$.

When plotting Q vs. τ_w for the Power Law fluids, the slope turns out as the following:

$$\frac{d \ln Q}{d \ln \tau_w} = \frac{1}{n} \quad (2.16)$$

The Rabinowitch equation becomes:

$$\dot{\gamma} = \left(\frac{3n+1}{4n} \right) \cdot \left(\frac{4Q}{\pi R^3} \right) \quad (2.17)$$

This equation represents the shear rate when a Power Law fluid flows under the effect of pressure forces in a high-pressure capillary rheometer.

2.4. Thixotropy

According to the IUPAC¹⁷, thixotropy is the continuous decrease of viscosity with time when flow is applied to a sample that has been previously at rest and the subsequent recovery of viscosity in time when the flow is discontinued.

The essential elements of the thixotropy definition are:

- 1- viscosity is the property that is usually used to express the thixotropy phenomena
- 2- Thixotropic behavior implies a time-dependent decrease in viscosity that is induced by flow
- 3- the effect of thixotropy is reversible when the flow is decreased or arrested.

In many industrial applications of thixotropic fluids, it is needed to have these fluids at a relatively low viscosity when high shear rates are applied, in order for the process to be applied properly to the product.

Thixotropic systems exhibit several rheological properties that can be measured, which provides a way to characterize individual fluids on the basis of some developed suitable models.

The difficulties that are coupled with measuring thixotropy can range from presence of particles and aggregates in the fluid's structure, to the extreme shear thinning and the time effects of the material studied. The transient behavior of the samples when changing shear rates can be used for measuring their thixotropy, and to decide whether it is important for measuring the rheology of a fluid or not

Several techniques can be utilised in measuring thixotropy such as¹⁸:

- 1- Investigating the hysteresis
- 2- Investigating the effect of a stepwise changes in shear rate or shear stress
- 3- Start-up and creep experiments

2.4.1. The relation between Thixotropy and viscoelasticity

Viscoelasticity is a property that some materials exhibit with both viscous and elastic behaviors when these materials are subjected to deformation. Time and shear history effects of a fluid can be expressed by both thixotropy and viscoelasticity. Thixotropic materials can display elastic effects. An elastic

¹⁷ IUPAC. Compendium of chemical terminology, electronic version <http://goldbook.iupac.org.W06691.html>. [Accessed January 2020]

¹⁸ J. Mewis, N. J. Wagner. Thixotropy. *Advances in Colloid and Interface Science* Volumes 147–148, 2009, pp:214-227. DOI: 10.1016/j.cis.2008.09.005

stress component can be detected during the flow of thixotropic materials. Some complex structure of some fluids induces a viscoelastic response even if the sample's viscosity changes indicates to a thixotropic behavior¹⁸.

These two properties must be taken into consideration, because thixotropic materials can be viscoelastic or not. To determine that, a simple method is used stepping-down in shear rate from a high to a low value and the shear stress is monitored in the sudden shear rate change region (figure 2.9.a). Viscoelastic fluids would react to the sudden drop in shear rate with a decrease of the shear stress to a new plateau value (figure 2.9.b). Under the same conditions the shear stress in an inelastic thixotropic material would drop immediately to a lower value, and then starts to increase gradually to its new steady state (figure 2.9.c).

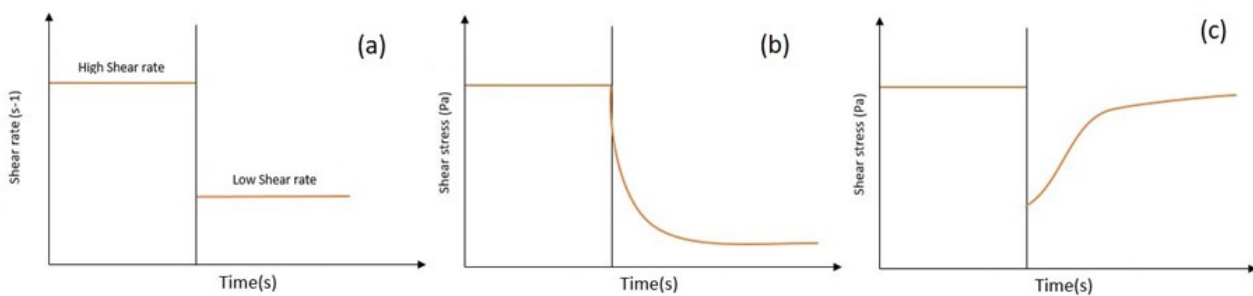


Figure 2.9: Shear stress response to a shear rate step down (a), b) viscoelastic, c) inelastic thixotropic ¹⁸.

Several authors have described this phenomenon in the literature, one of which¹⁹ described complex fluid systems—in a basic flow situation—as a small group of primary particles which form individual flocs. These flocs are considered the smallest unit of the system at the highest shear rate value during rheological measurements. Therefore, the system is considered a suspension of individual flocs at high shear rates. When the shear rate is decreased, these individual flocs form clusters through certain types of bonds, leading to the formation of structural units consisting of clustered individual flocs at a given shear rate.

If the system is at rest and not being imposed to any shear, these clusters will span a solid-like network structure with the individual flocs acting as fragile bonds at the interfaces of the structural units. The size of the structural units depends on the applied shear, and the higher the shear is, the smaller the size becomes. This size decrease is caused by the stretching of the links that keep the clusters network together and further broken down, leading to each network to result in smaller clusters as long as the shear rate value is still imposed. This explains the viscoelastic behavior described in (figure 2.10.b). On the other hand, Inelastic fluids have the ability to reverse the linkage break down when changing

¹⁹ D. Quemada. Rheological modelling of complex fluids: IV: Thixotropic and "thixoeelastic" behavior. Start-up and stress relaxation, creep tests and hysteresis cycles. The European physical journal applied physics AP 5, 191:207 (1999). DOI: 10.1051/epjap:1999128

the shear rate value, which leads to their structure regaining its properties at different shear rates²⁰ (figure 2.10.c)

2.4.2. Eliminating the time- effect (Pre- Shear)

Pre- shearing is used to improve the measurements of structural fluids, and in addition to understanding the thixotropic effect of the sample, pre- shearing can improve the ability to measure the right viscosity of the sample that is relevant to the application wanted. Pre- shearing the sample at a given shear rate for a certain period of time, until the steady state is reached, it is possible to achieve reproducible initial conditions with reproducible results.

The rheological properties of a structural fluid come from its internal network, which can be broken down at high shear rates and can be re- built over time at rest. Even though that these fluids are commonly measured, it can be challenging to perform consistent testing procedures. It is virtually impossible to avoid introducing shear and altering the microstructure of the measured material when loading a sample, and even small differences can result in huge measurements variations. Adding a pre-shear step before testing breaks down the structure in a way that is consistent from sample to sample which effectively erases the sample loading effects and therefore can produce repeatable results for fluids with time dependent behavior²¹. Another goal that needs to be investigated, is the ability of pre- shearing to eliminate the time effect of yogurt by studying the flow curve of the pre-sheared sample under different pre- shearing conditions. This requires determining the right pre- shearing technique with enough shearing speed and time and investigate if it is possible to eliminate this time effect completely. It also include comparing the rheological parameters for the different products and the different rheological models where the acquired data can be helpful in understanding how the time effect of yogurt can change during different parts of the production line which will allow for better CFD simulations²².

2.5. Elongation

When holding a drop of yogurt between the thumb and the forefinger it is felt that that yogurt is a little sticky, or tacky. This phenomenon can be measured using a Tack test, where Tack is the material ability to stick on a solid surface when applying very little pressure to it. The bonds that cause this adhesion cannot be measured directly, and what the Tack test does is measuring the force needed for breaking these bonds. Tack tests performed in the scientific literature on fluids, have found that the viscosity of these fluids play an important role in the tackiness of these fluids with liquids that have a moderately high viscosity showed higher tack, and when the viscosity decreases or increases the tack

²⁰ D. CHENG, F. EVANS. Phenomenological characterization of the rheological behavior of inelastic reversible thixotropic and antithixotropic fluids. Chemistry. 1965. DOI:10.1088/0508-3443/16/11/301

²¹ Santos, P.H., Carignano, M.A., & Campanella, O.H. (2017). Effect of Shear History on Rheology of Time-Dependent Colloidal Silica Gels. Gels. DOI:10.3390/gels3040045

²² D. Arlov. Rheology of Mayonnaise. Tetra Pak technical report. NOV-2016

decreases²³. The expected form of the break-up profile differs depending on the type of the fluid (figure 2.10)²⁴.

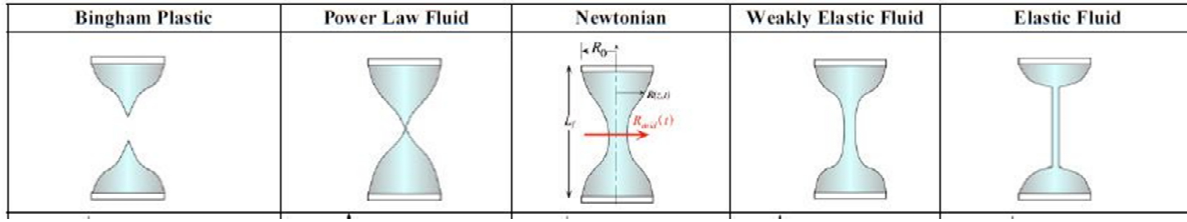


Figure 2.10: A summary of the most commonly- observed modes of capillary thinning and break-up ²⁴

In this study, it is good to understand the tack of different yogurt products, which will be a continuing work for the viscoelasticity investigation done in previous work²⁵, and the current investigation will focus on qualitatively comparing the different yogurt products.

2.6. Different regression methods for the prediction of data

Curve fitting is a process aimed to construct a curve that represent a mathematical function with one or more parameters in order to achieve the best fit possible to describe a series of data points²⁶.

Several sophisticated software are capable of performing several kinds of regression utilizing different regression methods with great accuracy. These software are not always available and requires some level of programming abilities. EXCEL sheets on the other hand are wildly accessible, and requires no programming skills, in addition to their high computational capacities in term of finding non- linear regression parameters. For these reasons, spreadsheets such as Microsoft Excel are widely suggested to make nonlinear parameter estimation²⁷.

The common method used for estimating the rheological parameters using Excel sheets is to plot the shear stress against the shear rate on a logarithmic axis scale, and using the trendline function for Power Law curves, the parameters generated are then exported to be used as Power Law parameters. The tightness of the fit is evaluated by the R^2 value where a closer value to 1 indicates to a tighter fit between the predicted values curve and the measured (real) values.

The mathematical process behind the TRENDLINE function can be described as follow; the software performs a log- transforming on the measured data and the predicted value and their residuals, and

²³ Charles L. Rohn, Rheological Analysis of Tack. TA Instruments USA. Report: AAN018e.

http://www.tainstruments.com/pdf/literature/AAN018_V1_Analysis%20of%20tack.pdf [Accessed DEC- 2019]

²⁴ Gareth H. McKinley. Visco-Elasto-Capillary Thinning and Break-Up of Complex Fluids. April 2005.

<http://web.mit.edu/fluids> [Accessed DEC- 2019]

²⁵ H. Williamson and R. Osterus. (2019) “Characterising the rheology of fermented dairy products during filling”. MA thesis. Sweden: Lund University.

²⁶ S.S. Halli, K.V. Rao. 1992. Advanced Techniques of Population Analysis. ISBN 0306439972 Page 165 (cf. ... functions are fulfilled if we have a good to moderate fit for the observed data.

²⁷ Berger RL (2007) Nonstandard operator precedence in Excel. Computational Statistics and Data Analysis, 51:2788–2791. DOI: 10.1007/s00180-014-0482-5

then minimizing the sum of square of these log-transformed residuals and evaluate the tightness of the fit based on the R-squared value (equation 2.18).

$$S = \min \sum [\log(y_i) - \log(y_j)]^2 \quad (2.18)$$

Concerns have been raised regarding this method for two main reasons, the first reason is that the R^2 value is not viable in describing the tightness of the fit in the case of non-linear regression²⁸. The other concern that arises with using trendline for non-linear regression appears when applying the Herschel-Bulkley model where the yield stress value must be measured separately and then inserted into the equation. To overcome this issue in previous study²⁹, the yield stress was measured using other methods (Tangent, Bayod...etc) and then inserted into the Herschel- Bulkley model. This approach simply includes inserting the static yield stress value into the model which is not relevant to the Herschel- Bulkley model that depends on the dynamic yield stress as a parameter.

The method adapted by the statistic literature for performing a nonlinear regression using an Excel sheet, is by utilizing the SOLVER function and minimizing the sum of squared residuals values in the solver set up until the curve of best fit is achieved.

Minimizing the sum of least square residuals (Ordinary Least square OLS) is the most commonly used method when determining parameters in regression, where the residual value is the difference between the measured value and the predicted value (equation 2.9).

With the measured data being (x_i, y_i) ; $i = 1, 2, 3, \dots, n$ and the predicted points are (x_i, y_j) ; $j = 1, 2, 3, \dots, j$, this gives the predicted model: $y_j = f(x_i) + \varepsilon_i$, with ε_i represents the error term (residual) for the data point

$$S = \min \sum [y_i - y_j]^2 \quad (2.19)$$

The OLS method is built on 7 main assumptions³⁰:

- 1- The regression model is linear in the coefficients and the error term
- 2- The error term has a population mean of zero
- 3- All independent variables are uncorrelated with the error term
- 4- Observations of the error term are uncorrelated with each other
- 5- The error term has a constant variance (no heteroscedasticity)
- 6- No independent variable is a perfect linear function of other explanatory variables
- 7- The error term is normally distributed (optional)

The assumptions for the OLS regression methods are sometimes violated. Several regression methods have been described in the literature, and it is interesting for the objectives of this study to review some

²⁸ Spiess, A. N., & Neumeyer, N. (2010). An evaluation of R^2 as an inadequate measure for nonlinear models in pharmacological and biochemical research: a Monte Carlo approach. *BMC pharmacology*, 10, 6. DOI:10.1186/1471-2210-10-6

²⁹ H. Williamson and R. Ostrich. (2019) "Characterising the rheology of fermented dairy products during filling". MA thesis. Sweden: Lund University.

³⁰ Barker, L. E., & Shaw, K. M. (2015). Best (but oft-forgotten) practices: checking assumptions concerning regression residuals. *The American journal of clinical nutrition*, 102(3), 533–539. DOI:10.3945/ajcn.115.113498

of these methods and discuss their relevance to the curve fitting of rheological models, the following methods will be investigated (table 2.1):

The regression method	The minimizing factor
Ordinary Least Squares (OLS)	$S = \min \sum [y_i - y_j]^2$
Least Absolut Residuals (LAR)	$S = \min \sum y_i - y_j $
Least Absolut Relative Residuals (LARR)	$S = \min \sum \frac{ y_i - y_j }{y_i}$
Least Squared Logarithmic Residuals (LSLR)	$S = \min \sum [\log(y_i) - \log(y_j)]^2$
Weighted Least Squares (WLS)	$S = \min \sum [(y_i - y_j) \cdot W_i]^2$

Table 2.1: A summary of the regression methods investigated for the rheological modelling

1- Least Absolut Residuals (LAR)

This method is similar to the OLS technique, where it attempts to find a function which closely approximates a set of data by minimizing the sum of the absolute residuals value (equation 2.20).

$$S = \min \sum |y_i - y_j| \quad (2.20)$$

It is more robust than the OLS method and this appears in the LAR method being more resistant to outliers, which makes it more applicable in studies where these outliers can be safely ignored. If it is important to pay attention to all outliers, then using the OLS method can be considered a better choice³¹.

2- Least Absolut Relative Residuals (LARR)

Another method suggested to control the effect of outliers is to put a weight on the residuals values before minimizing them which will lead to a better fit that can give a better prediction of the model analysed.

The simplest way to apply a weight on each residual is by dividing its absolute value over the real measured value, and by that it means to minimize the sum of the absolute relative residuals LARR (equation 2.11), instead of minimizing the sum of squared residuals mentioned in the OLS method earlier.

$$S = \min \sum \frac{|y_i - y_j|}{y_i} \quad (2.21)$$

3- Weighted Least Squares (WLS)

³¹ K. CHEN, Z YING. Analysis of least absolute deviation. <https://www.math.ust.hk/~makchen/papers/LAD.pdf> [Accessed DEC- 2019]

One of the assumptions for using the OLS method is that the error variance is constant for all the residuals. This assumption can be violated resulting in skewed residuals values were higher values will be clustered on either side of the residuals plot. This will affect the regression process as these data points with high residuals will act as outliers.

To overcome this, it is possible to turn to robust regression, and attach a weight to the residuals depending on their variance in a method called Weighted Least Squares (WLS). Using this method, the higher the variance of a point, the less weight it will have and therefore the less influence it the data point will have over the regression curve which will reduce the effect of outliers³²(equation 2.12).

With the measured data being (x_i, y_i) ; $i = 1, 2, 3, \dots, n$ and the predicted points are (x_i, y_j) ; $j = 1, 2, 3, \dots, j$, this gives the predicted model: $y_j = f(x_i) + \epsilon_i$, with ϵ_i represents the error term (residual) for the data point and $W_i = 1/(\sigma_i^2)$, where σ_i is the variance of each point.

$$S = \min \sum [(y_i - y_j) \cdot W_i]^2 \quad (2.22)$$

2.6.1. Evaluation the goodness of the regression

In order to evaluate the tightness of the fit, several steps are described in the literature. The first step in evaluating how tight is the fit produced by the rheological model and the regression method used is by simply looking at the curves in both Linear- and Log- axis scales, this can be a good way to give a preliminary idea of how good the fit is. The second step in evaluating the fit is to evaluate the sum of squared residuals (SSR) where the lower the value of SSR the better the fit is, and the closer the predicted model to represents the actual data set. The third step in evaluating the regression is usually done by performing a residual plot which consists of plotting the residuals values on the Y axis against the predicted values on the X axis, the first thing to evaluate in the residual plot is to check for the residuals with positive values which means the prediction was too low, while negative values mean the prediction was too high, and 0 means the prediction was exactly correct (figure 2.11). Ideally the residual plot for a good, healthy fit, has the following properties:

- 1- The points should be clustered around low residuals values.
- 2- The residuals should be symmetrically distributed with no clear pattern and tend to cluster toward the 0 value of the residuals.

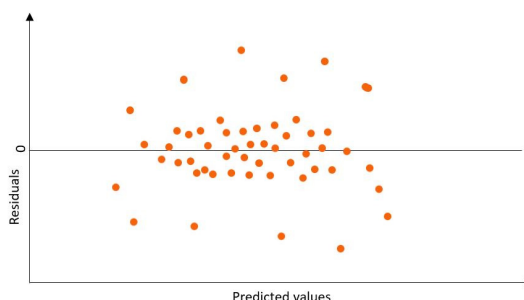


Figure 2.11: An example of a residual plot for a healthy regression with the residuals having a low value and clustered symmetrically around the 0 value of the residuals with no clear shapes

³² Zorn ME, Gibbons RD, Sonzogni WC. Weighted least-squares approach to calculating limits of detection and quantification by modeling variability as a function of concentration. *Analytical Chemistry*. 1997, 1;69(15):3069-75. DOI: 10.1021/ac970082i

2.6.2. Evaluating the propagated uncertainty produced by the regression

The uncertainty of the acquired parameters refers to the lack of knowledge about the exact real value of these parameters³³. The Monte Carlo (M-C) method is based on a theoretical probability distribution of a variable, where it creates a randomised noise of the predicted values using EXCEL spread sheet. The model's parameters were calculated for each simulation, and the acquired values for each parameter are then checked for normal distribution using a frequency distribution histogram with the bars representing the calculated parameters within certain ranges (bins) of values (figure 2.12).

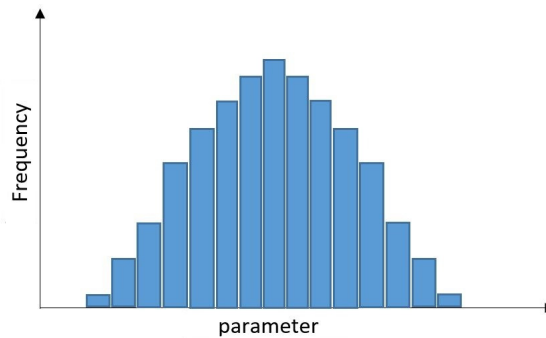


Figure 2.12: Example of a frequency distribution histogram showing a normal distribution of the parameter values produced by the simulations

The uncertainty of the regression method used is represented by the 95% confidence interval (CI), and here it is worth investigating the two types CIs³⁴, the first one is the 95% of the mean which represents the interval at which the chance of having the mean value is equal to 95%. While the other one is the 95% confidence interval of the range of values.

3. Methodology

This section will describe the materials and the methodology used for each experiment in this study.

3.1. Samples handling and loading

The measurements were performed using three products which were bought from a local supermarket and stored at refrigeration at $\sim 6^{\circ}\text{C}$.

The three products used in (figure 3.1) are:

³³ Tong L, Chang C, Jin S, Saminathan R (2012) Quantifying uncertainty of emission estimates in National Greenhouse Gas Inventories using bootstrap confidence intervals. *Atmos Environ* 56:80–87 DOI: 10.1016/j.atmosenv.2012.03.063

³⁴ Choudhary, D., & Garg, P. K. (2013). 95 % confidence interval: a misunderstood statistical tool. *The Indian journal of surgery*, 75(5), 410. DOI: 10.1007/s12262-012-0555-z

- 1- 1000 g Skånemejerier Vanilj yoghurt (2.5 % fat) Ingredients: Pasteurized milk, sugar 6.5%, modified corn starch, stabilizer (pectin), aroma, acid (citric acid), natural Vanilla aroma, yoghurt culture.
- 2- 1000 g Skånemejerier Naturell Lätt yoghurt (0.5 % fat) Ingredients: Pasteurized milk, milk protein, yoghurt culture, vitamin D
- 3- 1000 g Arla Långfil (3.0 % fat) Ingredients: Pasteurized milk, fil culture, vitamin D



Figure 3.1: Images of the three products studied in this thesis. From left to right, Vanilj, Naturell and Långfil

These products will be referred to as Vanilla, Naturell and Långfil respectively. The measurements were always done using freshly opened packages to avoid changes during storage after opening the package. The Products were also tested well within their best before date (2 weeks for the Vanilla and 1 week for the Naturell and Långfil)

These three products were chosen because of their different compositions which allows the measurements to give a better understanding of the yoghurt ingredients and how it might affect its rheological behavior. The Vanilla contains a small amount of added stabilizers while the Naturell contains added protein and vitamins, in addition to that, the manufacturing of Långfil is done using a different culture which results in the formation of different polymers than those in the other two products, these polymers have a higher molecular weight³⁵.

The sample handling and preparation for the measurements included the following:

- 1- The package was tilted up and down (180°): 10 times for both the Vanilla and Naturell, and 40 times for the Långfil.
- 2- The package carton was ripped carefully or cut with a scissors from the top
- 3- The package is then emptied in a glass or a plastic jar
- 4- The yogurt is then homogenised by stirring it using a spoon: 2 relatively slow stirs for the Vanilla and the Naturell, and 10 stirs for the Långfil. And this homogenisation step is done every 2 hours for the Vanilla and Naturell, and every 1 hour for Långfil to avoid phase separation.
- 5- The Cup of the rheometer is then filled gently using a spoon with ~15ml of yogurt

³⁵ Fondén, R., Leporanta, K. and Svensson, U. (2006) '7 Nordic / Scandinavian Fermented Milk Products. DOI: 10.1002/9780470995501.ch7

- 6- The temperature at which the measurement was performed and inputted into the rheometer was 20° C for all the measurements.
- 7- The resting time was set manually to ~60 seconds before each measurement, which is the time the product spends in the cup for the temperature to be adjusted and for the product to rest from any possible shearing effect due to the loading process.
- 8- No prior calibration was performed on the rotational rheometer
- 9- The default setting for the gap height and the lowering rate of the Bob was used for all the measurements.
- 10- All the measurements were done in 3 replicates.

3.2. Flow curve measurement

It is important to define some measuring parameters before describing the methodology used in this study. These parameters are:

- 1- The range of the measurement is the range of the shear rates (shear stress) values inputted into the measuring sequence. it can be at low shear rate range if the application is concerned with the sensory characterisation of the product, or high shear rate ranges if the measurements were concerned in flow behavior in pipes and filling equipment.
- 2- The Sampling points are the points of shear rates (shear stress) at which the rheometer capture the rheological data of the measured sample. increasing the sampling points will increase the degrees of freedom in the final data analysis, it is also possible that it will lead to get a more defined flow curve giving a more accurate description of the product under different flow situations.
- 3- The stabilizing time: when exposing a sample to a constant shear rate, the stabilizing time is the time required for the sample to achieve a near viscosity plateau situation within a 10 seconds interval, at which the change in viscosity is less than 5%. This method is used for products that are difficult to achieve a viscosity plateau.

The protocol used at Tetra Pak for the measurement includes a range of shear rates from 20 s⁻¹ to 200 s⁻¹ with 10 points per decade and a stabilizing time of 15-20 s.

Previous study has used a range of 0.7 s⁻¹ to 700 s⁻¹ with 7 sampling points for decade, and a stabilizing time of 40, 50 and 90 s for Vanilla, Naturell and Långfil respectively.

This study will try to increase the range of the measurement (1-1000 s⁻¹) in an attempt to acquire more information about yogurt rheological behavior in most of the production process situations. In addition to that, the number of sampling points will also be increased to get a more defined curve for each test (10 sampling points per decade).

Materials

- 1- Temperature controlled Malvern Kinexus rotational rheometer (Malvern Instruments limited Worcestershire UK). The methodology for using the Kinexus rheometer is explained in (Appendix § 6.1). The range and limitation of the Kinexus rheometer are presented in (Appendix § 6.2)
- 2- rSpace for Kinexus software

- 3- Serrated Bob geometry, 25 mm diameter, C25G A0009 SS
- 4- Serrated Cup geometry, 27.5 mm diameter, PC25G A0008 AL
- 5- The samples used had the following best before date:
 - 1- Dec for Vanilla, 29- Nov for Naturell and 2- DEC for Långfil

Method

- 1- The sample were loaded into the inserted geometry according to the protocol described in (§ 3.1)
- 2- The sequence used for the measurement was a table of shear rates up and down (Hysteresis Loop), this will help in getting additional understanding of the time effect when using different measuring method.
- 3- The range of the measurement was from 1 s^{-1} to 1000 s^{-1} , with 10 sampling point per decade (Logarithmic) (Figure 3.2)
- 4- The stabilizing time were 40 s, 50 s and 90 s for the Vanilla, Naturell and Långfil respectively (Stabilizing time was determined using the constant shear rate measurement for the Break-Down test § 3.8.1)
- 5- The results for the flow curve were analysed using different regression methods as described in (section §4.1)

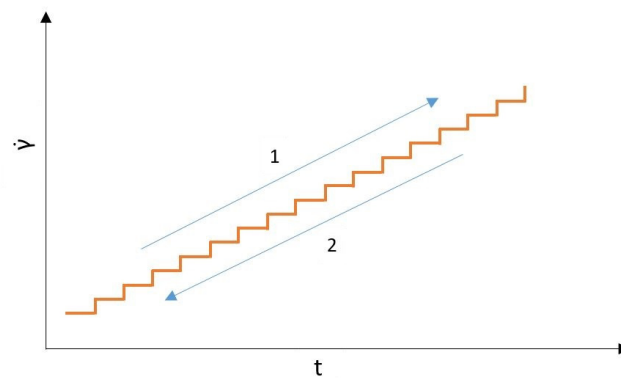


Figure 3.2: Hysteresis Loop test with sweeping up and down in shear rates for investigating the thixotropic effect and for achieving a flow curve

3.3. Assessment of Regression methods used in curve fitting

The methodology used to evaluate the different regression methods can be summarized as the following:

- The first step for investigating the regression methods is to perform a curve fitting using these methods
- The product chosen for the regression assessment was Vanilla
- The models chosen to be utilized in the assessment are
 - a) The Power Law model
 - b) The Power Law- viscosity equation
 - c) The Herschel- Bulkley model

- The OLS, LAR, LARR and LSLR methods are performed using EXCEL sheets for both models as detailed in the (Appendix § 6.3)
- The steps for performing WLS regression are explained in (Appendix § 6.4)
- For the parameter's uncertainty estimation, Monte- Carlo simulations were performed for each regression method for the Power Law model and the Power Law- viscosity equation as illustrated in the (Appendix § 6.5)
- The simulation results were checked for normal distribution using distribution frequency histograms
- Both types of 95% confidence intervals (CI of the mean and CI of the values) were estimated.

3.4. Batches variation

Yogurt products known for the existence of batch variation, and to determine the amount of deviation for the tested products, the Power Law parameters were one of the tools used for the compression for the three products. And to do that, the following methodology was used:

Materials

- 1- Temperature controlled Malvern Kinexus rotational rheometer (Malvern Instruments limited Worcestershire UK) with the rSpace for Kinexus software.
- 2- Serrated Cup and Bob geometry
- 3- A minimum of five batches of each product with different “Best before date” as shown in (table 3.1)

	Best before date					
Vanilla	28- Oct	3- Nov	24- Nov	1- Dec	8- Dec	31- Dec
Naturell	2- Nov	22- Nov	29- Nov	5- Dec	15- Dec	-
Långfil	16- Oct	20- Nov	27- Nov	2- Dec	9- Jan	-

Table 3.1: The “Best before date” for the batches used to investigate the batches variation

Method

To investigate the variation between the different batches of the three products, the measurements were performed for each batch as the following:

- 1- The sample were loaded into the inserted geometry according to the protocol described in (§ 3.1)
- 2- The sequence used for the measurement was a table of shear rates up and down (Hysteresis Loop)
- 3- The range of the measurement was from 1 s^{-1} to 1000 s^{-1} , with 10 sampling point per decade (Logarithmic)
- 4- The stabilizing time were 40 s, 50 s and 90 s for the Vanilla, Naturell and Långfil respectively
- 5- The results for the flow curve were analysed using the OLS regression method

3.5. Measurements using different geometries

The question regarding the right geometry for measuring yogurt rheology, and whether it has an effect over the resulting flow profile. Therefore, a methodology was developed to investigate the geometry choice.

Materials

- 1- Kinexus rotational rheometer- Malvern using the following geometries:
 - i) Serrated Cup and Bob geometry
 - ii) Smooth Cup and Bob geometry, (Cup: PC25G C0003, Bob: SS C25G C0004 SS)
 - iii) Serrated Cup and Smooth Bob geometry
- 2- Rheolab QC rotational rheometer- Anton Paar using the sand blasted Cup and Bob (CC27/S:SN 44579)
- 3- Three types of yogurt (Vanilla, Naturell and Långfil) with the “Best before date” of the samples illustrated in (table 3.2)

	Serrated Cup and Bob	Smooth Cup and Bob	Serrated Cup and Smooth Bob	Sand blasted Cup and Bob
Vanilla	1- Dec	17- Nov	17- Nov	24- Nov
Naturell	29- Nov	25- Dec	25- Dec	12- Nov
Långfil	2- Dec	1- Jan	1- Jan	14- Nov

Table 3.2: The “Best before date” for the batches used to investigate the different geometries effect

Method

- 1- The same Handling and loading protocol mentioned in (§3.1) was used for all the samples
- 2- The sequence used for the measurement was a table of shear rates up and down (Hysteresis Loop)
- 3- The range of the measurement was from 1 s^{-1} to 1000 s^{-1} , with 10 sampling point per decade (Logarithmic)
- 4- The stabilizing time were 40 s, 50 s and 90 s for the Vanilla, Naturell and Långfil respectively
- 5- The results for the flow curve were analysed using the OLS regression method

3.6. Static yield stress measurement

The methods chosen for the static yield stress determination were the ones that showed most repeatable results in previous study³⁶.

The tangent method (figure 3.3.a) depends on finding the lines of best fit for both the unyielded and the yielded regions, where the intercept of these lines represents the point where the curve starts deviating from its tangent, and the shear stress at this intercept represents the static yield stress value³⁷. The other method used in this study for the static yield stress determination is the bayod method (figure

³⁶ H. Williamson and R. Osterus. (2019) “Characterizing the rheology of fermented dairy products during filling”. MA thesis. Sweden: Lund University.

³⁷ Malvern Instruments (2012) Understanding Yield Stress Measurements. Available at: www.malvern.com/contact.

12.b) which depends on plotting the stress at the minimum value of the first derivative of the ratio of logarithms of shear stress to shear rate, at which the lowest value corresponds to the region that contains the beginning of the plastic deformation of the studied material ³⁸.

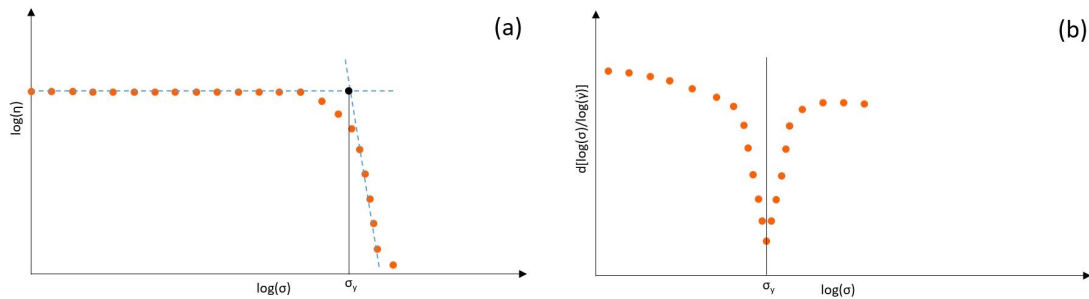


Figure 3.3: Examples for determining the static yield stress using a shear stress ramp with a. the tangent method and b. the bayod method

3.6.1. The tangent method

Materials

- 1- Temperature controlled Malvern Kinexus rotational rheometer (Malvern Instruments limited Worcestershire UK) with the rSpace for Kinexus software.
- 2- Serrated Cup and Bob geometry
- 3- Three types of yogurt with their best before date: Vanilla (22- Oct), Naturell (2- Nov) and Långfil (16- Oct)

Method

- 1- The same handling and loading protocol mentioned in (§3.1) was used for all the samples
- 2- The sequence used for the measurement was a linear shear stress ramp
- 3- The range of the measurement was from 1 Pa to 10 Pa, the ramp time was 20 min with 1 sampling point per second

3.6.2. The bayod method

Materials

- 1- Temperature controlled Malvern Kinexus rotational rheometer (Malvern Instruments limited Worcestershire UK) with the rSpace for Kinexus software.
- 2- Serrated Cup and Bob geometry
- 3- Three types of yogurt with their best before date: Vanilla (22- Oct), Naturell (22- Oct) and Långfil (16- Oct)

Method

- 1- The same handling and loading protocol mentioned in (§3.1) was used for all the samples
- 2- The sequence used for the measurement was a linear shear stress ramp

³⁸ Bayod, E. (2008) Microstructural and Rheological Properties of Concentrated Tomato Suspensions During Processing. Lund University.

- 3- The range of the measurement was from 0.01 s⁻¹ to 10 Pa, the ramp time was 10 min, 20 min and 30 min with 1 sampling point per second

3.7. Zero shear viscosity measurement

It was noticed in a previous study, when measuring η_0 using a shear stress ramp, the results were related to the time needed to perform a shear stress ramp, therefore, a method was developed to investigate this effect by using several different ramp times for the measurement.

Materials

- 1- Temperature controlled Malvern Kinexus rotational rheometer (Malvern Instruments limited Worcestershire UK) with the rSpace for Kinexus software.
- 2- Serrated Cup and Bob geometry
- 3- Three types of yogurt with their best before date: Vanilla (22- Dec), Naturell (5- Dec) and Långfil (2- Dec)

Method

- 1- The same handling and loading protocol mentioned in (§3.1) was used for all the samples
- 2- The sequence used for the measurement was a linear shear stress ramp
- 3- The range of the measurement was from 0.01 Pa to 10 Pa, the ramp time was 10 min, 20 min and 30 min with 1 sampling point per second

3.8. Infinite shear viscosity measurement

The infinite shear viscosity measurement was done at the material lab at Chalmers university. The method planned for measuring η_∞ was to perform a sweep of shear rates from 1000 s⁻¹ to 10000 s⁻¹ and analyse the results to find a plateau of viscosity with the increased shear rate values. This was not possible due to the formation of bubbles and not being able to achieve a steady state for the measurements to be reliable. Therefore, an alternative method was developed.

Materials

- 1- Göttfert 2002 capillary rheometer with a GX5 die (L=30 mm, D= 0.5 mm) (figure 3.4)
- 2- Two litres of each yogurt products with the following best before dates: Vanilla (24- Nov), Naturell (22- Nov) and (20- Nov).



Figure 3.4: An image of the die (to the left) and the high- pressure capillary rheometer (to the right) used for the determination of the η_∞

Method

- 1- The samples were loaded into the rheometer's reservoir, but the loading protocol was not followed due to the high viscosity of yogurt. This required inserting a metal rod into the reservoir in an attempt to eliminate the forming bubbles.
- 2- The sequence used were a constant shear rate at ten values, shown in (table 3.3)
- 3- The results were analysed using the OLS regression method

Step number	1	2	3	4	5	6	7	8	9	10
Shear rate (s^{-1})	1000	1292	1668	2154	2783	3594	4642	5995	7743	10000

Table 3.3: The shear rate values used for the constant shear rate test using the high- pressure capillary rheometer

3.9. Thixotropy measurements

It is possible to evaluate the Thixotropic effect of the sample based on the methodology for the hysteresis loop test (described in § 3.2).

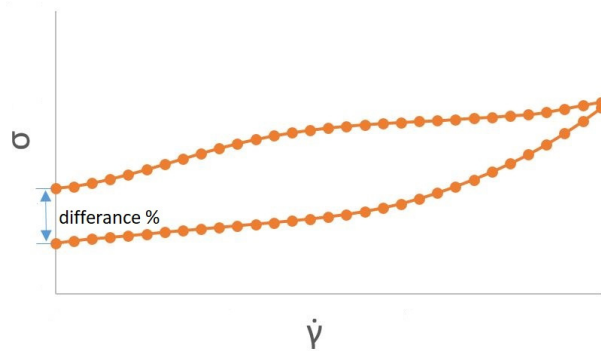


Figure 3.5: An example of a hysteresis loop and determining the difference between the initial and final shear stress values to estimate the time effect of the sample.

the amount of hysteresis is calculated based on the difference percentage in the shear stress between the initial and the last sampling point for the hysteresis loop for compression between the products (figure 3.5). In addition to that, several measuring methods were developed as detailed in the following subsections:

3.9.1. Break down test

The Break- down test was used to investigate the viscosity plateau and the stabilizing time.

Materials

- 1- Temperature controlled Malvern Kinexus rotational rheometer (Malvern Instruments limited Worcestershire UK) with the rSpace for Kinexus software.
- 2- Serrated Cup and Bob geometry
- 3- Three types of yogurt with their best before date: Vanilla (15- Oct), Naturell (14- Oct) and Långfil (10- Oct)

Method

- 1- The same handling and loading protocol mentioned in (§3.1) was used for all the samples
- 2- The sequence used for the measurement was a constant shear rate test (table 3.4) and was applied for all the samples.

Constant shear rate value (s^{-1})	Time for the measurement (s)	Sampling intervals (per second)
100	300	1
300	300	1
900	300	1

Table 3.4: The protocol used for the Break- down investigation

The measured viscosity data is plotted against time, and the graphs are checked for a viscosity plateau, which is the phenomenon of the viscosity becoming constant no matter how long we shear the product. The 10 seconds interval at which the viscosity drop is less than 5% is called the stabilizing time (figure 3.6), which will be used as an indication for an equilibrium state in other measurements.

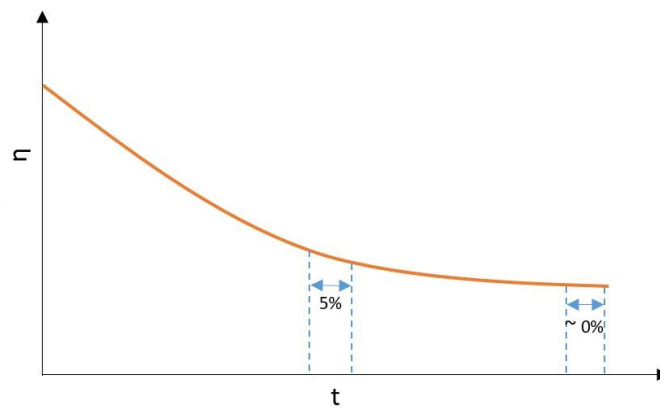


Figure 3.6: An example showing the viscosity plateau (0%) and the protocol used for estimating the stabilizing time

3.9.2. Build up test

The measurement designed for investigating the Build- up ability of yogurt is derived from one of the tests done in a previous research³⁹ (figure 3.7).

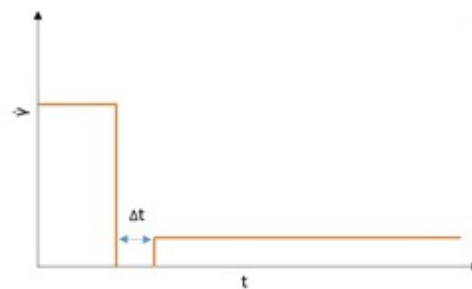


Figure 3.7: An example of the shear rates applied to perform a Build- up test

³⁹ Y. Wei, M.J. Solomon. Quantitative nonlinear thixotropic model with stretched exponential response in transient shear flows. Published: October 2016. DOI: 10.1122/1.4965228

Materials

- 1- Temperature controlled Malvern Kinexus rotational rheometer (Malvern Instruments limited Worcestershire UK) with the rSpace for Kinexus software.
- 2- Serrated Cup and Bob geometry
- 3- Three types of yogurt with their best before date: Vanilla (22- Dec), Naturell (5- Dec) and Långfil (27- Nov)

Method

- 1- The same handling and loading protocol mentioned in (§3.1) was used for all the samples
- 2- The sequence used for the measurement contains a pre- shear step at constant shear rate. The sample is then rested for different resting times Δt and afterwards sheared at constant low shear rate (table 3.5)

Pre- shear step (s^{-1})	Δt (s)	Build- up step (s^{-1})
100	0	1
	30	
	90	
	300	
300	0	
	30	
	90	
	300	

Table 3.5: The protocol used for the Build- up test

3.9.3. Varied shear rate step test

To get a bigger overall picture of the changes in viscosity in transient shear rate situations, a varied shear rate step test was performed, and the shear stress and viscosity values were recorded (figure 3.8).

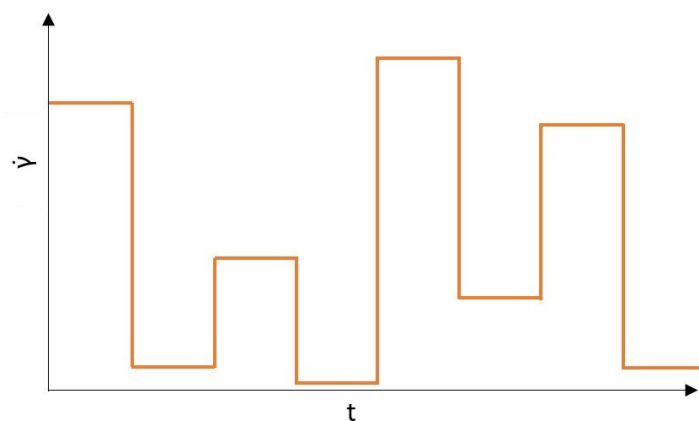


Figure 3.8: Example of a varied shear rate test used to examine the Build- up and Break- down (thixotropy) of a sample by changing the shear rate value at different time intervals

Materials

- 1- Temperature controlled Malvern Kinexus rotational rheometer (Malvern Instruments limited Worcestershire UK) with the rSpace for Kinexus software.
- 2- Serrated Cup and Bob geometry
- 3- Three types of yogurt with their best before date: Vanilla (31- Dec), Naturell (12- Nov) and Långfil (27- Nov)

Method

- 1- The same handling and loading protocol mentioned in (§3.1) was used for all the samples
- 2- The sequence used for the measurement contains varied constant shear rate values (steps) with 2 min per step (table 3.6)

Step	1	2	3	4	5	6	7	8	9	10
Shear rate (s^{-1})	1	300	0.01	70	0.1	100	0.001	500	0.01	300

Table 3.6: The protocol used for the varied shear rate step test

3.10. Pre- shearing

For the measurements using pre-shearing in this study, two techniques were used, the first one is by applying a constant shear rate for a period of time just before measuring the samples, this pre-shearing step varies in speed and duration to investigate thoroughly the effects of pre-shearing on the samples (figure 3.9.a). The second technique was to perform multiple hysteresis loops on the samples and analyse the results from each one of these loops to investigate the possibility of eliminating the time effect of the samples (figure 3.9.b).

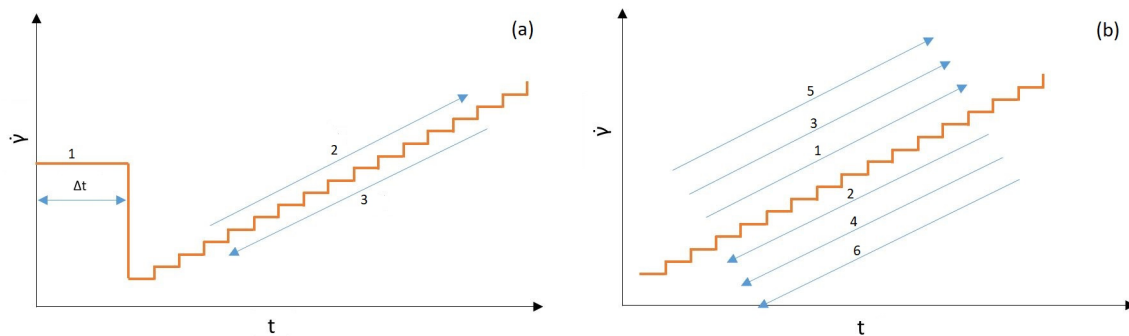


Figure 3.9: Example of the pre-shearing methods used in this study, a. pre-shearing using CSR at a certain speed for certain period Δt . b. multiple hysteresis loops

3.10.1. Pre- shearing using constant shear rate

Materials

- 1- Temperature controlled Malvern Kinexus rotational rheometer (Malvern Instruments limited Worcestershire UK) with the rSpace for Kinexus software.

- 2- Serrated Cup and Bob geometry
- 3- Three types of yogurt with their best before date: Vanilla (28- Oct), Naturell (3- Nov) and Långfil (20- Nov)

Method

- 1- The same handling and loading protocol mentioned in (§3.1) was used for all the samples
- 2- The sequence used for the measurement contains a pre- shear step at a constant shear rate value (s^{-1}) for Δt (s). The sample is then introduced to a hysteresis loop test without being rested as detailed in (§ 3.2) (table 3.7)

Pre- shearing speed (s^{-1})	Pre- shearing time (s)			
	30	90	300	600
30	V- N- L	V- N	V- N	
100	V- N	V- N- L	V- N	
300	V- N	V- N	V- N- L	
900				V- N- L

Table 3.7: The protocol used for measuring with constant shear rate for pre-shearing, Vanilla: V, Naturell: N and Långfil: L

3.10.2. Multiple hysteresis loops test

Materials

- 1- Temperature controlled Malvern Kinexus rotational rheometer (Malvern Instruments limited Worcestershire UK) with the rSpace for Kinexus software.
- 2- Serrated Cup and Bob geometry
- 3- Three types of yogurt with their best before date: Vanilla (17- Nov), Naturell (5- Dec) and Långfil (27- Nov)

Method

- 1- The same handling and loading protocol mentioned in (§3.1) was used for all the samples
- 2- The sequence used for the measurement contains a multiple hysteresis loops test (3 Loops) with no rest in between. The hysteresis loop adheres to the protocol detailed in (§ 3.2)

3.11. Elongation (Tack test)

Materials

- 1- MCR rheometer from Anton Paar
- 2- Parallel plates geometry
- 3- Three types of yogurt with their best before date: Vanilla (24- Nov), Naturell (12- Nov) and Långfil (12- Nov)

Method

To investigate the tack of the three yogurt products, two measuring methods were used, using different measuring gap.

The methodology for performing the first method were:

- 1- Driving to the measuring gap of $d = 5$ mm
- 2- Moving up the measuring plate with the constant removal speed of $v = 5$ mm/s
- 3- Filming the tests using a mobile camera in slow motion

The methodology for performing the first method were:

- 1- Pre- shearing the sample at 1000 s^{-1} for 1 s
- 2- Driving to the measuring gap of $d = 1$ mm
- 3- Moving up the measuring plate with the constant removal speed of $v = 5$ mm/s

4. Results and discussion

This section will present the results and the analysis of the experiments described earlier, with the discussion and the findings for each section.

4.1. Regression method evaluation

The five regression methods were applied to perform a curve fit on the resulting flow curve for the three products, the first model applied was the Power Law model which showed different K and n values with each method used as shown in (table 4.1) for Vanilla. The results for applying the different regression methods on the Naturell and Långfil measurements can be found in (Appendix §6.6).

The standard deviation resulting from using the different methods was up to 2 Pa.s^n for the K value in the case of Långfil, and up to 0.87 Pa.s^n for the K value of the Vanilla, and up to 0.04 for the n value in the case of Naturell, this makes determining the most relevant regression method more important as these differences can affect further applications of these models. In addition to that, it is worth mentioning that the only regression method that was able to determine the dynamic yield stress of Långfil was the WLS method.

	OLS	LAR	LARR	LSLR	WLS	SD
K (Pa. s^n)	5.91	7.44	8.35	8.16	7.74	0.87
n (-)	0.35	0.30	0.26	0.28	0.29	0.03
SSR	317.65	456.30	992.93	617.15	527.30	-

Table 4.1: The results of the Power law curve fitting using different regression methods (Vanilla)

	OLS	LAR	LARR	LSLR	WLS	SD
A (Pa. s^b)	1.06	1.10	2.35	2.59	1.18	0.67
b (-)	0.59	0.58	0.46	0.45	0.57	0.06
τ_0 (Pa)	10.23	10.68	7.90	7.18	9.91	1.38
SSR	60.12	69.00	172.99	147.87	61.11	-

Table 4.2: The results of the Herschel- Bulkley curve fitting using different regression methods (Vanilla)

Another observation from the results is that the OLS method gave the best fit judging only on the SSR value for all the measurements, which is a good indication on the tightness of the fit it produces, but still it needs to be evaluated later when examining the residual plots to check if the fits are good, with violation of the assumptions of the OLS method.

The second step in evaluating the regression is to check for the tightness of the fits by examining the flow curves on a linear and a logarithmic scale for the three models when applied for the vanilla (figure 4.1, 4.2, 4.3) while the curve flow curve fitting of Naturell and Långfil using the different regression methods can be found at (Appendix § 6.6). The examination of these curves indicates that the five methods appear to produce a good fit on a logarithmic scale axis plots for the three mentioned figures, but this type of plotting can be misleading to the untrained eyes when evaluating it⁴⁰. It is also observed from the linear and the logarithmic scale plots in the figures mentioned above, that the LARR method produces the best fit for the left segment of the measured points while it also produces the worst fit among the regression methods on the right segment of the flow curves.

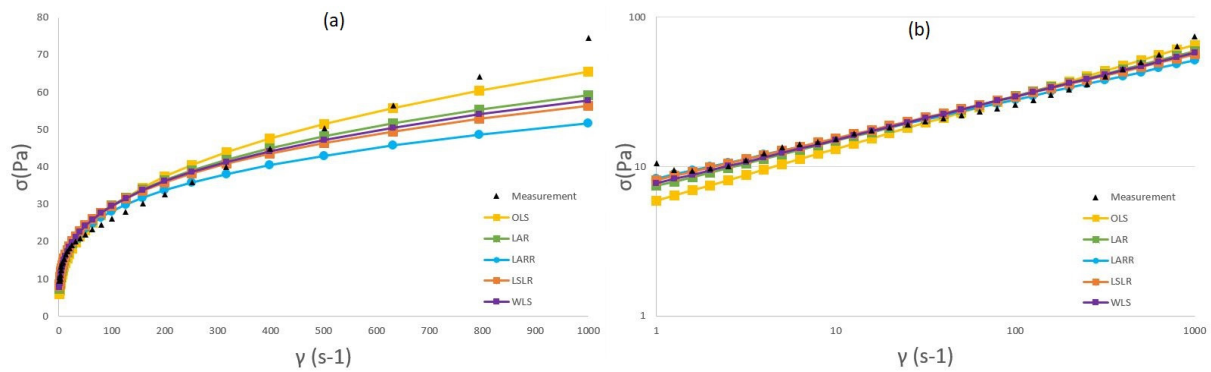


Figure 4.1: The flow curve resulting from the Power law curve fitting using the different regression methods (Vanilla)

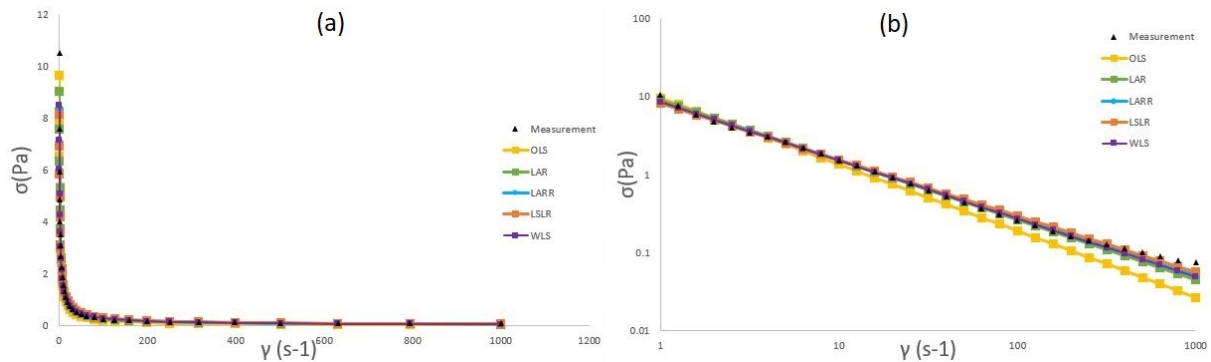


Figure 4.2: The flow curve resulting from the Power law viscosity equation curve fitting using the different regression methods (Vanilla)

⁴⁰ H. Motulsk. The Use and Abuse of Logarithmic Axes. June- 2009.

<https://s3.amazonaws.com/cdn.graphpad.com/faq/1910/file/1487logaxes.pdf> [Accessed DEC- 2019]

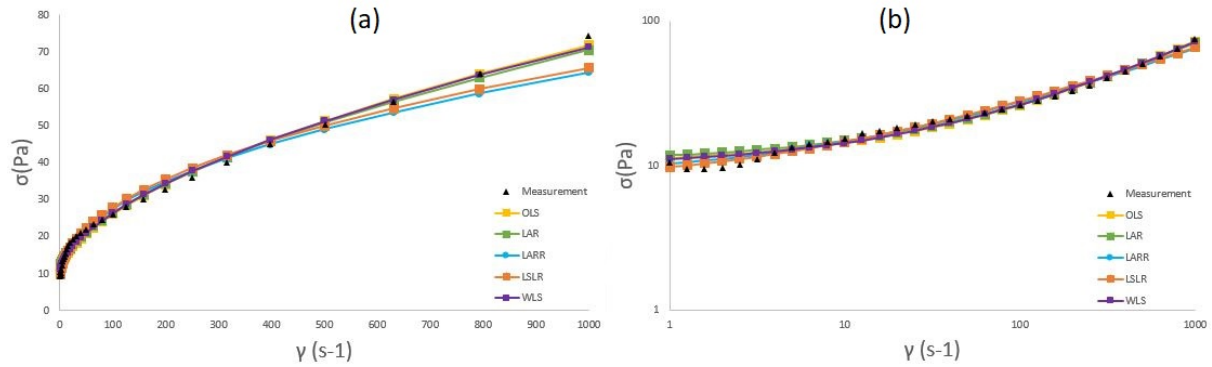


Figure 4.3: The flow curve resulting from the Herschel- Bulkley curve fitting using the different regression methods (Vanilla)

4.1.1. Evaluating the tightness of the fit for the regression methods

For a further examination for the regression analysis done using the five regression methods, residual plots of the curve fitting used to model the Vanilla were graphed (figure 4.4, 4.5 and 4.6), the residuals plots for the Naturell and Långfil can be found at (appendix § 6.7).

The residual plot tool provided a good approach to examine the tightness of the fit more accurately along the range of the measured data points.

By looking at the curves in the figures, it can be noted that the residuals values increase with the increased predicted values. This is logical since the measured data point were sampled using a logarithmic scale. But a trend can also be observed, is that the LARR method produced lower predicted values than the other methods, in addition to that, the residuals of the LARR are the biggest —among the other methods— at the high measured range. This reveals that the LARR suffers from overfitting in the beginning of the curve and thus, fail to produce a good fit at the end of the curve, were an overfitted model represents the noise rather than relationships in the population, the problems due to overfitting appear also when trying to fit an over fitted model of a sample to another sample that has its own error distribution and this reduces the generalizability outside the model produced by the analysed dataset⁴¹. The LSLR, LAR and the WLS methods shows a degree of overfitting too, but still less than the overfitting observed to a certain extent in the LARR method. It is also noted that the WLS, OLS and LAR methods improve drastically when applied to the Herschel- Bulkley model, which might indicate to the fact that an added parameter to the model might be better to get a better fit to describe the real values.

⁴¹ Babyak, MA., (2004), What You See May Not Be What You Get: A Brief, Nontechnical Introduction to Overfitting in Regression-Type Models, Psychosomatic Medicine 66:411-421.

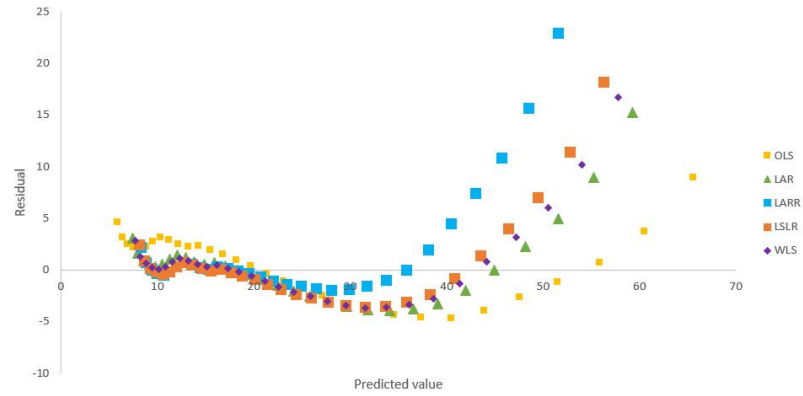


Figure 4.4: The residual plot resulting from the Power law curve fitting using the different regression methods (Vanilla)

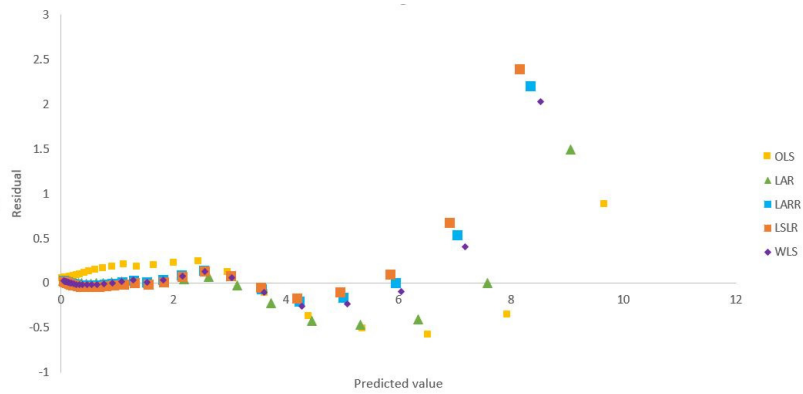


Figure 4.5: The residual plot resulting from the Power law viscosity equation curve fitting using the different regression methods (Vanilla)

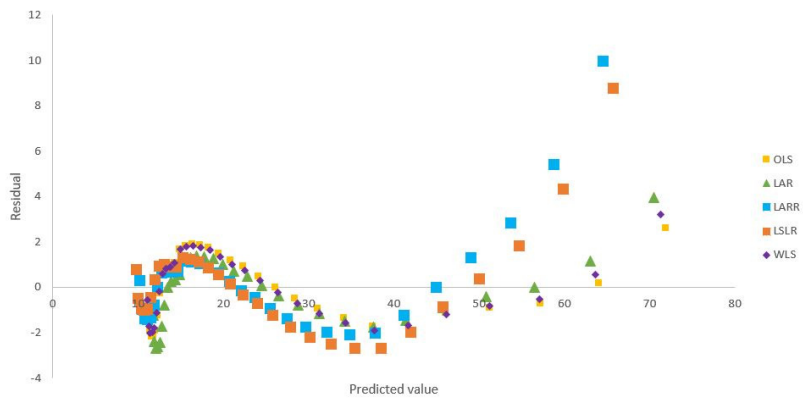


Figure 4.6: The residual plot resulting from the Herschel- Bulkley curve fitting using the different regression methods (Vanilla)

By squaring the residuals, the OLS method gives more weight to larger residuals, these large residuals can be outliers (outliers in regression are predicted values with residuals that have a high value compared to most of the other predicted values), and this will lead to the predicted values in some

cases being far from the actual measurements. The outliers can simply be removed from the dataset, but this practice can raise concerns since it decreases the degrees of freedom, especially when the number of the data points is not big.

Comparing the stability of the solutions provided by the OLS and the LAR methods shows that the OLS method provide a more stable solution with the regression parameters being continuous functions of the measured data, and by stability it is meant that a small adjustment of the x value of a data point will not affect the regression line greatly. On the other hand, the LAR method provide a continuous solution for some data configuration, but a small change in the X value of a data point can deviate the regression line greatly which will produce a bigger change in the regression parameters⁴².

Even though this method seems attractive because of the very close fit it can produce in some cases, the theoretical justification of using the relative error is still a challenging task for mathematicians, and under general conditions, the consistency of this method has not yet been established. In addition to that, in the studies that have been done so far, the relative error was defined as the spread between the measured data and the predicted value divided by the predicted value, this can be inadequate when the predicted value is large and the measured value is relatively small which can lead to the problem of overfitting in some cases⁴³.

4.1.2. Evaluating the propagated uncertainty of the regression methods

The following step in analysing the regression methods is to investigate the uncertainty propagated by each method. This was done using the Monte Carlo simulations with 400 simulation on each regression method for the two models, the Power Law model and the Power Law viscosity equation.

The Monte Carlo simulation was not able to perform on the LSLR method, this was due to the fact that the simulations produced negative values that cannot be logged; therefore, an uncertainty investigation of this regression method will not be included in this study.

The simulations are studied first by investigating frequency distribution histograms of the resulting parameters K and n for the Power Law model (figure 4.7) and for the Power Law- viscosity equation (figure 4.8). The histograms show a normal distribution for both the parameters K and n for all the methods used, which agree with the assumption associated when performing the Monte Carlo simulation. and therefore, makes it more credible in determining the propagated uncertainty of the regression methods investigated. The frequency distribution histograms resulting from applying the Monte Carlo simulation on the Power Law viscosity equation can be found in (Appendix \$ 6.8)

⁴² Steven P. Ellis, Instability of least squares, least absolute deviation and least median of squares linear regression. *Statist. Sci.* Volume 13, Number 4 (1998), 337-350.

⁴³ Chen, K., Guo, S., Lin, Y., & Ying, Z. (2010). Least Absolute Relative Error Estimation. *Journal of the American Statistical Association*, 105(491), 1104–1112. DOI:10.1198/jasa.2010.tm09307

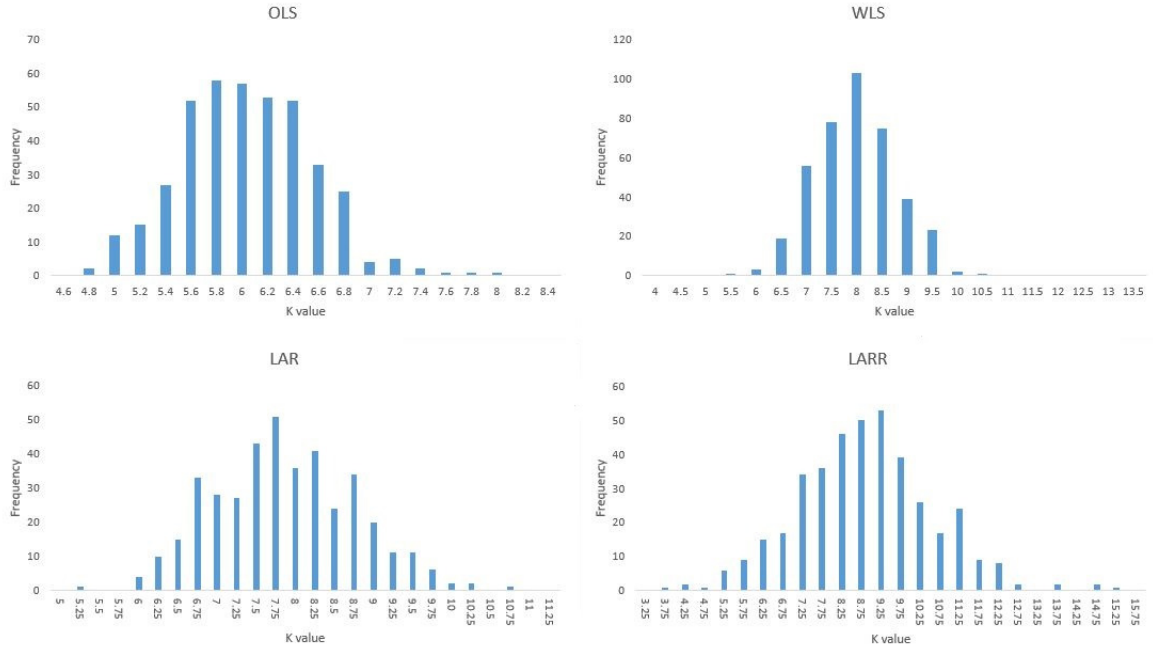


Figure 4.7: The frequency distribution histogram of K, for the Power law model curve fitting using different regression methods (Vanilla)

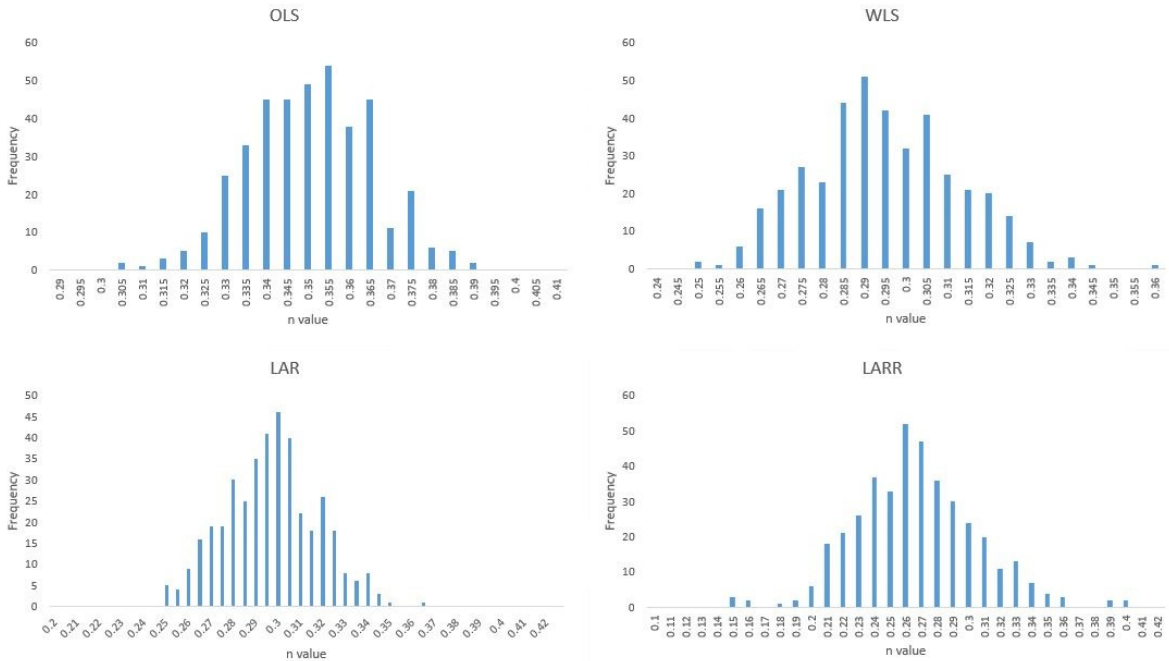


Figure 4.8: The frequency distribution histogram of n, for the Power law model curve fitting using different regression methods (Vanilla)

The next step in studying the uncertainty is to determine both the 95% confidence intervals of the values and the 95% confidence intervals of the mean mentioned. The confidence intervals for the regression methods when applied on the Power Law model are presented in (table 4.3 and table 4.4),

and the confidence intervals for the regression methods when applied on the Power Law- viscosity equation are presented in (Appendix § 6.8).

For both the parameters in both models, the LARR method had the largest intervals (which correlate with the fact that this method produce a case of overfitting that has a negative effect on the generalization of this method), while the OLS method appeared to have the smallest intervals. This points out to a clear advantage of the OLS method due to the fact that it is the least sensitive to uncertainty propagation. This makes the OLS method more reliable than the other methods. The WLS and the LAR methods performed well compared to the LARR method but slightly more sensitive than the OLS method, which makes them a good choice to use if one of the assumptions for applying the OLS regression is violated.

	OLS		WLS		LAR		LARR	
	95%CI of mean	95%CI of value	95%CI of mean	95%CI of value	95%CI of mean	95%CI of value	95%CI of mean	95%CI of value
Upper bound	5.99	7.01	7.83	9.37	7.83	9.52	8.77	11.83
Lower bound	5.89	4.96	7.67	6.25	7.66	6.13	8.43	5.38
Upper- Lower limit	0.10	2.05	0.16	3.12	0.18	3.39	0.34	6.45

Table 4.3: The uncertainty of the K value when using different regression methods to apply the Power law model

	OLS		WLS		LAR		LARR	
	95%CI of mean	95%CI of value	95%CI of mean	95%CI of value	95%CI of mean	95%CI of value	95%CI of mean	95%CI of value
Upper bound	0.35	0.38	0.29	0.33	0.30	0.34	0.27	0.35
Lower bound	0.35	0.32	0.29	0.26	0.29	0.26	0.26	0.20
Upper- Lower limit	0.00	0.06	0.00	0.07	0.00	0.08	0.01	0.15

Table 4.4: The uncertainty of the n value when using different regression methods to apply the Power law model

As expected, the OLS method is a reliable method when performing a curve fitting and none of the assumptions for this method are violated. Analysing each regression performed looking for Heteroscedasticity and over fitting is a troublesome task and require time, especially when rapid analysis for a big set of measurements is needed. The use of the WLS and LAR method seems like a good solution to some of the problems that the OLS faces. Although the LAR method is robust and simpler to use than the WLS method, but still the WLS combine the stable solution provided by the OLS method and the robustness that comes with the LAR method. The WLS method has shown acceptable sensitivity when performing the Monte Carlo simulation which gives it a good level of reliability, therefore the WLS method will be used only for the measurements for the rheological modelling of this study, but because of the time limitations, the rest of the measurements will be utilizing the OLS method as it is more rapid and simpler to use.

4.2. Rheological modelling results

Performing a hysteresis loop measurement for the studied samples resulted in the flow curves presented in (figure 4.9). This section will focus on the curve fitting to the measured data using several rheological models and will focus on the upward sweep, while in further section, the discussion will expand to include other angles on how to interrupt the hysteresis loop data. The measurement protocol at Tetra Pak labs and the protocol used in a previous study included a smaller range of shear rates and less sampling points. The method developed in this study tried to increase the range and the sampling points to get an overall picture of the rheological behavior over a wider range of applications.

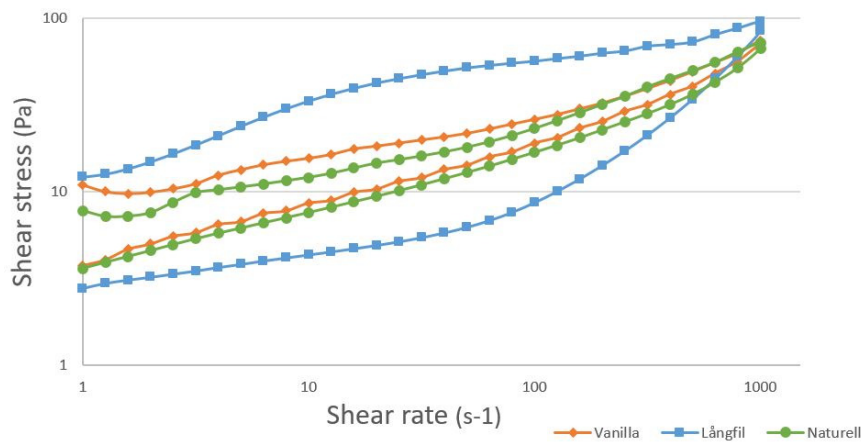


Figure 4.9: The results of the Hysteresis loop tests for different yogurt products

The common way to perform the curve fitting, the upward sweep is regressed to the available model, and as stated in (section § 4.1), the Weighted Least Square regression method was used for the determination of the rheological parameters using the SOLVER function in EXCEL sheets.

4.2.1. Power Law model

The results from using the Power Law model (equation 2.1) to fit the measured data to the upward sweep of the flow curves (figure 4.10), and a summary of the resulting parameters are presented in (table 4.5). These measurements were done with no pre-shearing.

The resulting K and n values seems to be reasonable when comparing between the samples. n value is lower than 1 and this is expected from yogurt products as these products are categorized as shear thinning fluids when a Power Law model is fitted to their flow curves. K value is the consistency index, and it was found that Långfil has a higher K value than Naturell and Vanilla, which indicates that Långfil is thicker in consistency when compared to the other two products. The SSR value is used to evaluate the goodness of the fit, the lowest SSR value was observed in the case of Naturell, which indicates that the Power Law model is more suitable to describe the rheological behavior of Naturell

compared to Vanilla and Långfil. On the other hand, Långfil had the highest SSR value, in addition to the highest measurement uncertainty which can be translated from the high value of the standard deviation when applying the Power Law model.

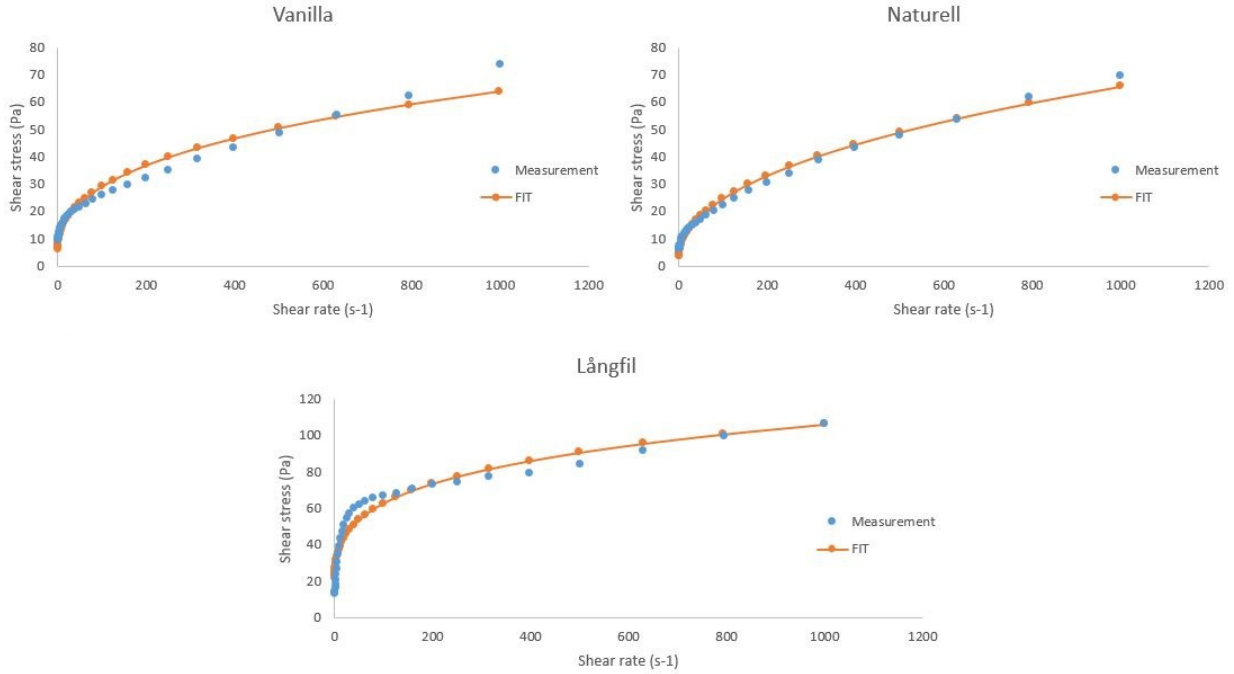


Figure 4.10: The results from the Power Law curve fitting

	Vanilla	Naturell	Långfil
$K [Pa \cdot s^n]$	8.16 ± 0.3	3.73 ± 0.2	25.28 ± 6.5
$n [-]$	0.28 ± 0.0	0.41 ± 0.0	0.20 ± 0.0
$SSR [Pa^2]$	620.08 ± 30.7	174.08 ± 29.4	988.79 ± 327.9

Table 4.5: The results of the Power law parameters using the WLS curve fitting method

The Power Law viscosity equation (equation 2.2) is applied to the viscosity-based flow curves in order to acquire the Power Law parameters (figure 4.11)

The resulting parameters are compiled in (table 18), the resulting K and n values are different from the ones acquired from the Power Law model which can be the result from the difference in the variance of the residuals and their distribution during the regression which affects the weight of each predicted value.

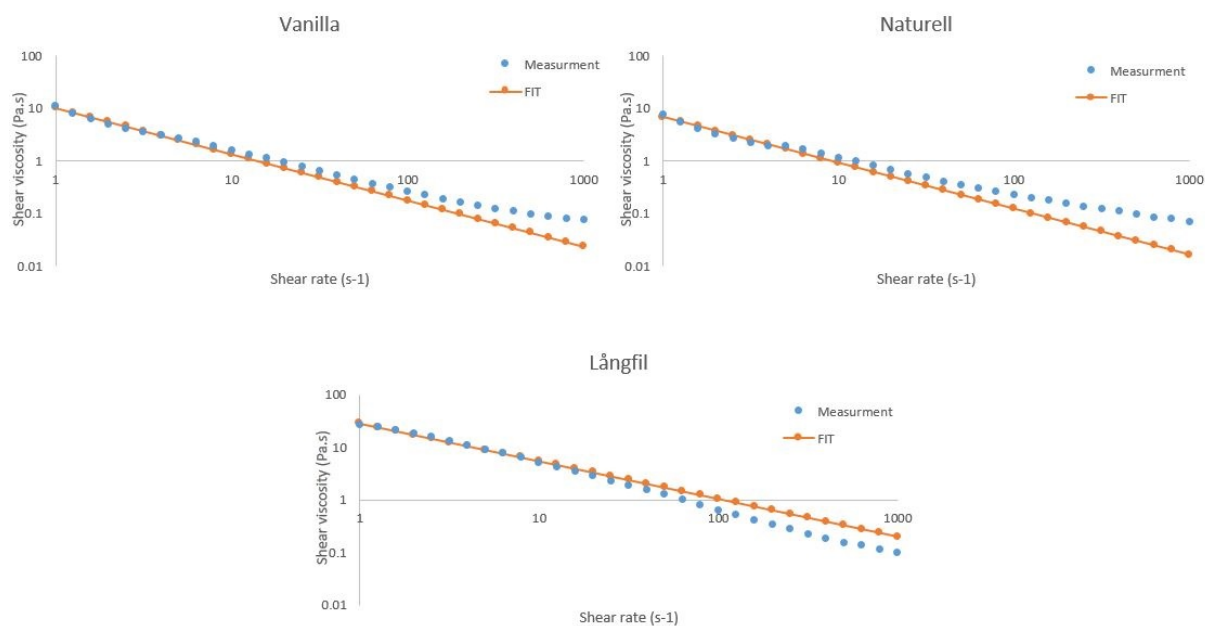


Figure 4.11: The results from the Power Law viscosity equation curve fitting

	Vanilla	Naturell	Långfil
K [Pa·s ⁿ]	8.79 ± 0.3	5.60 ± 0.3	23.94 ± 8.0
n [-]	0.25 ± 0.0	0.31 ± 0.0	0.27 ± 0.1
SSR [(Pa.s) ²]	4.75 ± 0.6	6.52 ± 1.6	223.68 ± 291.8

Table 4.6: The results of the Power law parameters using the WLS curve fitting method

By examining the Power Law constants (K and n) in (table 4.5 and table 4.6) that result from the Power Law model and the Power Law viscosity equation, it can be noticed that there is a difference between the values resulting from these models. This can be explained by the viscosity equation having the condition $\dot{\gamma} \neq 0$. This condition makes the viscosity equation fails at predicting the shear stress value at very low shear rate values approaching zero.

4.2.2. Herschel- Bulkley model

The use of the SOLVER function instead of TRENDLINE function, provided the ability to determine the dynamic yield stress directly from the flow curve. It is also worth mentioning again that the WLS regression method was the only method to provide a yield stress value among the other regression methods (table 4.7). The value of b is between 0 and 1 as for the Power Law parameter (n), therefore the Herchel- Bulkly model indicates to a shear thinning behavior for the three products. From the results and by examining (figure 4.12), it is clear also that Långfil has a higher degree of shear thinning behavior than the other products.

The magnitude of A value indicates that Långfil has a thicker consistency than Naturell and Vanilla which correlates with the Power Law results. The SSR values indicate that the Herchel- Bulkly model performed well in describing the curve flow of the Naturell followed by Vanilla, while its accuracy decreases for Långfil.

The standard deviation for the Vanilla and Naturell is very low for all the parameters, which indicates a high reliability produced by the Herchel- Bulkly model (equation 2.3). On the other hand, the standard deviation for the Långfil was high (higher than the case of the Power Law model), this might lead to the conclusion that the Herchel- Bulkly is not the best choice for describing Långfil flow.

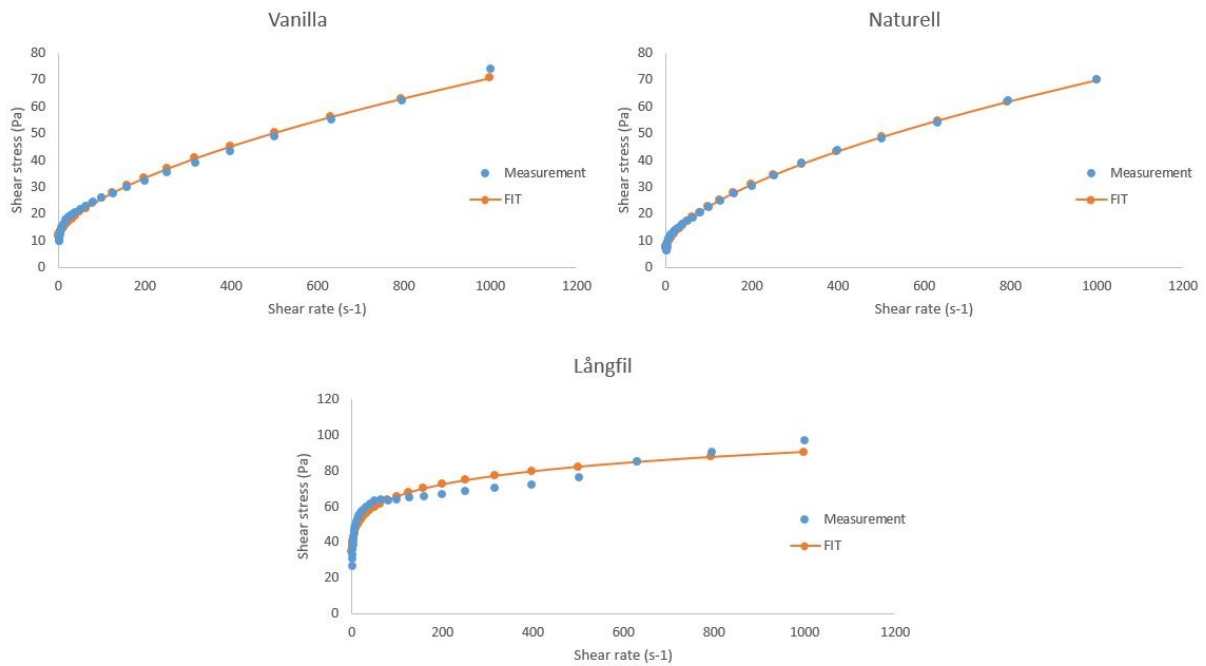


Figure 4.12: The results from the Herchel- Bulkly curve fitting

	Vanilla	Naturell	Långfil
A [Pa·s ⁿ]	1.03 ± 0.1	1.01 ± 0.1	20.92 ± 9.6
b [-]	0.59 ± 0.0	0.60 ± 0.0	0.23 ± 0.1
τ ₀ [Pa]	10.55 ± 0.2	6.83 ± 0.5	6.85 ± 5.1
SSR [Pa ²]	72.19 ± 6.4	11.32 ± 4.7	1256.52 ± 525.5

Table 4.7: The results of the Herchel- Bulkly parameters using the WLS curve fitting method

When fitting the measured data to the Herchel- Bulkly viscosity equation (equation 2.4), the fitted curve produced by this model is presented in (figure 4.13) which presents also a good fit for the three products. Looking at the resulting parameters presented in (table 4.8) it is noted that the standard deviation resulting from this model is higher compared to the Herchel-Bulkly model, which indicates to less reproducibility between the measured three replicates. Another observation is the lack of this model ability to predict the yield stress value of Långfil.

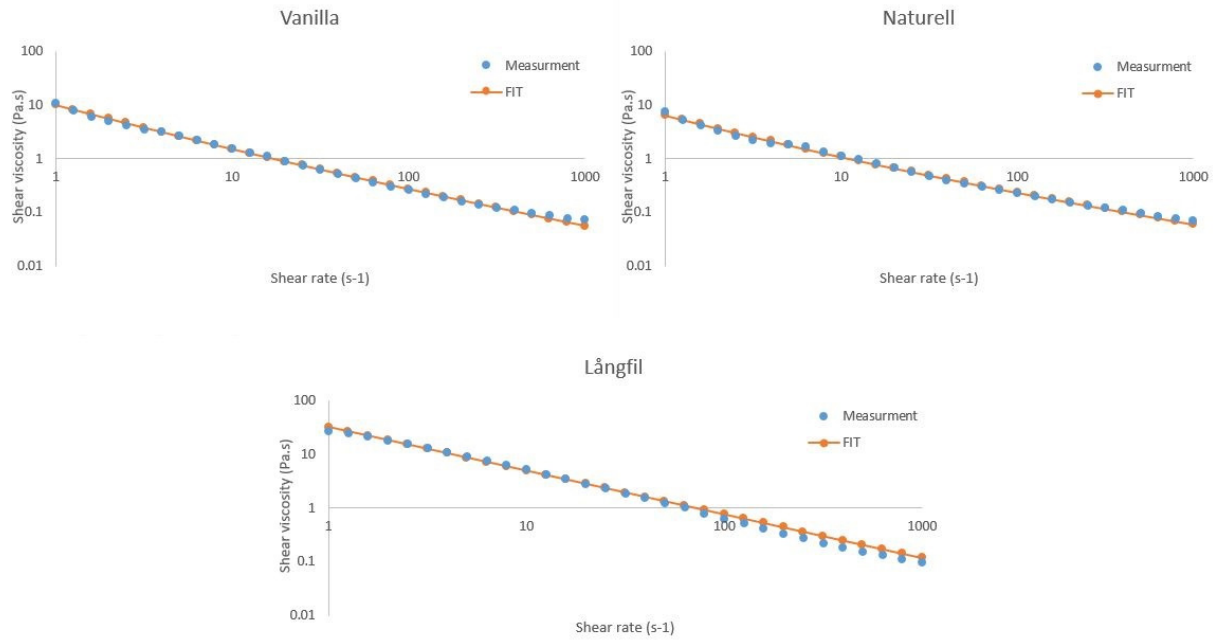


Figure 4.13: The results from the Herschel- Bulkly viscosity equation curve fitting

	Vanilla	Naturell	Långfil
A [Pa·s ⁿ]	4.27 ± 1.9	1.31 ± 0.7	18.87 ± 9.2
b [-]	0.37 ± 0.1	0.57 ± 0.1	0.35 ± 0.1
τ_0 [Pa]	5.77 ± 2.9	6.65 ± 1.8	0.00 ± 0.00
SSR [(Pa. s) ²]	3.06 ± 0.9	2.86 ± 1.0	12.61 ± 14.1

Table 4.8: The results of the Herschel- Bulkly viscosity equation parameters using the WLS curve fitting method

The Herschel–Bulkley model is very suitable for evaluating the shear stress dependence on the shear rate for the three studied products.

The attempt to increase the range of the measurements resulted in acceptable values compared to the values in the previous study (the methodology in the previous study used a range of shear rates between 0.7- 700 s⁻¹). To investigate more into the range used in this study, the upward sweep measurements of one Vanilla replicate was divided into three parts, each part was fitted to the Power law model (figure 4.14), The results of the Power law parameters for each part are shown in (table 4.9).

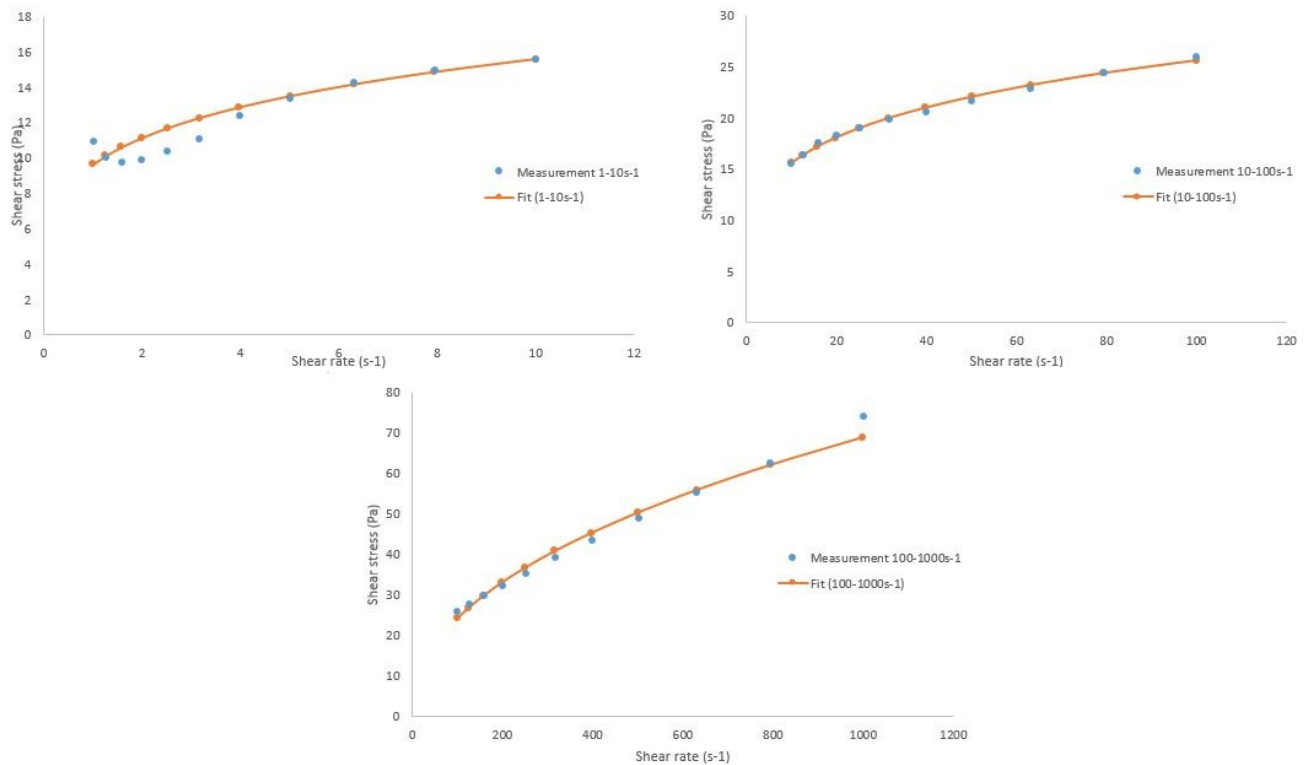


Figure 4.14: The curve fitting of the Power law model to the partitioned upward sweep (Vanilla)

	Range			
	1- 1000 s ⁻¹	1- 10 s ⁻¹	10- 100 s ⁻¹	100- 1000 s ⁻¹
K (Pa.s ⁿ)	8.2	9.6	9.5	3
n (-)	0.3	0.2	0.2	0.5

Table 4.9: Power law parameters for three parts of the shear rate sweep, a decade per part (Vanilla)

By looking at the two first decades, the values of the parameters are nearly the same, but for the third decade, the K value decreases drastically and the n value increase in a more than double its value in the first two decades. The values of these parameters indicate to the sample losing its consistency and an increased flow, and that adheres well to reality since the shear rate is increasing. Therefore, it is recommended to choose the right range, according to the wanted application before performing the measurements, as it has a huge effect on the resulting model. Low ranges would be useful for the sensory characteristics of the product and, mid ranges would be suitable for studying the rheological behavior of the product during flow in processing lines, while high range measurements would be useful when characterising the product at high shear processing conditions, such as filling and processing lines. This approach maybe applicable for other products, and not only the studied yogurt products used in this investigation.

The number of sampling points is also a relative measuring parameter, since increasing the sampling points will increase the degrees of freedom of the regression (curve fitting) analysis, but this benefit comes with a price, the drawback of having a high number of sampling points will increase the time

required for performing the measurements. The time required to perform a single hysteresis loop using the protocol developed in this study was 40 min, 50 min and 90 min for Vanilla, Naturell and Långfil respectively.

This study provides two recommendations based on the above findings; the first one is to measure at a large range of shear rate, and then fit the model to the segment of the flow curve that is relevant to the wanted application. The second suggestion is to measure using the range that is relevant to the wanted application and performing the curve fitting to this chosen range only.

4.3. Batch variation

During performing the tests. It was noted that there was a batch variation in viscosities in some samples from different production dates. The results from the batches variation measurements are presented in this section. (Figure 4.15) represents the difference in hysteresis loops for several batches for each product. A quick look at the figure leads to the conclusion of the Vanilla having the most deviation between the different batches, where the thixotropic effect varies from batch to batch judging on the difference between the initial and the last shear stress values of the loops. To get a mathematical proof of that and to quantify these differences, the upward sweep of each loop was curve fitted to the Power Law model using the OLS regression method and the results are presented in (table 4.10).

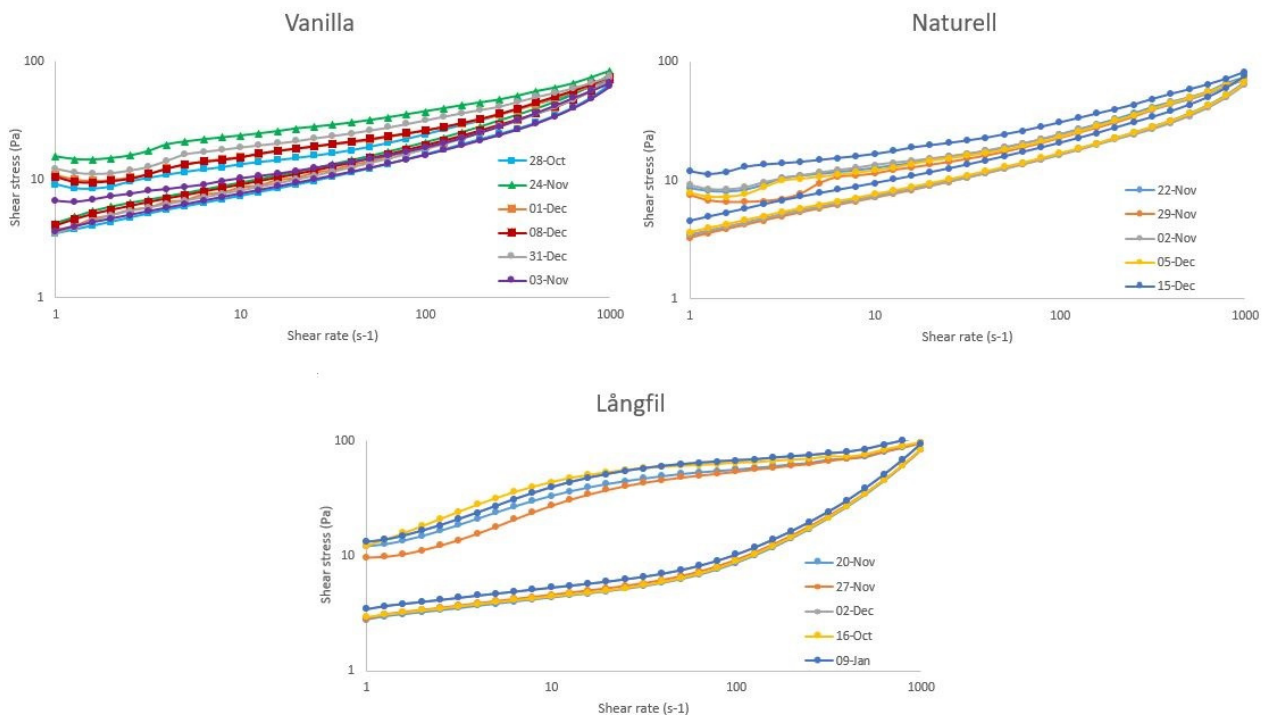


Figure 4.15: the results of the Hysteresis loop tests performed on several batches for each product (the products are marked by their best before date)

Vanilla		31-Dec	01-Dec	08-Dec	22-Dec	24-Nov	03-Nov	Standard Deviation	COV (%)
	K (Pa.s ⁿ)	8.66	8.16	6.08	4.87	11.50	2.80	3.1	48
	n (-)	0.31	0.28	0.35	0.38	0.27	0.44	0.1	22
Naturell		15-Dec	05-Dec	22-Nov	29-Nov	02-Nov	-	Standard Deviation	COV (%)
	K (Pa.s ⁿ)	6.47	3.81	4.30	3.63	4.52	-	1.1	28.5
	n (-)	0.35	0.41	0.40	0.42	0.38	-	0	8.4
Långfil		20-Nov	27-Nov	16-Oct	02-Dec	09-Jan	-	Standard Deviation	COV (%)
	K (Pa.s ⁿ)	18.19	16.51	17.23	25.68	13.84	-	4.4	27.8
	n (-)	0.24	0.26	0.25	0.20	0.27	-	0	13

Table 4.10: The Power law parameters for the different batches of the three products

Looking at (table 4.8), there is a clear variation between the batches. Even though, great care was taken when performing the measurements to ensure measuring the products within the first two weeks of their production date, and using a freshly opened pack when measuring, and following the handling and loading of the samples, the variation between the samples could not be avoided. Vanilla has shown the greatest variation, while Naturell was the most resistant to batch variation. The possible explanation for the variation is the possible different in activity between the bacterial cultures used for fermenting the yogurt products. Even though it was expected to have the highest variation for the Långfil, the results showed that Vanilla was the most subjected product to batch variation.

4.4. Measuring using different geometries

The hysteresis loops resulting from using the different chosen geometries are presented in (figure 4.16). The different level of bending in the curves suggests that there is a presence of the effect of wall slip when using smooth surface geometries, but these results cannot tell the whole story since they were done using different batches for most of the geometries (table 3.2 in § 3.5), so the disagreement between the curves can also be explained by batch variations. A closer look on the graphs reveals that the Serrated Cup and Bob Geometry caused the least bends in the flow curves, which can confirm that it reduces the wall slip effect resulting in a more linear curve compared to the other geometries.

From the (table 4.11) it becomes more obvious that the geometry used can hugely affect the Power Law parameters, which in return can affect the characterization process of the rheological behavior. But still this effect is subjected to batch variations when performing these tests.

	Serrated Cup and Bob	Smooth Cup and Bob	Serrated Cup and Smooth Bob	Sand Blasted Cup and Bob
--	----------------------	--------------------	-----------------------------	--------------------------

	K (Pa. s ⁿ)	n	K (Pa. s ⁿ)	n	K (Pa. s ⁿ)	n	K (Pa. s ⁿ)	n
Vanilla	8.16 ± 0.30	0.28 ± 0.00	6.24 ± 0.22	0.35 ± 0.00	5.76 ± 0.34	0.36 ± 0.01	7.03	0.31
Naturell	3.73 ± 0.22	0.41 ± 0.01	5.59 ± 0.15	0.37 ± 0.00	4.86 ± 0.02	0.38 ± 0.00	4.24	0.35
Långfil	25.28 ± 6.54	0.20 ± 0.04	14.32 ± 0.40	0.28 ± 0.00	12.38 ± 0.27	0.29 ± 0.00	12.51	0.26

Table 4.11: The Power law parameters resulting from measurements using different geometries

It is difficult to handle the batch variation as they interfere in the results of this test. Therefore, the values of K and n cannot be depended on very much, and by observing the graphs in (figure 4.16) it is clear that each product exhibit a pattern of behavior during measuring, but the magnitude of this pattern varies depending on the geometry use.

Care must be taken when choosing the right geometry, and it is recommended to perform the measurements with more than one geometry and to repeat these measurements with more than one batch in order to capture the COV% and the standard deviation between these methods and batches.

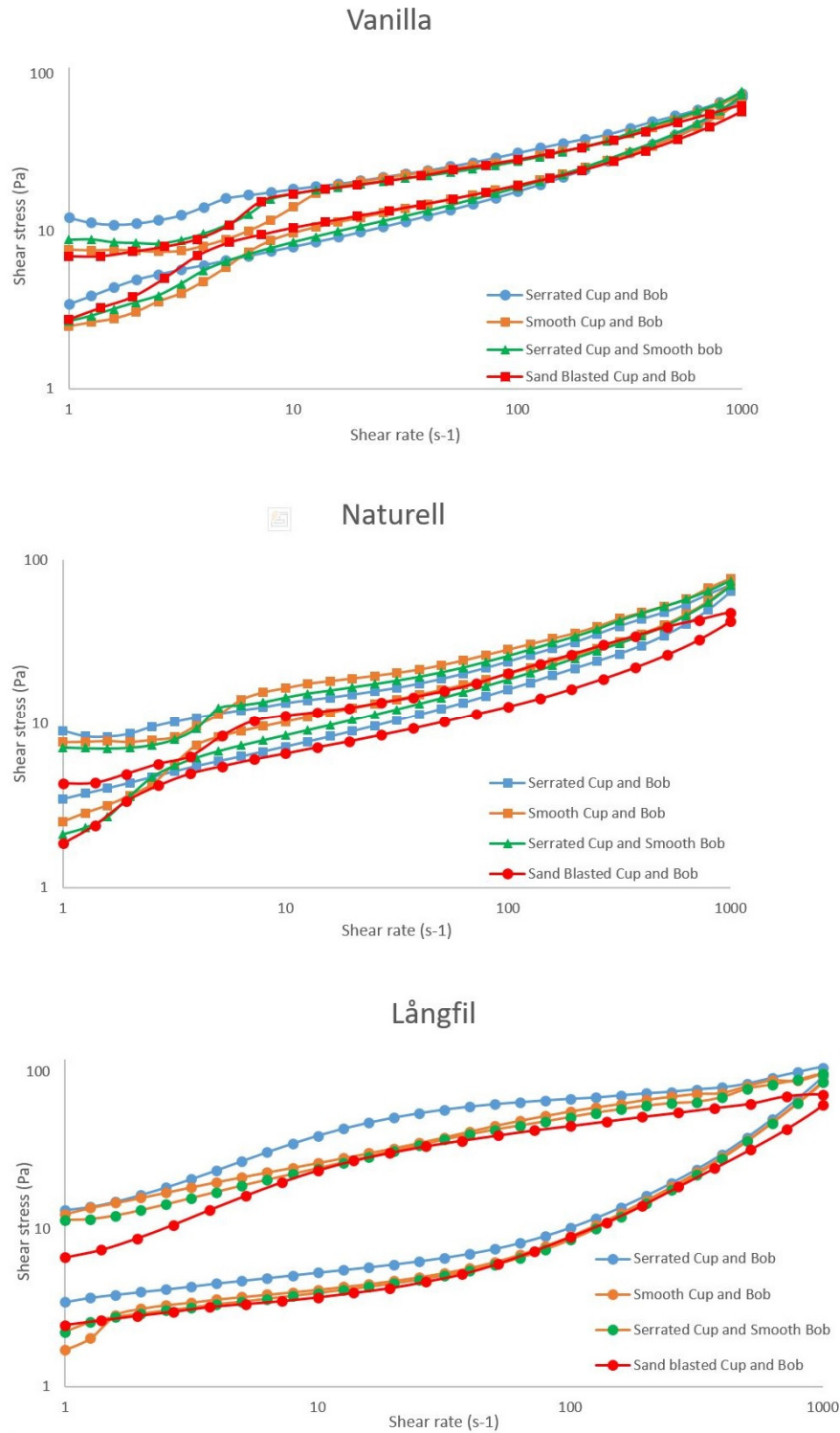


Figure 4.16: The Hysteresis loop measurements using different geometries for the three products

In an attempt to overcome the batch variation when investigating the effect of the used geometry, the measurements done using the same batch were compared. These measurements were done using the

smooth cup and bob, and the serrated cup and smooth bob (results in table 4.11 and the orange and green curve respectively). Comparing only these results there is still a slightly different in the resulting parameters and the flow curves. This suggests that the geometry used, and the batch variation can affect the acquired results. Therefore, it is recommended to perform the measurements using different batches using several geometries for each batch, this will help understand the effect of these factors on the results.

4.5. Yield stress

The results of both the methods used for the determination of the static yield stress are presented in (table 4.12). The results of using the two different methods indicates to a good level of agreements were both the methods resulted is very similar values.

	Vanilla	Naturell	Långfil
τ_0 (Pa) Tangent method	7.3 ± 0.9	7.5 ± 0.2	5.9 ± 0.1
τ_0 (Pa) Bayod method	7.9 ± 0.0	7.4 ± 0.5	6.1 ± 0.4
τ_0 (Pa) Herchel- Bulkly	10.56 ± 0.2	6.8 ± 0.5	6.9 ± 5.1

Table 4.12: The static yield stress results from the tangent and the bayod methods

The estimated yield stress using the tangent and the bayod method is called the static yield stress, while the yield stress calculated from the Herchel- Bulkly curve fitting is the dynamic yield stress. The literature suggests that the dynamic yield stress should be lower than the static yield stress⁴⁴, this is true only in the case of Naturell, while it doesn't agree with the results of the Vanilla and Långfil. The reason behind this can be due to batch variation again.

Therefore, the recommendation for the yield stress measurement is that it should be done using different methods with different batches and different geometries, performed on the same batch.

4.6. Zero shear viscosity

The concept of zero shear viscosity is illustrated in (section § 2.1.5). Performing the shear stress ramps using different ramp times resulted in different viscosity plateau values (figure 4.17).

The results of the viscosity plateaus for the measured shear stress ramps are presented in (table 4.13). The value of η_0 is very dependent on the ramping time and therefore it is difficult to decide if these results are reasonable or related to the real value if there is such a value, or it is just not possible to measure η_0 with the available equipment. However, this parameter is required for the CFD simulations and an estimation is better than having nothing.

⁴⁴ Parmar, Kps & Méheust, Yves & Fossum, Jon. (2006). Electrorheological suspensions of laponite in oil: rheometry studies under steady shear.

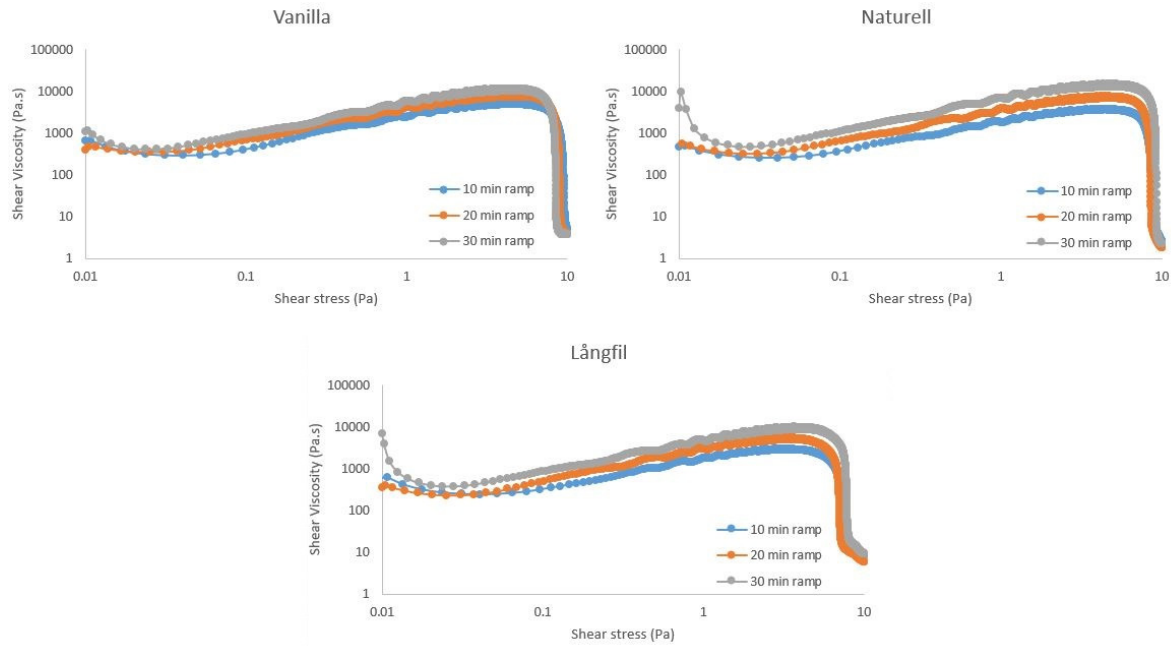


Figure 4.17: The results of shear stress ramps using different ramp times to determine η_0

The trend observed in the three different ramps, Vanilla and Naturell resulted in a relatively similar η_0 values while Långfil resulted in the lowest value (which is not consistent with a previous study that found Långfil to have the highest value). The values chosen to be used in further application is the values resulted from the 30 min ramp.

	10 min ramp	20 min ramp	30 min ramp
η_0 (Pa) Vanilla	4618 ± 523	7692 ± 834	11867 ± 1115
η_0 (Pa) Naturell	3622 ± 44	7026 ± 688	11463 ± 931
η_0 (Pa) Långfil	2926 ± 60	5103 ± 199	8543 ± 372

Table 4.13: The results of shear stress ramps for the determination of η_0

From the results it can be seen that there is a level of inconsistency between the different ramp time used for testing, this can be a sign of the yogurt products having a yield stress, and not having a zero shear viscosity, or it can't be measured with the available equipment.

To expand the search for the connection between η_0 and τ_0 , the Tangent method was used to estimate the yield stress for the η_0 measurements, and the results are illustrated in (table 4.14)

	10 min ramp time	20 min ramp time	30 min ramp time	COV%
τ_0 (Pa) Vanilla	5.8	8.2	6.7	18
τ_0 (Pa) Naturell	8.2	8.1	6.7	11
τ_0 (Pa) Långfil	6.0	9.0	7.5	20

Table 4.14: The results of the static yield stress using the Tangent method when applied to the η_0 measurements

The results are also inconsistent, even though the measurements were done using the same batch, this confirms the assumption of the possibility that the used measurement instruments are not able to capture it, or that the products do not possess a zero shear viscosity.

4.7. Infinite shear viscosity

The measurements using the capillary rheometer faced difficulties due to the formation of bubbles which made it difficult to achieve an equilibrium state. In addition to that, the pressures recorded are below the sensitivity of the transducer and the yogurt samples appeared to get stuck in the 0.5 mm die. The raw data were plotted in (figure 4.18). As seen in the graphs, it is clear that a steady state was difficult to achieve due to the reasons mentioned earlier. The sampling points were chosen manually by monitoring the pressure drop and taking the sample points if the pressure drop read is constant for more than 10 seconds.

For each shear rate value, the most repeatable pressure drop value was chosen to continue the analysis. Afterwards, the viscosity values were calculated for each shear rate value, and then these values were plotted against their corresponding shear rate (figure 4.19)

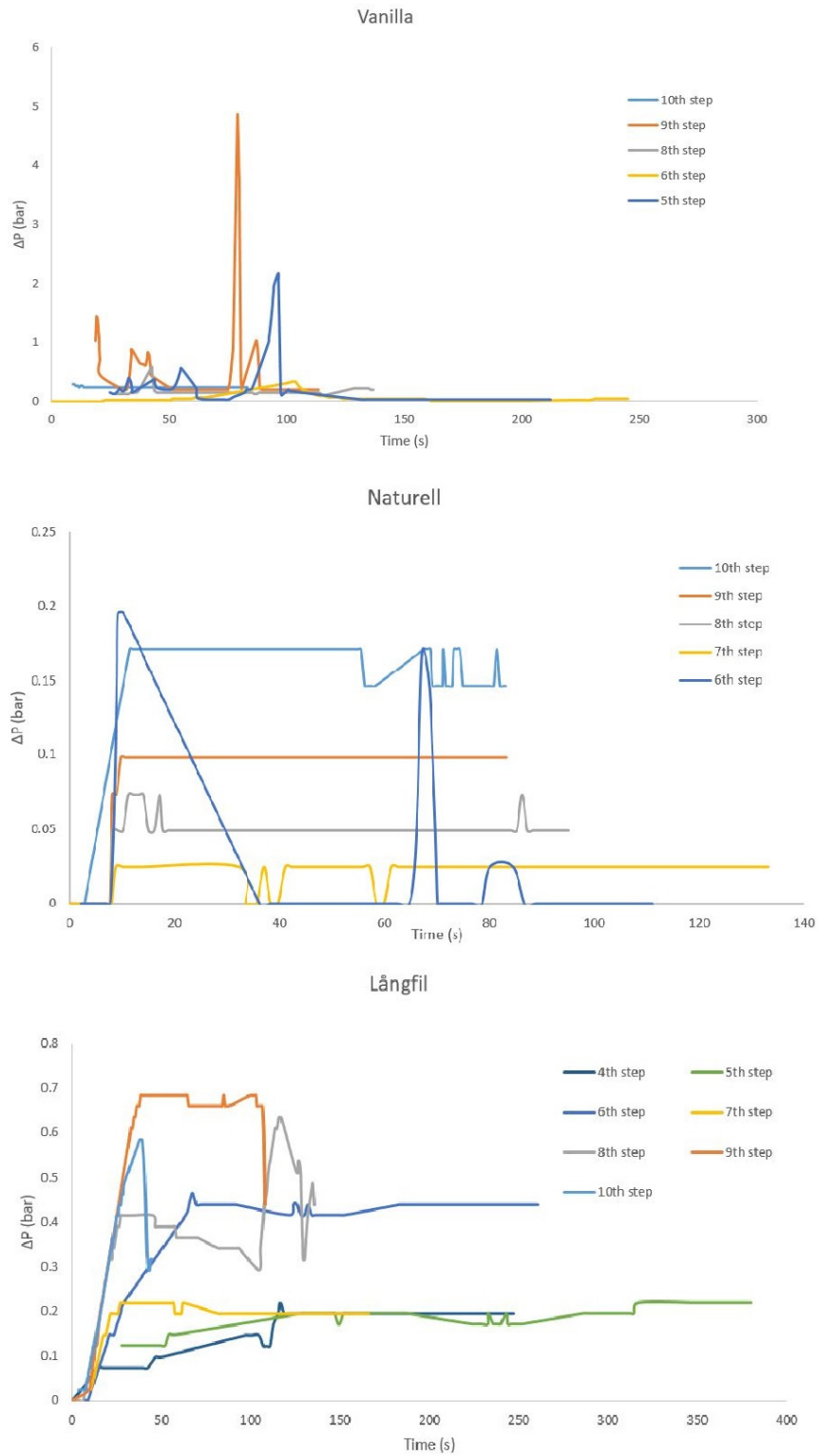


Figure 4.18: The pressure drop raw data for the capillary rheometer measurements

The viscosity flow curves (figure 4.19) appears to be unpredictable were the viscosity values do not follow the typical behavior of yogurt, especially for the case of Långfil.

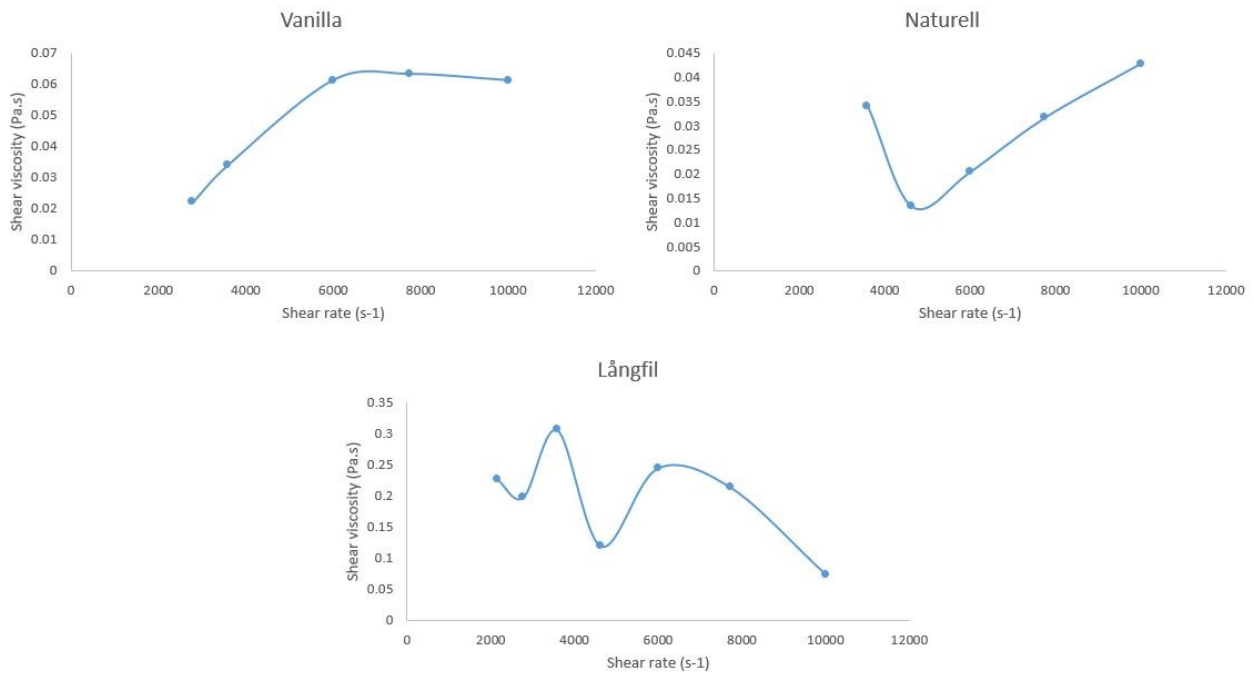


Figure 4.19: The viscosity flow curves resulting from performing the measurements for each shear rate separately using a high- pressure capillary rheometer.

The results of these measurements are not reliable and there is no guarantee that they are relevant to reality, but still, having an acceptable value is better than nothing for the CFD simulations. Therefore, the lowest viscosity value resulting from the analysis will be adapted as the infinite shear viscosity and these values are combined in (table 4.15).

	η_{∞} [Pa. s]
Vanilla	0.022
Naturell	0.013
Långfil	0.073

Table 4.15: The resulting η_0 from the Capillary rheometer measurements

To compare the Capillary rheometer measurements with the rotational rheometer measurements, both data were plotted in the same flow curve (figure 4.20). From the graphs it is noted that the measurements were done at a much higher shear rates than the intended range to be used, (10,000-100,000 s⁻¹) instead of (10,000- 100,000s⁻¹), this reduces the reliability of the results.

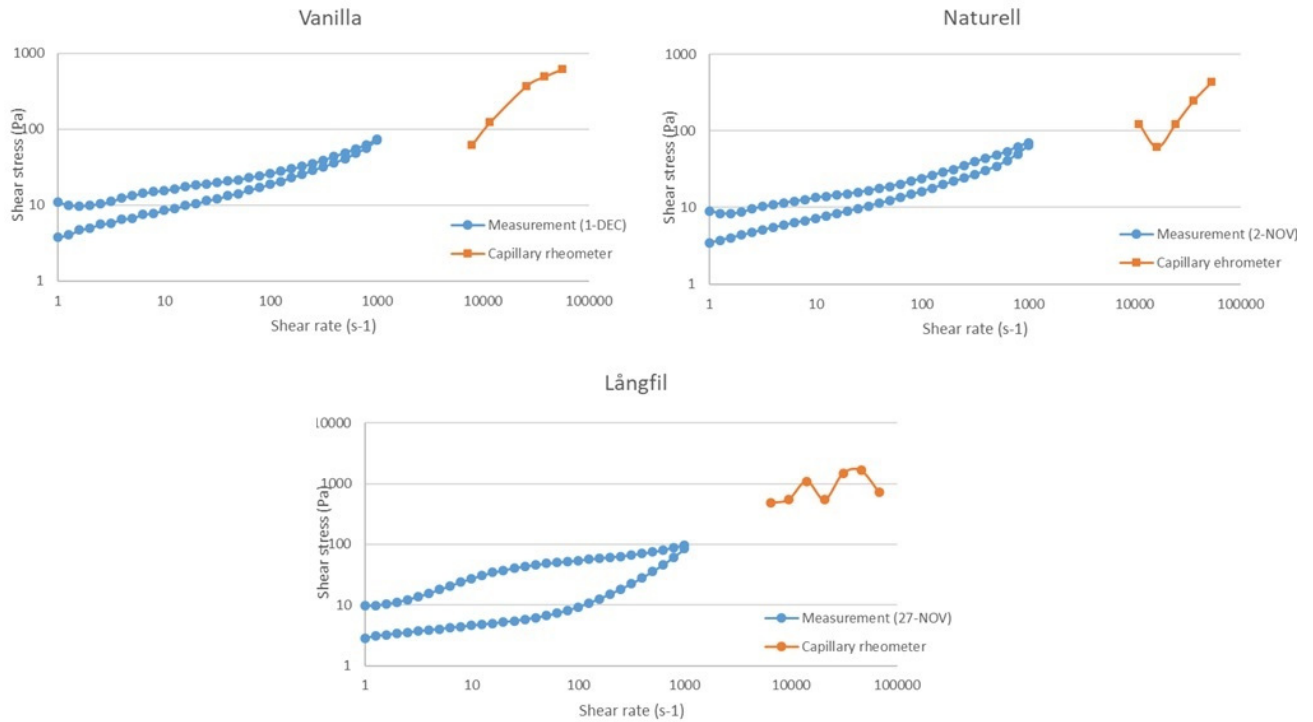


Table 4.20: Co-plot of the rotational rheometer and the capillary rheometer data

The Power law model was fitted to the acquired flow curves, and the Power law parameters are shown in (table 4.14). The results for the Vanilla and Naturell are rational to a certain extent where the n value indicates to an extensive flow which can describe the flow situation during the capillary rheometer measurements. To compare the results of the capillary rheometer with the rotational rheometer results, a coplot is shown in (figure 4.21) where the Power law predicted model using the rotational rheometer is coplotted to the capillary rheometer measurements. The results from the co-plotting is somewhat unrealistic and difficult to interrupt any conclusions from.

	Vanilla	Naturell	Långfil
$K \text{ (Pa} \cdot \text{s}^n)$	0.03	0.00	83.49
$n \text{ (-)}$	0.90	1.22	0.25

Table 4.16: The results of the Power law curve fitting to the capillary rheometer results

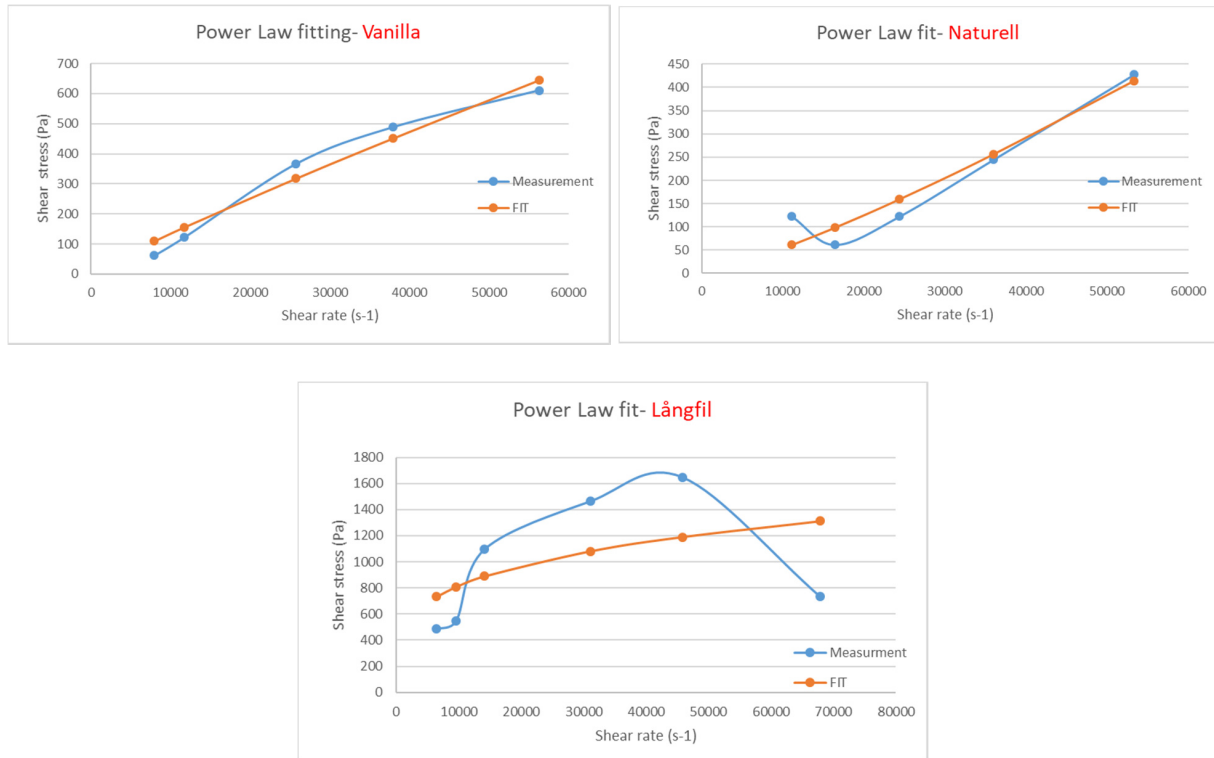


Figure 4.21: Coplot of the measured yogurt products using the capillary rheometer (blue) and the predicted model using the power law model and the rotational rheometer (orange)

4.8. Cross model

One of the benefits of having η_0 and η_∞ values, is that they set limits for the viscosity values for the Power Law model, otherwise the viscosity will trend to infinity. Even though, the values found in this study can be more or less unreliable, but still an approximate value can be useful in some situations. The cross model with the approximate limitations is presented in (figure 4.22).

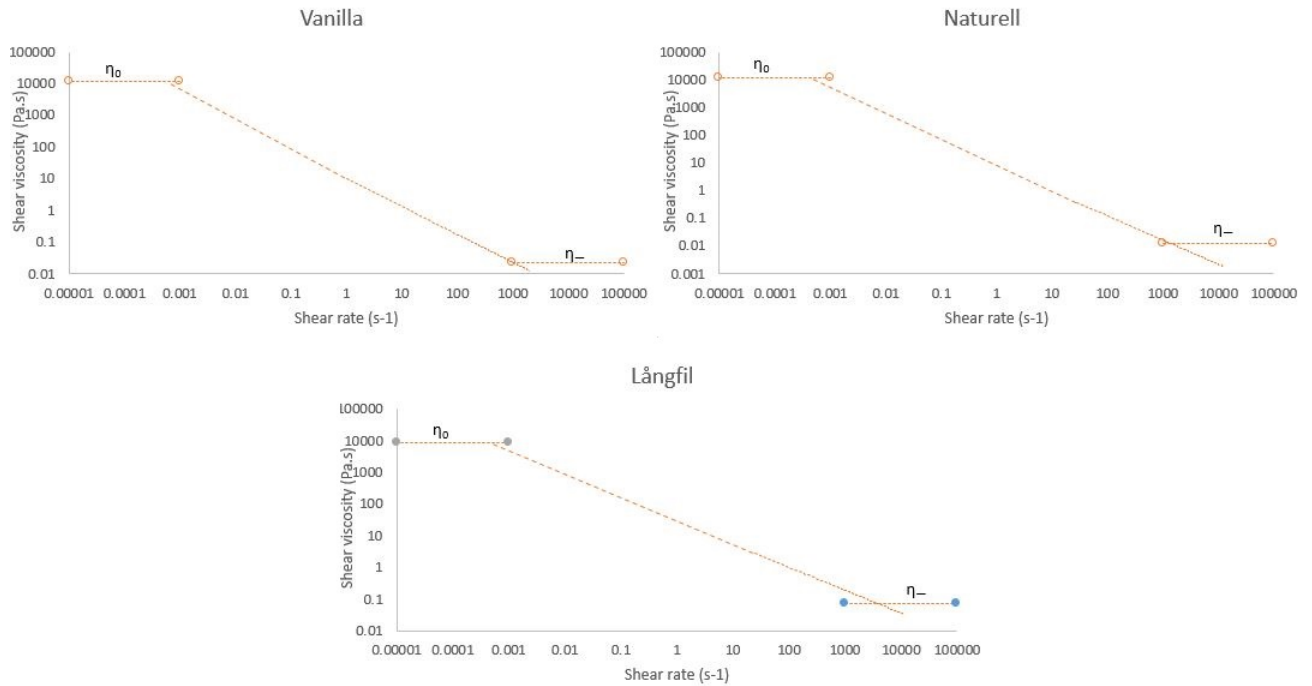


Figure 4.22: Inserting η_0 and η_∞ values into the Power law model results

Cross model can be written as the following:

$$\text{Vanilla: } \eta = 0.22 + \frac{(11867 - 0.22)}{1 + (8.16\dot{\gamma})^{-0.28}}$$

$$\text{Naturell: } \eta = 0.13 + \frac{(11463 - 0.13)}{1 + (3.73\dot{\gamma})^{-0.41}}$$

$$\text{Långfil: } \eta = 0.73 + \frac{(8543 - 0.73)}{1 + (25.28\dot{\gamma})^{-0.2}}$$

4.9. Thixotropy

Hysteresis loop tests for the three products were performed for the rheological modelling, but the results are also relevant to the thixotropy investigation of these products. As seen in (figure 4.9), it is clear that the products are thixotropic since they did not regain a lot of their structure after sweeping up and down. A complete structure rebuild might be achieved after removing the shear forces with longer resting time that can be up to several hours. It is also clear that Långfil had the most decrease in shear stress during the downward sweep, which is combined with the loss of its structure after testing. Vanilla on the other hand showed a slightly higher resistance to shear, which makes sense as it is the only product among the three tested products that contain added stabilizers. The thixotropic effect was evaluated based on the difference between the initial and the final shear stress value (1 s^{-1}) (table 4.17).

	Difference %
Vanilla	47 ± 1
Naturell	61 ± 1
Långfil	77 ± 1

Table 4.17: the difference between the initial and the final shear stress values resulting from a Hysteresis loop test

The hysteresis loops of the three products proves the thixotropic effect because the shear stress is lagging behind the shear rate. The shape of the hysteresis loops can vary strongly between the three samples, which indicates that there is a difference in the thixotropic effect of these products. It is possible that the conditions prior to shear during loading, might interfere with the hysteresis results. The small standard deviation between the replicates exclude any major interference from sample handling on the results (table 4.15). A remaining question, is whether the damage to the structure during the hysteresis loops is irreversible, because of the high shear value applied to the samples at the top of the loop, this would have been investigated by leaving the sample for a 24 hours rest and remeasuring again. The bend in the curve after the beginning of the upward sweep can be explained by the breakdown of the initial structure after starting up starting to dominate the time evolution of the stress, resulting in a stress overshoot⁴⁵.

4.9.1. Break down test

The results from the Break- down tests are presented in (figure 4.23). As expected, when applying a constant shear on the yogurt samples, the viscosity will keep decreasing with time. The amount of shear applied will also affect the initial viscosity of the sample which is also associated with fluids with shear thinning behaviors as these fluids' viscosity decreases with shear rate.

The two key findings during the break down tests were the following:

- 1- It was obvious from (figure 4.23) that the applied shear did not result in a viscosity plateau, and the viscosity kept decreasing as long as the constant shear is still applied and regardless of which product it is.
- 2- For investigating the concept of the stabilizing time (described in §2.1.1) the results are found in (table 4.18). It appeared that with different constant shear values, the stabilizing time was different. Which indicates that the amount of shear rate applied on the sample play a role in determining the time needed for the viscosity to become close to a plateau situation

⁴⁵ Jan. Mewis Norman, J.Wagner, (2009), Thixotropy, Advances in Colloid and Interface Science, Volumes 147–148, 214-227, DOI: 10.1016/j.cis.2008.09.005

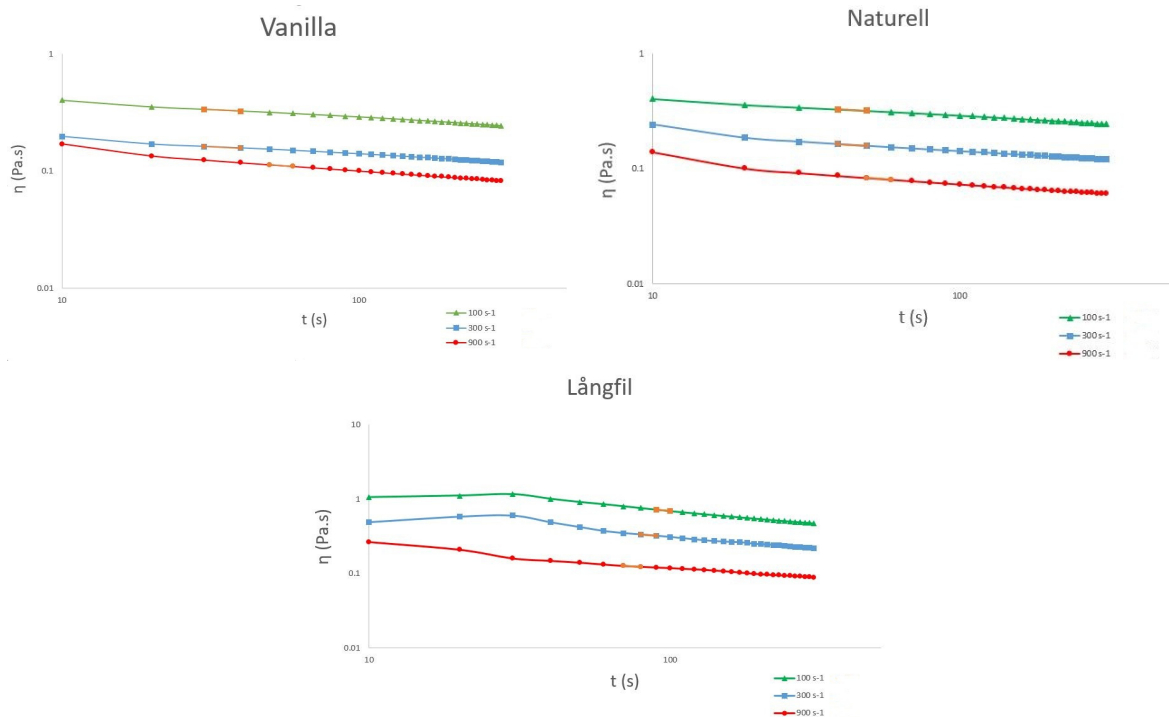


Figure 4.23: The results from the Break- down test for the three products, using constant shear rate at 100s^{-1} , 300s^{-1} and 900s^{-1}

	100 s^{-1}	300 s^{-1}	900 s^{-1}
Vanilla	30 sec	30 sec	40 sec
Naturell	40 sec	40 sec	50 sec
Långfil	90 sec	80 sec	70 sec

Table 4.18: The stabilizing time results using different shear rate values for the measurements

It is noted that the viscosity increases slightly for a short period of time for the Långfil at 100 s^{-1} and 300 s^{-1} constant shear rates, because the sample is suddenly subjected to a constant shear rate after it has been at rest. Applying the constant shear rate resulted in an overshoot stress (except for långfil at 900s^{-1}) followed by a gradual structure decay, but the steady state was not achieved (constant viscosity with continuous shearing).

For the Vanilla and Naturell, the viscosity starts decreasing as soon as the shear is applied but the viscosity plateau is also not achieved. The time effect of the samples is affecting the viscosity reads depending at the time when the data point is sampled, and the more the sample is sheared the less the viscosity value read will be. This is a dilemma for the rheological measurements since it requires to record the viscosity (shear stress) at a steady state (viscosity plateau). Tetra Pak protocol introduces the concept of stabilizing time (§ 3.1), which helps to improve the measuring results compared to the measurements done without taking into account the sample going into a steady state during sampling.

It is worth mentioning that plotting (fig 4.24) on a linear axis will make it difficult to read the results as the magnitude of the viscosity decrease will be less obvious (fig 4.18), therefore it is recommended to plot the data on a logarithmic scale axis for a proper evaluation.

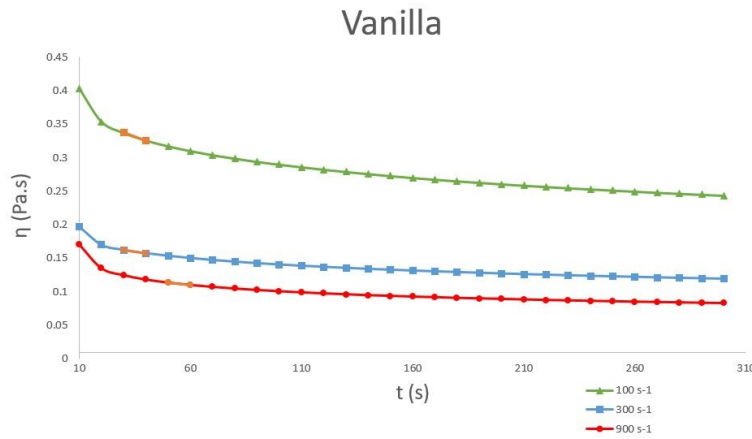


Fig 4.24: The results from the Break- down test for the three products (Linear scale), using constant shear rate at $100s^{-1}$, $300s^{-1}$ and $900 s^{-1}$

4.9.2. Build up test

The results from the Build- up tests are plotted in (figure 4.25, 4.26 and 4.27). from the graphs. Note that the first 3-5 sampling points in the ($dt=0$) curve must be ignored, since the raw data showed that the rheometer needs a few seconds to adjust its speed from $100s^{-1}$ or $300s^{-1}$ to $1s^{-1}$ which makes these points not meaningful for the measurements done.

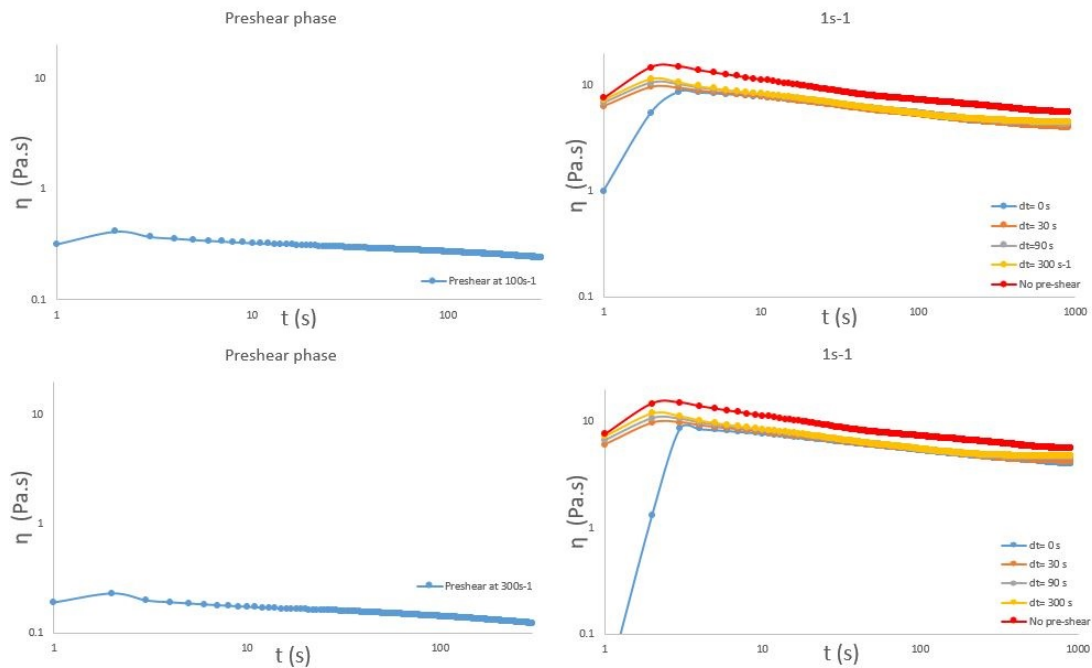


Figure 4.25: The results from the Build- up tests performed on Vanilla

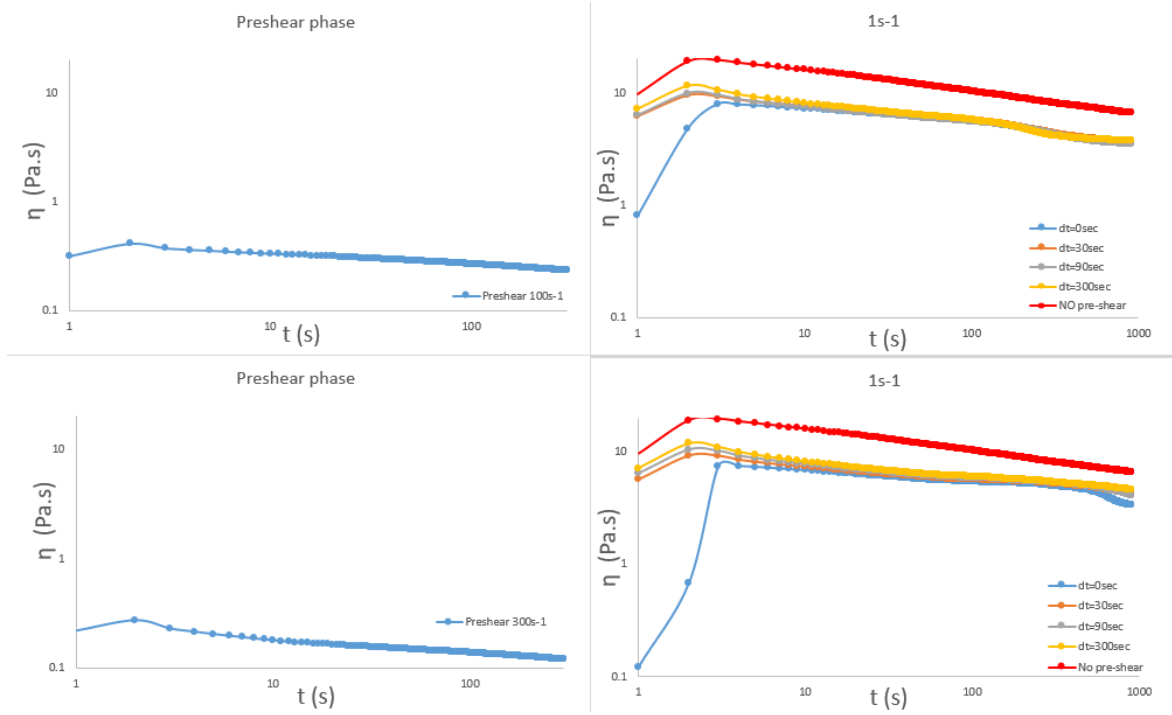


Figure 4.26: The results from the Build-up tests performed on Naturell

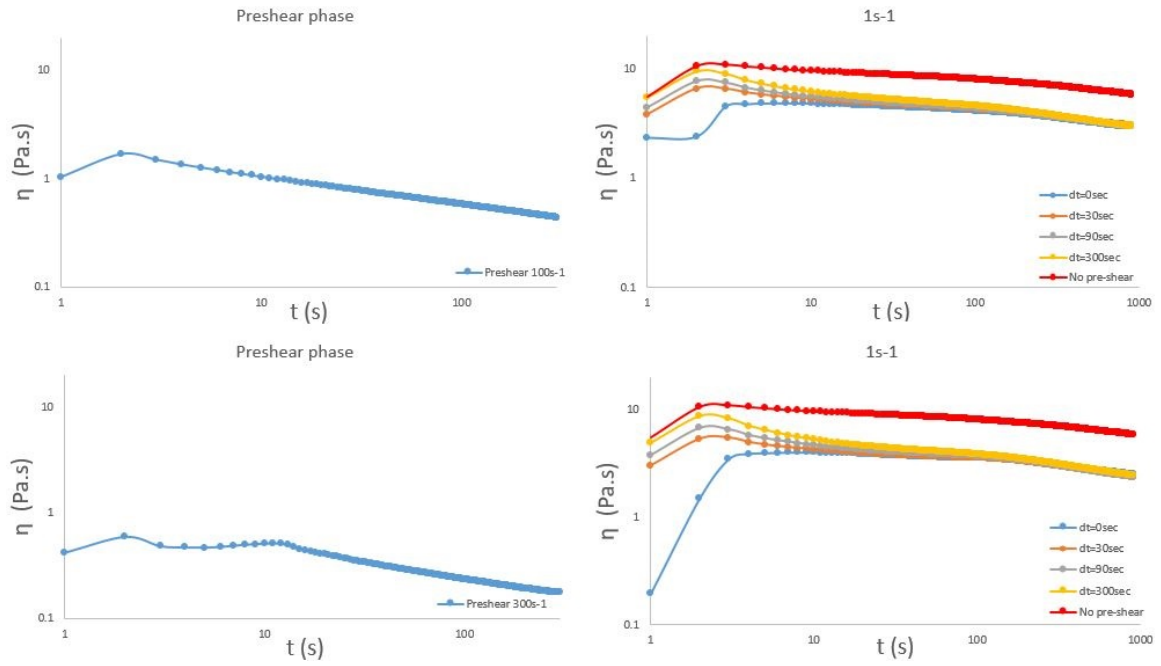


Figure 4.27: The results from the Build-up tests performed on Långfil

By shearing the sample at a high shear rate (100 s^{-1} and 300 s^{-1}) the viscosity keeps decaying without achieving a steady state, and when suddenly stepping down the shear rate, the viscosity increases depending on the resting time provided for the sample, where the longer the time given for the sample to rest, the more it was able to rebuild itself. This reflects the changes in microstructure under well-defined flow conditions between shearing and rest and. Compared to the samples measured with no pre-shear, the highest amount of Build- up were the samples that were left resting for the longest period of time (300 s), as these samples flow curves were the closest to the viscosity of the samples with no pre-shear. this proves the previous findings that the structural build-up of yogurt is very dependent on the time effect, as long as there is no permanent structural destruction of the samples. In addition to that, the growth of the viscosity that occurs immediately after the sudden decrease in shear rate provides a dominating indication of thixotropy.

In order to qualitatively investigate the viscoelasticity of the yogurt samples, it seems useful to plot the recorded shear stress during the build-up test with $\Delta t=0$, where the shear rate value drops from 300 s^{-1} to 1 s^{-1} with no resting time, (figure 4.28) represents the plot of the shear stress values against time.

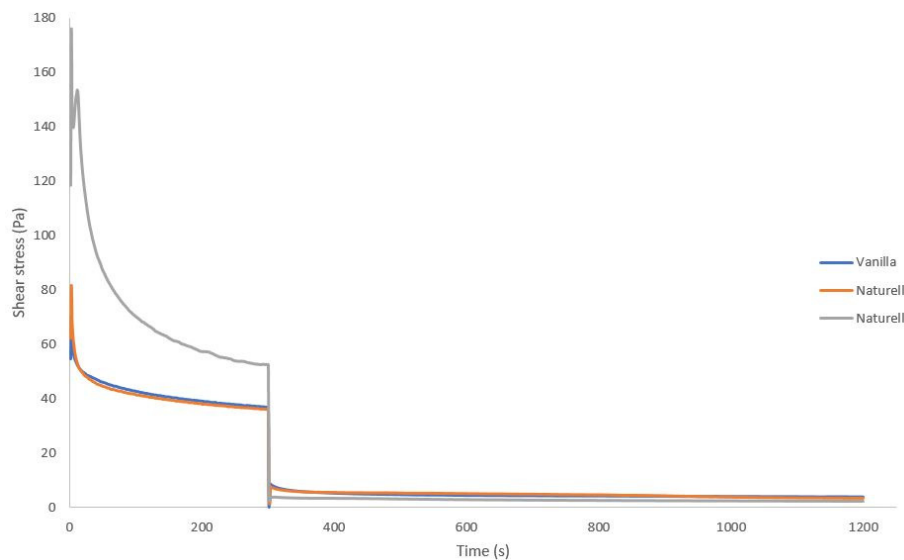


Figure 4.28: The shear stress response during a stepdown in shear rate from 300 s^{-1} to 1 s^{-1} with no resting time

As it appears from the graph, the shear stress decreases immediately to a new plateau value which indicates to the microstructure regaining its structure to a new steady state, which means that the three types of yogurt have thixotropic and viscoelastic properties.

4.9.3. Varied shear rate steps test

This test was performed to provide an overview of the Break- down and Build- up of the three products when applying varied shear rate values. The results are presented in (figure 4.29) and it shows a slight Break- down in all the products when comparing the first and the final upward steps (both are at 300 s^{-1}), where the shear stress value at the final step is slightly lower than the first step. It is also noted that the shear stress at the first upward step goes into a phase of general decline, while in the last

upward step it is relatively constant. The downward steps at (0.01 s^{-1} and 0.1 s^{-1}) can reveal the occurrence of a microstructural Build- up in the case of going down to these steps from a shear rate value $\geq 100 \text{ s}^{-1}$.

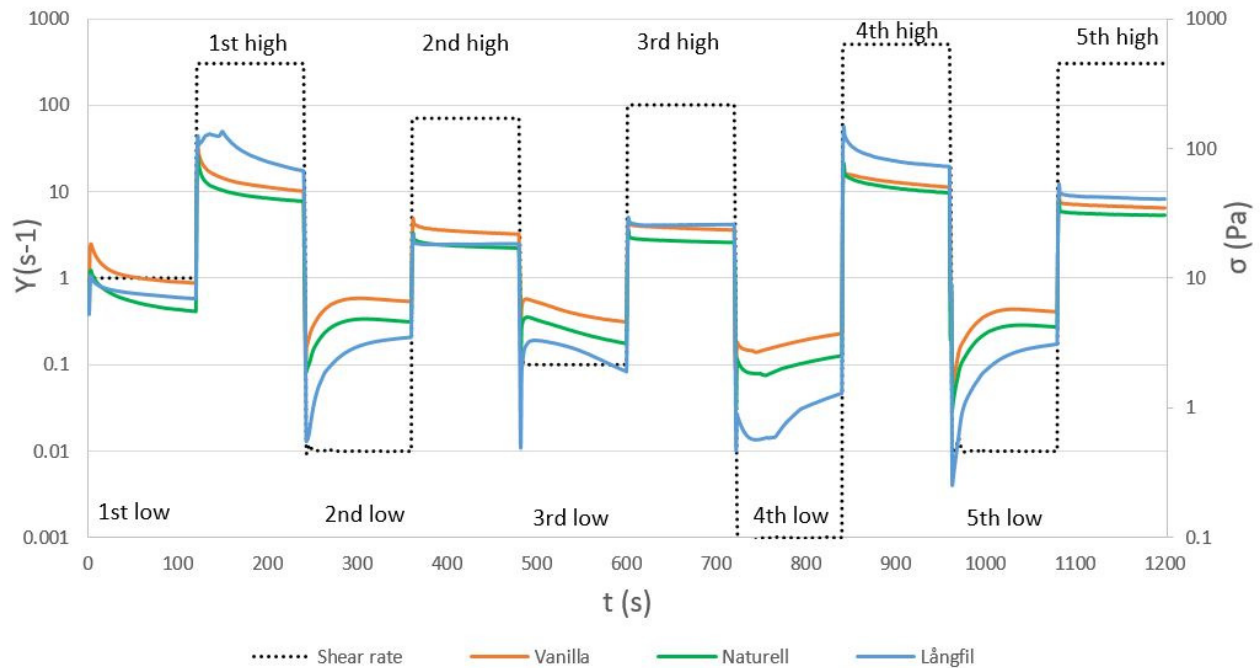


Figure 4.29: The results of the varied shear rate step test for the three yogurt products (shear stress)

The structural break down and build up becomes more visible when plotting the curve with the viscosity measurements instead of the shear stress (figure 4.30). it is worth noting the difference between the first and last high steps, the time effect has almost disappeared during the last high step, and this is due to the pre- shearing that was applied during the previous high steps; This is an indication of the possibility to eliminate the time effect, which might be a good way to improve the rheological measurements.

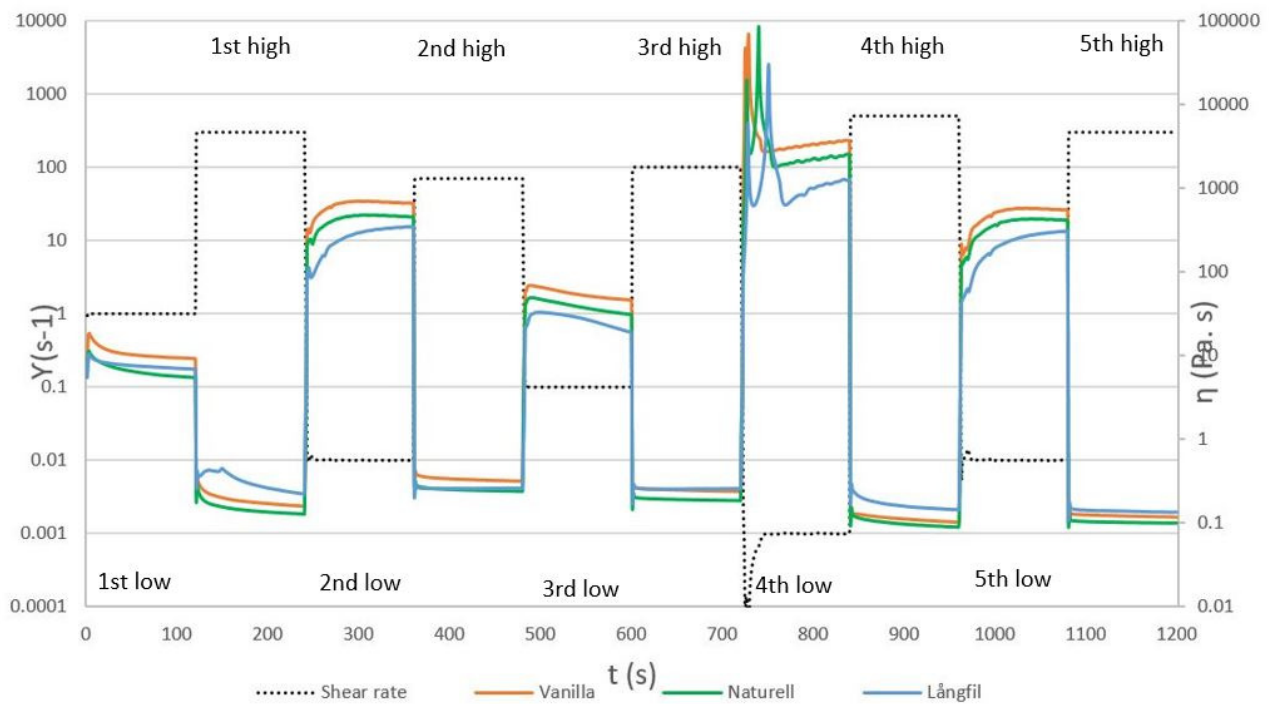


Figure 4.30: The results of the varied shear rate step test for the three yogurt products (viscosity)

4.9.4. Investigating the effect of pre- shearing

The investigation of the pre- shearing role in eliminating the time effect included two methods of pre-shearing, these methods are using a constant shear rate right before the measurement, and the second one includes a multiple hysteresis loops measurement.

4.9.4.1. Pre- shearing using constant shear rate

As concluded earlier, thixotropy plays a role in measuring the right viscosity values, therefore, pre-shearing techniques were used to eliminate the time effect and improve the results of the measurements, and to measure the right properties of the sample.

The hysteresis loops measurements that were done immediately after applying a constant shear with varied speeds, for varied periods of time on the three products is represented in (figure 4.31, 4.32 and 4.33). The three types of yogurt have proven to be time dependant, and this is apparent by the different flow curves of the pre-sheared samples and the samples that were measured without pre-shear, it is also observed that the degree of hysteresis decreases with the increasing pre-shearing speed and duration.

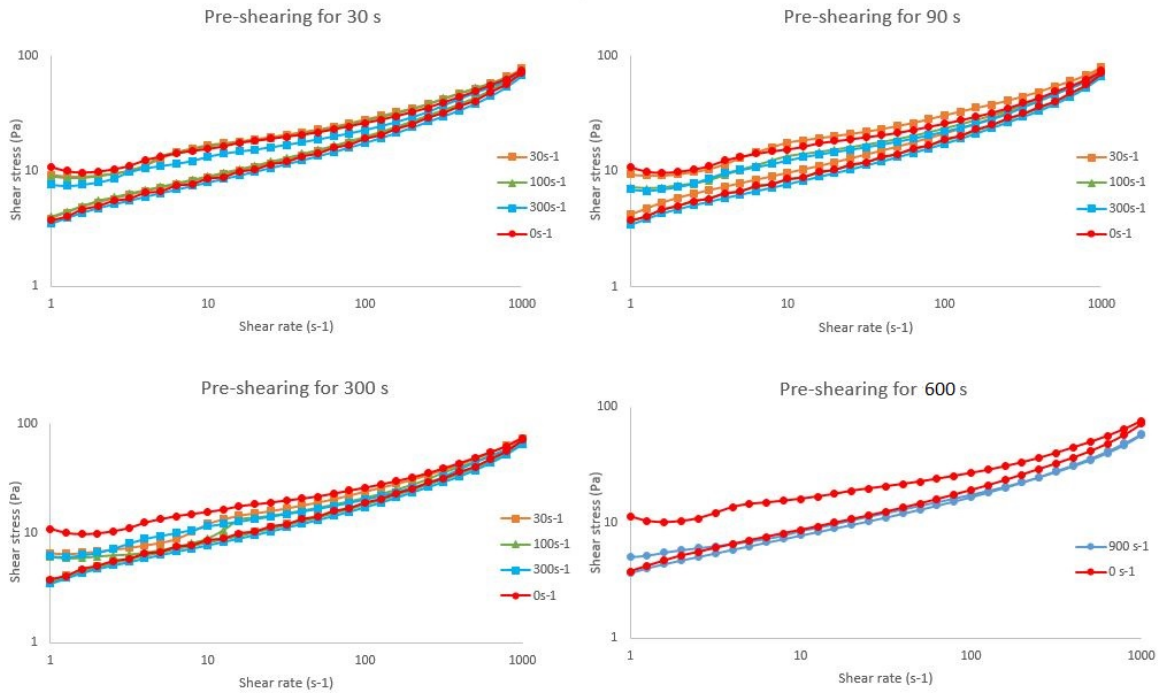


Figure 4.31: The hysteresis loops resulting from different pre-shearing speeds and times (Vanilla)

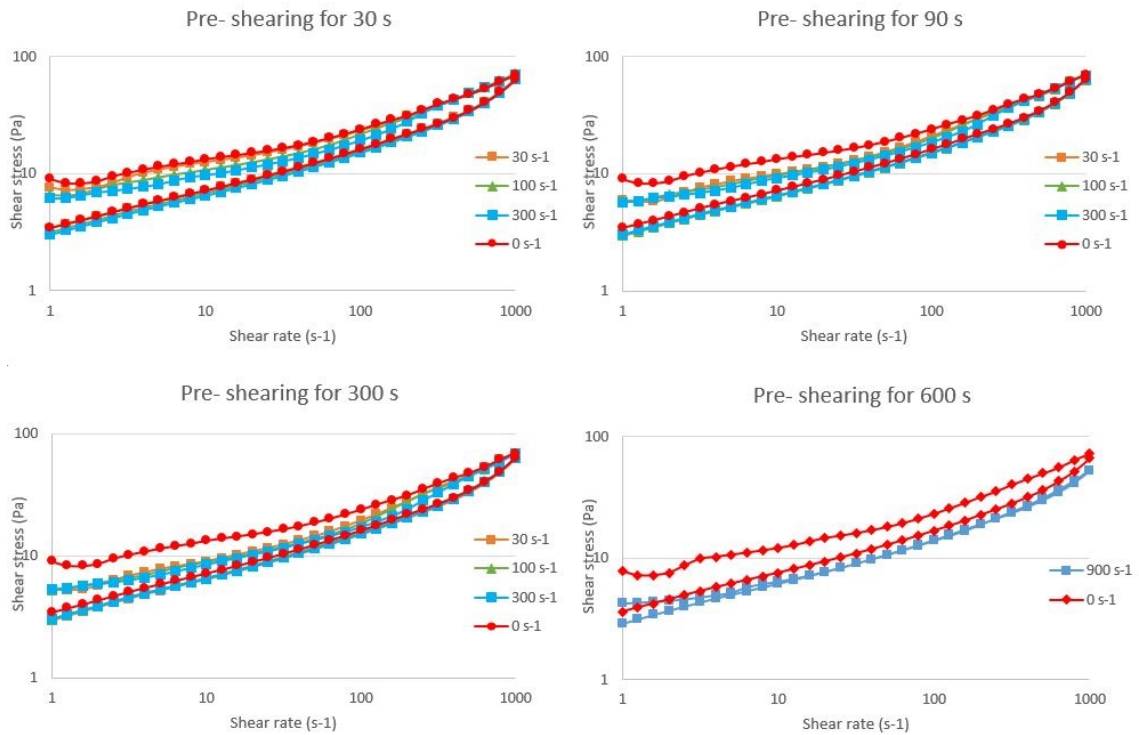


Figure 4.32: The hysteresis loops resulting from different pre-shearing speeds and times (Naturell)

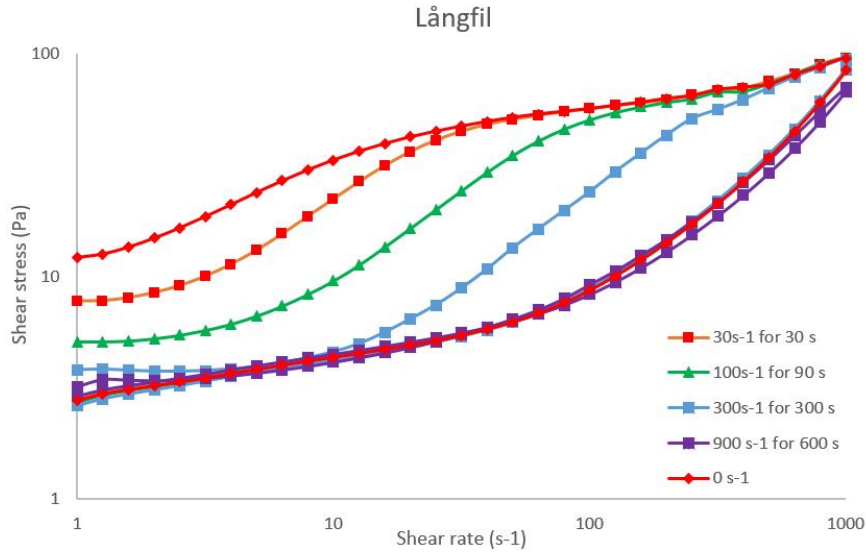


Figure 4.33: The hysteresis loops resulting from different pre-shearing speeds and times (Långfil)

To further investigate the effect of pre-shearing -using constant shear rates- on the measurements, each upward sweep of the tests was curve fitted to the Power Law model using the OLS regression method, and the results are compiled in (table 4.19, 4.20 and 4.21). The results of the Power Law curve fitting agree with the hysteresis loops results as it appears that the K value decreases, and the n value increases with the increased pre-shearing. This makes sense since the K value represents the consistency of the sample, and a decrease in the consistency by pre-shearing the sample will cause a decrease in the K value. In addition to that, the n value increase indicates to the increased flow due to the increased pre-shearing. It also appears from the Power Law modelling, that the loss in shear thinning behavior was the biggest for Långfil as the K and n values were the closest to unity when pre-shearing at 900 s^{-1} .

Pre-shearing time [s]	Pre-shearing speed [s^{-1}]									
	0		30		90		300		900	
	K [$\text{Pa} \cdot \text{s}^n$]	n [-]	K [$\text{Pa} \cdot \text{s}^n$]	n [-]	K [$\text{Pa} \cdot \text{s}^n$]	n [-]	K [$\text{Pa} \cdot \text{s}^n$]	n [-]	K [$\text{Pa} \cdot \text{s}^n$]	n [-]
0	6.09	0.34								
30			5.73	0.36	5.74	0.36	4.25	0.39		
90			5.80	0.36	4.25	0.39	3.92	0.40		
300			3.99	0.41	3.15	0.44	3.25	0.42		
600									2.61	0.43

Table 4.19: The Power law parameters resulting from the measurements of pre-sheared samples using different shearing speeds and times (Vanilla)

Pre- shearing time [s]	Pre- shearing speed [s^{-1}]									
	0		30		90		300		900	
	K [Pa. s^n]	n [-]	K [Pa. s^n]	n [-]	K [Pa. s^n]	n [-]	K [Pa. s^n]	n [-]	K [Pa. s^n]	n [-]
0	4.52	0.38								
30			4.15	0.40	2.98	0.45	2.45	0.48		
90			2.73	0.46	2.66	0.46	2.24	0.49		
300			2.38	0.47	2.16	0.49	1.78	0.51		
600									1.63	0.49

Table 4.20: The Power law parameters resulting from the measurements of pre- sheared samples using different shearing speeds and times (Naturell)

Pre- shearing time [s]	Pre- shearing speed [s ⁻¹]									
	0		30		90		300		900	
	K [Pa. s ⁿ]	n [-]	K [Pa. s ⁿ]	n [-]	K [Pa. s ⁿ]	n [-]	K [Pa. s ⁿ]	n [-]	K [Pa. s ⁿ]	n [-]
0	18.19	0.24								
30			12.66	0.30						
90					6.53	0.40				
300					1.60		0.60			
600									0.13	0.90

Table 4.21: The Power law parameters resulting from the measurements of pre- sheared samples using different shearing speeds and times (Långfil)

It was also noted from the pre-sheared samples flow curves that the downward ramps are very similar, this suggests that it would be better to perform the rheological modelling on the downward ramps instead, as it appears that it would provide more reproducible results. The power law parameters of the downward ramp are presented in table (4.22, 4.23 and 4.24).

Pre- shearing time [s]	Pre- shearing speed [s^{-1}]									
	0		30		100		300		900	
	K [Pa. s^n]	n [-]	K [Pa. s^n]	n [-]	K [Pa. s^n]	n [-]	K [Pa. s^n]	n [-]	K [Pa. s^n]	n [-]
0	1.97	0.5								
30			2.05	0.5	2.14	0.49	1.85	0.5		
90			2.23	0.49	2	0.5	1.85	0.5		
300			2.02	0.5	1.94	0.5	1.86	0.5		
600									2.25	0.45

Table 4.22: The Power law parameters resulting from the downward ramp of the measurements of pre- sheared samples using different shearing speeds and times (Vanilla)

Pre- shearing time [s]	Pre- shearing speed [s^{-1}]									
	0		30		100		300		900	
	K [Pa. s^n]	n [-]	K [Pa. s^n]	n [-]	K [Pa. s^n]	n [-]	K [Pa. s^n]	n [-]	K [Pa. s^n]	n [-]
0	1.25	0.55								
30			1.50	0.52	1.21	0.55	1.18	0.56		
90			1.20	0.55	1.20	0.55	1.22	0.55		
300			1.13	0.56	1.17	0.55	1.13	0.56		
600									1.76	0.48

Table 4.23: The Power law parameters resulting from the downward ramp of the measurements of pre- sheared samples using different shearing speeds and times (Naturell)

Pre- shearing time [s]	Pre- shearing speed [s^{-1}]									
	0		30		100		300		900	
	K [Pa. s^n]	n [-]	K [Pa. s^n]	n [-]	K [Pa. s^n]	n [-]	K [Pa. s^n]	n [-]	K [Pa. s^n]	n [-]
0	0.06	1.03								
30			0.05	1.08						
90					0.05	1.07				
300							0.06	1.05		
600									0.08	0.97

Table 4.24: The Power law parameters resulting from the downward ramp of the measurements of pre- sheared samples using different shearing speeds and times (Långfil)

By comparing the Power law model when fitted to the downward sweep, it is clear that the results are more reproducible, with an acceptable coefficient of variance (COV%), as shown in table (4.25), in the table below, the coefficient of variance for all the pre-shear condition is calculated, and it looks like it is enough to perform a hysteresis loop in the range of ($1 - 1000 s^{-1}$), as it create enough damage to the yogurt structure to eliminate the time effect, and then fit the power law model to the downward ramp.

	Standard deviation		COV	
	K (Pa. s^n)	n (-)	K (Pa. s^n)	n (-)
Vanilla	0.14	0.02	7%	3%
Naturell	0.26	0.02	15%	4%
Långfil	0.01	0.04	20%	4%

Table 4.25: The standard deviation and the coefficient of variance for the power law parameters when fitted to the downward ramp of the hysteresis loops with and without pre- shearing

4.9.4.2. Multiple hysteresis Loops

The second approach for investigating the pre- shear effect was to perform a multiple hysteresis loops for the three products by sweeping the table of shear rates up and down three times with no rest in between. The results of these tests are in (figure 4.34), and it appears that performing additional loops almost eliminated the time effect of the three products, but again this amount of pre- shearing is huge and its relevance to defining a measuring method is questionable since it totally destroy the yogurt structure.

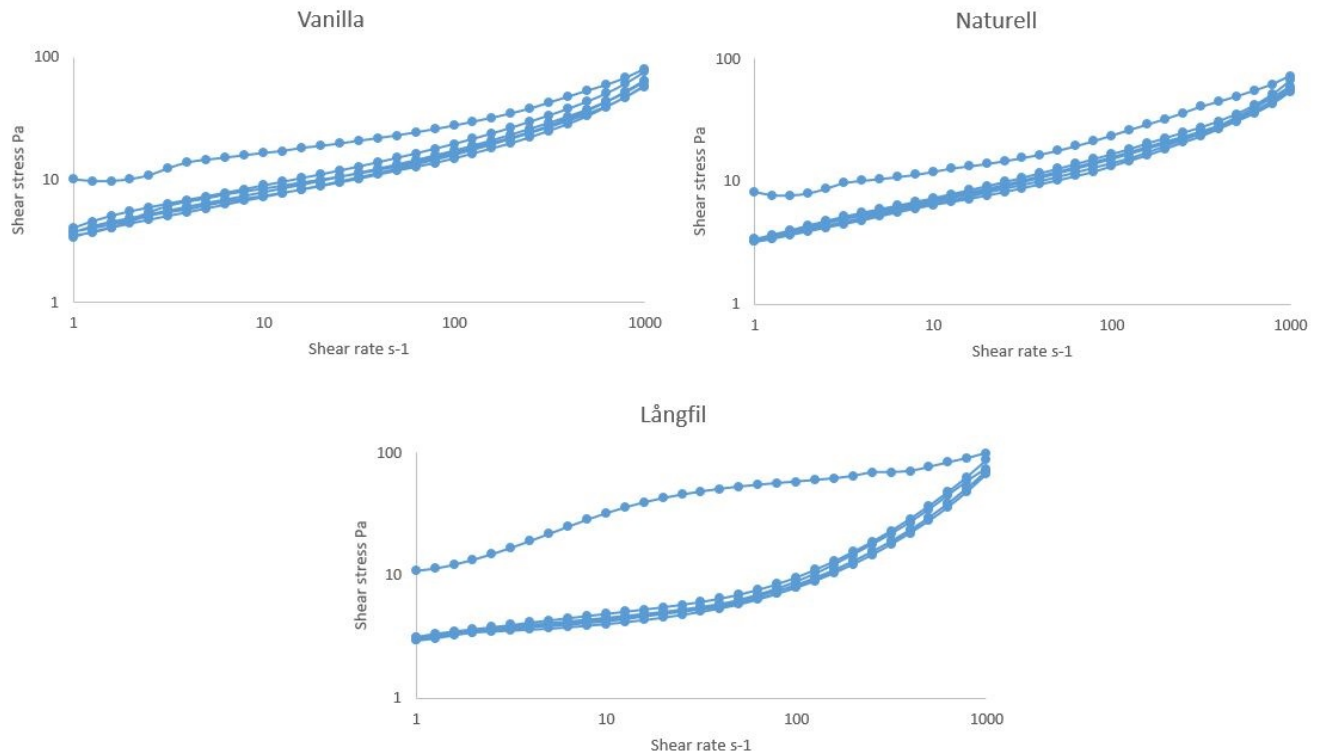


Figure 4.34: The flow curves resulting from the multiple hysteresis loop tests (3 loops)

The Power Law model was fitted for both the upward and the downward sweeps of each loop of the three products, and the results for the K and n values are compiled in (table 4.26). The K and n values indicates to the decrease in the time effect. A significant difference is observed between the first upward sweep and the first downward sweep. Therefore, the shear forces applied to the sample during the first upward sweep seems to be high enough to completely break down the yogurt network. A small hysteresis loop was observed (almost negligible) when the second upward sweep and a second downward sweep were compared, and in addition to that, no structure recovery was observed. It is also worth mentioning that Långfil was the most affected product by pre-shearing, as it seems from the K value of the downward sweeps which approaches zero, and this is an indication of a huge loss in consistency.

	1 st Upward sweep		1 st Downward sweep		2 nd Upward sweep		2 nd Downward sweep		3 rd Upward sweep		3 rd Downward sweep	
	K [Pa. s ⁿ]	n [-]	K [Pa. s ⁿ]	n [-]	K [Pa. s ⁿ]	n [-]	K [Pa. s ⁿ]	n [-]	K [Pa. s ⁿ]	n [-]	K [Pa. s ⁿ]	n [-]
Vanilla	6.27	0.35	1.98	0.50	1.79	0.50	1.95	0.49	1.58	0.50	1.89	0.48
Naturell	4.03	0.41	1.54	0.42	1.22	0.55	1.75	0.48	1.25	0.53	1.83	0.47
Långfil	16.51	0.26	0.07	1.02	0.10	0.96	0.08	1.00	0.08	0.97	0.07	0.98

Table 4.26: The Power law parameters resulting from each upward sweep of the multiple hysteresis loops

From the results in (sections §4.9.4.1 and §4.9.4.2) it can be concluded that pre- shearing was able to minimize (nearly eliminate) the time effect of the three studied product, although the pre- shearing technique using a constant shear rate prior to the measurement proved that yogurt require a high amount of shear, and also the results were only repeatable when fitting the downward sweep. In addition to that, performing a multiple hysteresis loop resulted in eliminating the time effect with the first downward sweep, with the following downward sweeps producing almost the same results. Based on these findings, it is recommended to perform a one loop hysteresis loop and perform the curve fitting only on the downward sweep in order to eliminate the time effect of the tested yogurt products.

It is also worth mentioning that this has proven to be applicable for Naturell, Vanilla and Långfil with a range of the measurements between 1 and 1000 s^{-1}) where 1000 s^{-1} was enough to pre- shear the samples , therefore, care must be taken when applying this method to different products that might require a higher or lower shear rate for pre- shearing.

4.10. Elongation

The results of the tack test when using a 5 mm gap with no pre-shear (figure 4.35), and when using a 1 mm gap with pre-shear (figure 4.36). The tack of the yogurt products seems to be similar for the three products, although Långfil appears to have a more elastic property than Vanilla and Naturell. To decide which type of fluid the three yogurt samples represent based on these figures, then Vanilla and Naturell appears to have a Power Law behavior (especially the pre-sheared Vanilla sample), Långfil on the other hand has a clear elastic behavior which may suggest the models used in this study are not enough to characterize its rheological behavior.

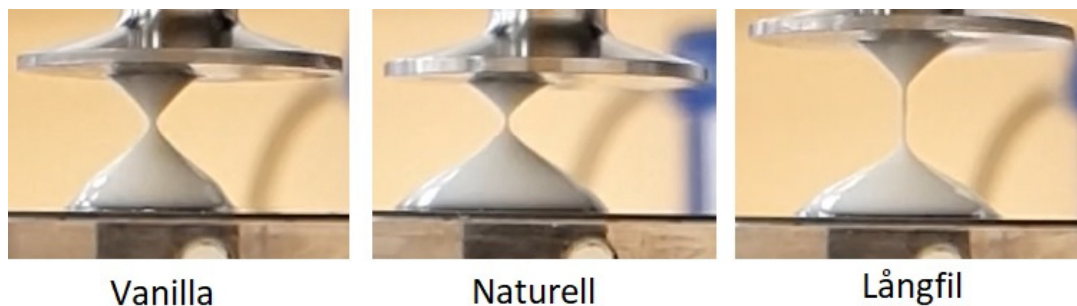


Figure 4.35: Images of the point of breakage during the Tack test without pre- shearing and an initial 5mm gap

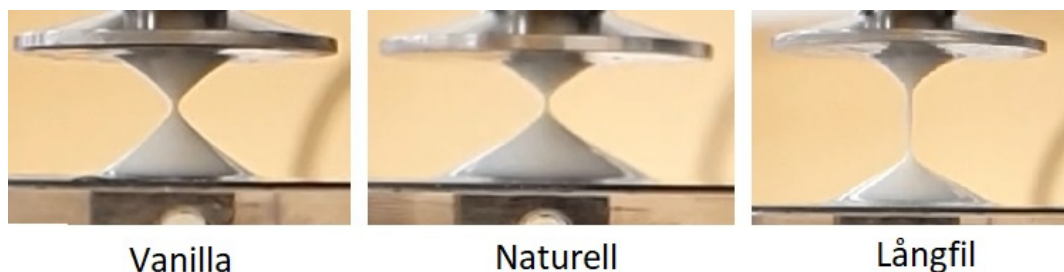


Figure 4.36: Images of the point of breakage during the Tack test without pre- shearing and an initial 1mm gap

The data from the tack test with pre-sheared samples were analysed and resulted in (figure 4.37) which shows that the minimum force values and the surface area are also shown in (table 4.22).

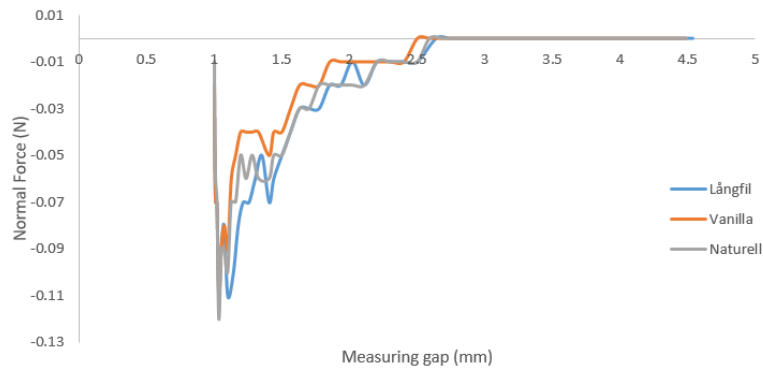


Figure 4.37: The analysis of the Tack test for the pre-sheared samples with 1mm gap

	Minimum F_N (N)	Surface area (Nmm)
Vanilla	-0.11	0.062
Naturell	-0.12	0.053
Långfil	-0.11	1.51

Table 4.27: The estimated minimum force and the surface area for the Tack test with pre-shear and 1mm initial gap

As shown in (figure 4.30) the force readings for the three products are not clear, and therefore it is difficult to draw any conclusions from the Tack test.

5. Conclusion and remarks

Several factors play a role in the rheological measurement for fermented dairy products, although an optimized method that suit all kind of products seems difficult, this study provided several recommendations and critical points that must be taken into consideration for fermented dairy products measurements.

5.1. General remarks

To provide a review of several rheological characterization methods (objective I), it was important first to develop a curve fitting method that can provide the solution with both stability and robustness using EXCEL sheets. The commonly used method is the Trendline function in EXCEL. The concern around this method was raised in some of the literature suggesting that its validity is only related for linear regression situations. While this study was focusing on non- linear regression situations it was important to investigate several alternatives. The Regression methods investigated were adapted from the statistic literature and focused on evaluating the goodness of the fit produced by each method, with a low propagated uncertainty. Keeping in mind that having residuals is something unavoidable when

regressing the measured data. Each one of the studied methods proved to be useful based on the situation it is used for. The ordinary least squared method (OLS) was recommended, since it provided a stable solution for the measurements and the models used in this study. In addition to that it proved to be a user-friendly method to apply using EXCEL sheets, the concern regarding the OLS method was the possibility of the data to violate one or more of its 7 assumptions (section § 2.7), such as having heteroscedasticity or a non- constant variance. The proposed solution for this is to use the weighted least squares (WLS) method, which was able to add a robustness aspect to the OLS method by giving each point a certain weight based on its variance, with a lower weight for outliers (data points with higher variance). In addition to that, the Herschel- Bulkley model produced a better fit than the Power Law model, which can be an indication that the added yield stress parameter improves the model ability to predict the measured data.

Based on the above it is recommended to perform an OLS regression for the curve fitting of the data, unless it was suspected that one of the assumptions is violated with outliers, it is important to treat these outliers, and the WLS is the go to method to overcome this. And this was shown in this study with the WLS method being the only one able to predict certain parameters (The yield stress of Långfil).

The next step in answering (objective I) was to develop a method for measuring the rheology of three fermented dairy products. The protocol used at Tetra Pak labs for measuring fermented dairy products is to sweep the shear rate up and down between ($20\text{-}200\text{ s}^{-1}$) with 10 sampling points per decade and a stabilizing time of (10- 15 s). The method developed in this study tried to increase the range of the measurement by increasing the shear rate range to ($1\text{-}1000\text{ s}^{-1}$) using a serrated cup and bob geometry, and the sampling points to 10 points per decade, and by taking the stabilizing time into consideration (40 s, 50 s and 90 s for Vanilla, Naturell and Långfil respectively) to guarantee measuring at a steady state situation, and to get an overall picture of the rheological behavior over a wider range of applications.

The results from this study showed differences in the flow curves for each part of the flow curve. Therefore, this study suggests two measuring methods when it comes to the range of the measurement, when time is not a limitation, it is recommended to perform the measurement on a large range, and then perform the rheological modelling on the segment that is relevant to the wanted application. The other recommended method is used when time is a limitation and a fast measurement needs to be performed, this method includes measuring at a range that is relevant to the wanted application. Regarding the number of sampling points, it is important to have a number that provides an acceptable degree of freedom, but this is not always possible due to time limitation. Therefore, it is recommended to not use less than 10 points per decade.

During the measurements, batch variation played a huge role in decreasing the consistency and repeatability of the results. This is common for fermented dairy products, and it is difficult to avoid. Therefore, it is recommended to perform the measurement on several batches and estimate the coefficient of variance (COV%) to understand how this variation can affect the acquired results. The results also showed that the chosen geometry plays a role in preventing wall slip and provide accurate results, for fermented yogurt products it is recommended to use the serrated cup and bob.

Some application requires the determination of the yield stress value, and this is considered a part of the rheological characterization of a given fluid (objective I). For the three fermented dairy products, the yield stress measurements showed good agreement for both of the used methods (tangent and

bayod) for the static yield stress, therefore it is recommended to use one of these methods, but again it has to be done on several batches to estimate the COV%.

Another goal of this study is to develop a method for measuring zero- and infinite- shear rate viscosities of different yogurt products (objective II). The results for estimating η_0 showed a pattern of increasing η_0 value with increasing the ramp time of the shear stress. This suggests that the products do not possess a zero-shear viscosity with a yield stress, or that the equipment used is not able to measure η_0 . When measuring η_∞ , difficulties in achieving a steady state were faced. In addition to that, the pressures recorded are below the sensitivity of the transducer and the yogurt samples appeared to get stuck in the 0.5 mm. Therefore, the results of these measurements are not to be trusted. And this was confirmed when these results were compared to the rotational rheometer data.

In order to describe the time effect of the three measured products (objective III), several measurements were performed. The hysteresis loops measurements for the three products proved the time dependant behavior of these products. It was clear that all the samples continued to break down and did not reach a viscosity plateau regardless of the shear rate applied. It was also observed that the three products required 40s, 50s and 90s to achieve a steady state (according to the protocol used at Tetra Pak labs), and this shows that thixotropy has an effect on the rheological measurements, and stresses on the importance of using the right stabilizing time in order to avoid the overestimation of the viscosity when using a shorter stabilizing time when measuring yogurt products. The description of the time effect (objective III) required further measurements, the build-up tests showed that the time needed for the samples to recover is longer than the time required for breaking down the samples. The results also showed that increasing the resting time results in more structure build up. It also showed that a low shear rate of 1 s^{-1} was enough to cause a structural break up, and to allow for a better structural build up measurement, it is required to measure at a lower shear rate than 1 s^{-1} . The results of plotting the shear stress values against time during the build- up test also showed that the three investigated yogurt samples are thixotropic viscoelastic products. The varied shear rate test concluded that the lower the shear rate applied, the more structural build up can be achieved, it also showed that Långfil is the most sensitive to break down and build up conditions among the three investigated products.

The next goal of this study was to eliminate the time effect of the three products in order to improve the repeatability and relevancy of the rheological measurements (objective IV). Two techniques were tested, with applying a constant shear rate prior to testing, and the second technique included performing a multiple hysteresis loops test (3 loops). The results showed that it is enough to measure using a hysteresis loop with a large range of shear rates (up to 1000 s^{-1} in this study), and then measure the downward sweep.

To perform a qualitative compression of the elongation properties for the three tested products (objective V). The results from the elongation tests proved that Långfil has more elastic properties than the other samples, with the Vanilla and Naturell having a Power Law behavior when compared to the data and the graphs in the literature. On the other hand, it was not possible to quantify this elongation behavior due to the force readings being not clear enough for any estimations.

5.2. Suggestions for future work

The regression method suggested in this study showed good results with an acceptable rational for the range of the investigated products, and the next step should be to use these methods to regress more complicated flow curves and analyse several more products to expose its strengths and weaknesses

even more. The method developed during this study showed good results for the tested types of yogurt, therefore it will be interesting to also investigate its performance with a wider range of products, where a larger range of shear rates is used for the characterization of other products. The data acquired in this study are suggested to be correlated with real flow situations, such as flow in pipes and filling machines.

It is also suggested to expand the thixotropic behavior investigation to check for the ability to build a thixotropic model that can describe the behavior of the investigated products. Adding a 24- 48 hr rest after shearing the samples will confirm the build-up time needed for the microstructure of the samples to recover.

Another interesting, and useful investigation would be to correlating pressure drop measurements with rheology measurement.

Other variables such as the relation between the pH, composition and temperature of the samples on the flow and time effect behavior of these products.

6. Appendices

6.1. Kinexus rheometer use instructions

- 1- Make sure to open the compressed air valve before starting the rheometer
- 2- Start the Kinexus rheometer by pressing the On/Off button on the back of the device and remove the thermal cover and the protective bob.
- 3- Start the computer connected to the Kinexus rheometer using the login information provided in the Kinexus instruction next to the rheometer and start the rSpace software located on the screed Desktop.
- 4- Insert the geometry you intend to use (the geometries are in a black case on the shelves next to the rheometer.
- 5- Allow the rheometer to perform a zero-gap initialization by following the instructions on the screen.
- 6- Homogenise the sample according to the method described in §3.1.
- 7- Load the sample (~15ml) into the Cup using a measuring spoon and press 'Load sample' and follow the instructions on the screen
- 8- Choose the sequence needed to perform the test, (e.g. XX03 Table of shear rate UP) and if the sequence needed is not available, then it is needed to be programmed.
- 9- Once the sequence is chosen, enter the operating conditions in the inputs screen. Common input conditions are:
 - a) Temperature- the temperature applied during the measurement
 - b) Samples per decade - the number of sampling points to be taken per linear or logarithmic decade
 - c) Sampling interval - the time between sampling points
- 10- Shear stress/rate range - the start and end shear stress or shear rate values
- 11- Start the sequence and wait one minute for the temperature to stabilise and the sample to rest, then press 'skip'. If this is not done, the sequence will start automatically if the set temperature is reached within five minutes.

- 12- When the sequence is complete the raw data can be found under the 'Table' tab. The table can be selected by clicking in the top, left, empty square. Right click on the selected data, and choose 'send to main menu', select all the data and, right click and choose 'Export' and choose a location for the exported file in a (csv.) format.
- 13- Once the measurement is done and the results are saved, remove the thermal cover and press 'Unload sample' and follow the instructions on the screen
- 14- Clean the geometry with water and dry them with paper or leave them to dry.
- 15- Put the geometry back in its case and return it on the shelf
- 16- Reinsert the protective bob and the thermal cover and turn off the Kinexus and turn off the compressed gas
- 17- Close the software and turn off the computer

6.2. Kinexus rheometer range and limitations

pro+	
Rheometer platform	Meeting rheological needs in research and development
Standard operating modes	n control; Shear rate control; Shear
Torque range – Viscometry (rate and stress control)	5.0 nNm - 225 mNm
Torque range – Oscillation (strain and stress control)	1.0 nNm - 225 mNm
Torque resolution	0.1 nNm
Position resolution	<10 nrad
Angular velocity range	1 nrad/s to 500 rad/s
Step change in strain	<10 ms
Frequency range	6.28 $\mu\text{rad/s}$ to 942 rad/s ⁻¹ (1 μHz to 150 Hz)
Motor inertia	12 $\mu\text{N.m.s}^2$
Normal Force range	0.001 N - 50 N
Normal Force resolution	0.5 mN
Normal Force response time	<10 ms
Vertical lift speed	0.1 $\mu\text{m/s}$ to 35 mm/s
Vertical lift range (measurable)	230 mm
Gap resolution (over full vertical lift range)	0.1 μm

Figure 6.1: Kinexus rheometer range and limitations

6.3. Applying the OLS regression method using EXCEL sheets

- 1- List the applied shear rate values as the independent variable in column B and measured shear stress values as the dependent variable in column A (figure 6.2).
- 2- Set the parameters values in column G temporarily to $K=7$ and $n=0.3$
- 3- Insert the model required to fit in column C using the parameters in column G ($\tau = K\dot{\gamma}^n$ in the example)
- 4- Calculate the residuals values for each data point in column D using the equation ($r = \tau_i - \tau_j$)
- 5- Calculate the square of each residual (r^2) in column E

- 6- Calculate the sum of squared residuals (SSR) in cell G4 (SSR= sum(r^2))
- 7- Using the SOLVER function, minimize the SSR in G4 value by changing the model parameters values in cells G2 and G3 (figure 6.3)
- 8- Insert a scatter plot for both of the measured flow curve ($x = \dot{\gamma}_i$ and $y = \tau_i$) and of the predicted model ($x = \dot{\gamma}_i$ and $y = \tau_i$) and name these curves as Measured and FIT, respectively.

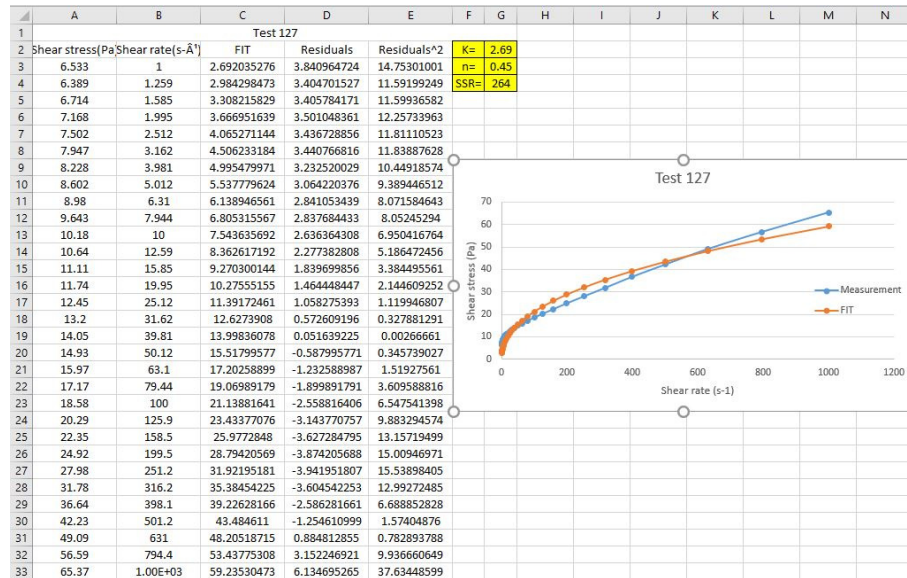


Figure 6.2: Example of the utilization of the OLS regression method using EXCEL sheets

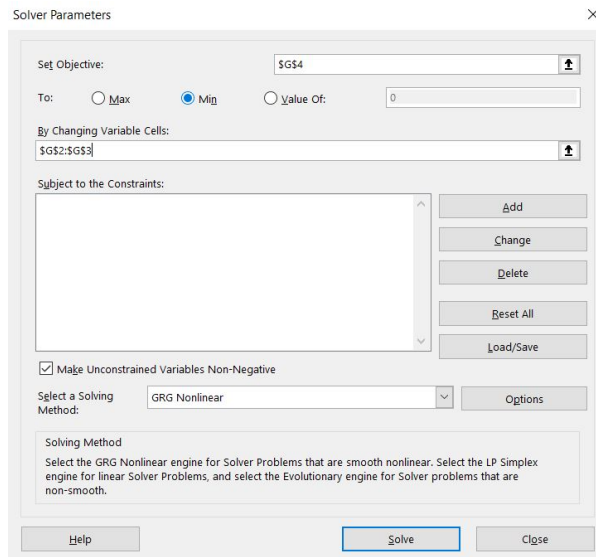


Figure 6.3: Example of the interface of the SOLVER function for performing a nonlinear regression using the OLS method

6.4. Applying the WLS regression method using EXCEL sheets

- 1- Perform a normal OLS regression
- 2- Copy the resulting sheet and save the cells as values removing the formulas
- 3- Find the absolute value for each residual
- 4- To find the variance for each point perform the following:
 - a) Create a plot with Y axis: |residuals| and X axis: the predicted values from the OLS method
 - b) Perform a linear regression for the resulting set of points using the equation:

$$Y = \alpha.X + \beta$$

- 5- Create a column of weights using the equation $W_i = \frac{1}{\sigma_i}$
- 6- Create a column of weighted residuals by multiplying each weight to its corresponding residual from the OLS method
- 7- Using the SOLVER function, minimize the sum of squared weighted residuals to find the model parameters.

6.5. The methodology for the Monte- Carlo simulation

The methodology for performing the Monte- Carlo simulation was adapted from the literature⁴⁶.

- 1- To initiate the Monte- Carlo simulation, reassemble the measured data and the predicted values as shown in (figure 6.4) with df refers to the degrees of freedom
- 2- Insert the function needed for the simulation in cell L3:

$$\tau_{L3} = \$E3 + NORM.INV(RAND(),0,SQRT\left(\frac{SSR}{df}\right))$$

- 3- The τ values in the other rows in column L are simulated in a similar way.
- 4- The simulated values for a new dependent variable τ are demonstrated in cells L3-L33
- 5- The same Monte Carlo simulations are performed from column M to column OU. Therefore, a total of 400 sets of simulated τ are obtained.
- 6- copy the simulated τ data to a new sheet by right-clicking “Paste Special” and selecting “Values” in the dialogue of “Paste Special”. Afterwards, copy the simulation values and over paste them on the simulation results in the original sheet.
- 7- Organize the SSR values and the K and n parameters for each simulation as shown in (figure 6.4)
- 8- Because the maximum number of variables SOLVER can solve is 200, we can minimize the SSR values for 100 simulations at one time by minimizing the sum of SSR values of 100 simulations in cells F35, F36, F37 and F38

⁴⁶ Wei Hu, Jing Xie, Henry Wai Chau, Bing Cheng Si. Evaluation of parameter uncertainties in nonlinear regression using Microsoft Excel Spreadsheet. Environmental Systems Research (2015) 4:4 DOI 10.1186/s40068-015-0031-4

	A	B	C	D	E	F	G	H	I	J	K	L	M	N	O
1	Test 355				Predicted										
2	Shear rate Shear stress (Pa)				FIT							M-C			
3	1	10.55			5.91038							12.4756	4.68348	8.03189	6.59194
4	1.259	9.553			6.40407							6.97302	12.7589	9.85854	5.33043
5	1.585	9.431			6.93888							4.17888	6.47965	7.8953	10.0869
6	1.995	9.692			7.51781							8.04895	12.4373	9.49609	5.86215
7	2.512	10.13			8.14611							6.66394	4.34529	9.32622	15.2876
8	3.162	11.09			8.82597							12.7022	9.79166	6.30383	3.04353
9	3.981	12.34			9.56324							16.1164	11.9837	10.0423	5.02093
10	5.012	13.48			10.362							5.58712	9.71105	9.93413	4.22162
11	6.31	14.12			11.2275							12.683	12.8555	14.2234	7.71252
12	7.944	14.67			12.1652							14.4706	14.983	13.7044	6.11377
13	10	15.4			13.1806							14.0155	20.3998	16.5939	17.6586
14	12.59	16.6			14.2816							16.4864	14.6508	8.31781	17.1099
15	15.85	17.42			15.4743							11.4558	12.8524	9.18515	18.098
16	19.95	18.29			16.7654							22.279	17.1146	19.0375	15.6641
17	25.12	19.14			18.1665							22.6185	17.541	24.9485	16.7867
18	31.62	20.06			19.6826							17.2972	18.2097	22.3069	22.1085
19	39.81	20.98			21.3268							20.6446	20.1597	22.4311	22.7402
20	50.12	22.01			23.1081							21.4675	25.9529	24.0425	23.6054
21	63.1	23.29			25.0382							20.1452	25.8192	21.6241	30.4018
22	79.44	24.61			27.1293							26.9571	22.164	29.5869	28.1331
23	100	26.11			29.3939							33.7876	26.886	28.0785	26.4547
24	125.9	27.94			31.8492							33.6097	35.3107	30.6171	31.3062
25	158.5	30.15			34.5089							33.7694	31.8672	33.7738	33.5347
26	199.5	32.76			37.3881							37.3123	36.2582	42.0138	41.9812
27	251.2	35.85			40.5128							44.0185	42.8299	40.5122	38.0502
28	316.2	39.98			43.8939							39.6589	45.5175	47.5631	48.2777
29	398.1	44.94			47.5606							43.5198	51.1137	53.0572	51.8012
30	501.2	50.4			51.533							50.5661	44.9443	49.0264	50.3225
31	631	56.54			55.8373							60.0438	54.8998	58.2545	56.0979
32	794.4	64.24			60.5006							68.7003	60.5581	60.3324	55.4621
33	1.00E+03	74.48			65.5508							60.8119	65.2367	65.8252	65.9684
34															
35	SSR=	317.649				1-100		31733				SSR=	415.786	275.411	265.819
36	K=	5.91038				101-200		31492				K=	6.31901	6.40363	6.33966
37	n=	0.34832				201-300		33700.1				n=	0.33843	0.3334	0.34015
38	df=	29				301-400		30372.2							0.34608
39															

Figure 6.4: Example of performing a Monte- Carlo simulation for the parameters of the Power Law model when applied to Vanilla yogurt

9- The frequency distribution of K and n are plotted on a separate sheet (figure 6.5).

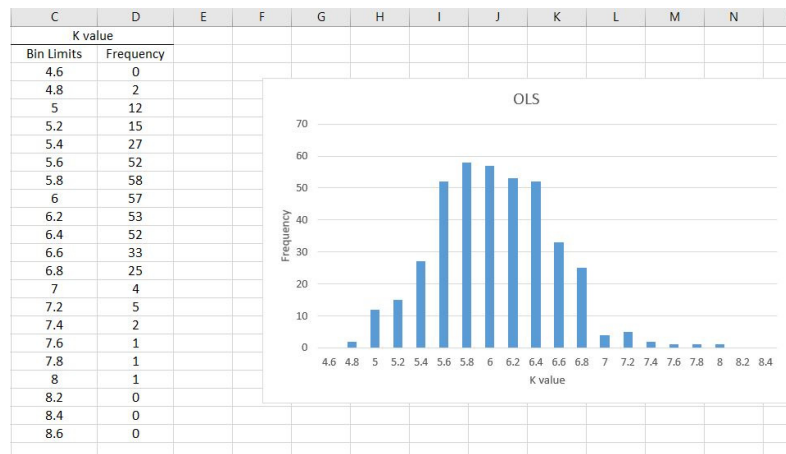


Figure 6.5: Example of the frequency distribution histogram of the K value when performing a Monte- Carlo simulation for the Power Law model

- 10- To calculate the 95% confidence interval of values of K or n values of the 400 simulations, copy all the fitted K or n values, then paste them to a new sheet by right clicking “Paste Special” and selecting “Transpose” in the dialogue of “Paste Special” to list all the fitted K or n values in one column. Select the transposed data, and rank them in an ascending order using Sort tool in Data tab.
- 11- Find the value of α and n corresponding to the 2.5 percentile and 97.5 percentile, which are the lower limit and upper limit, respectively, at a 95% confidence.

6.6. The results of the curve fitting for Naturell and Långfil using different regression methods

The resulting parameters produced using different regression methods for Naturell

	OLS	LAR	LARR	LSLR	WLS	SD
K (Pa. s ⁿ)	3.47	3.46	4.88	5.17	3.49	0.77
n (-)	0.43	0.42	0.35	0.34	0.43	0.04
SSR (Pa ²)	132.55	141.08	616.19	455.06	132.60	-

Table 6.1: The results of the Power law curve fitting using different regression methods (Naturell)

	OLS	LAR	LARR	LSLR	WLS	SD
K (Pa. s ⁿ)	6.74	6.08	4.89	5.17	5.48	0.66
n (-)	0.13	0.27	0.35	0.34	0.31	0.08
SSR (Pa. s ²)	1.69	2.62	8.15	6.19	4.55	-

Table 6.2: The results of the Power law viscosity equation curve fitting using different regression methods (Naturell)

	OLS	LAR	LARR	LSLR	WLS	SD
A (Pa. s ^b)	1.22	1.09	1.64	1.75	1.34	1.06
b (-)	0.57	0.59	0.53	0.52	0.56	0.07
σ_y	5.82	6.35	4.58	4.70	5.55	0.67
SSR (Pa ²)	16.56	18.12	27.94	35.05	163.65	-

Table 6.3: The results of the Herchel- Bulkly curve fitting using different regression methods (Naturell)

The resulting parameters produced using different regression methods for Långfil

	OLS	LAR	LARR	LSLR	WLS	SD
K (Pa. s ⁿ)	14.45	14.67	9.74	10.79	13.43	2
n (-)	0.27	0.27	0.34	0.34	0.28	0.03
SSR	577.60	580.50	1343.44	1529.64	629.38	-

Table 6.4: The results of the Power law curve fitting using different regression methods (Långfil)

	OLS	LAR	LARR	LSLR	WLS	SD
K (Pa. s ⁿ)	8.97	8.89	9.74	10.79	9.76	0.69
n (-)	0.43	0.43	0.34	0.34	0.40	0.04
SSR	1.86	1.88	3.76	9.61	3.52	-

Table 6.5: The results of the Power law viscosity model curve fitting using different regression methods (Långfil)

	OLS	LAR	LARR	LSLR	WLS	SD
A (Pa. s ^b)	14.45	14.70	9.83	10.79	10.62	2.07
b (-)	0.27	0.27	0.34	0.34	0.31	0.03
σ_y	0.00	0.00	0.00	0.00	5.91	2.36
SSR	577.60	580.67	1310.47	1529.64	786.26	-

Table 6.6: The results of the Herchel- Bulkly curve fitting using different regression methods (Långfil)

Fitted flow curves using different regression methods for Naturell

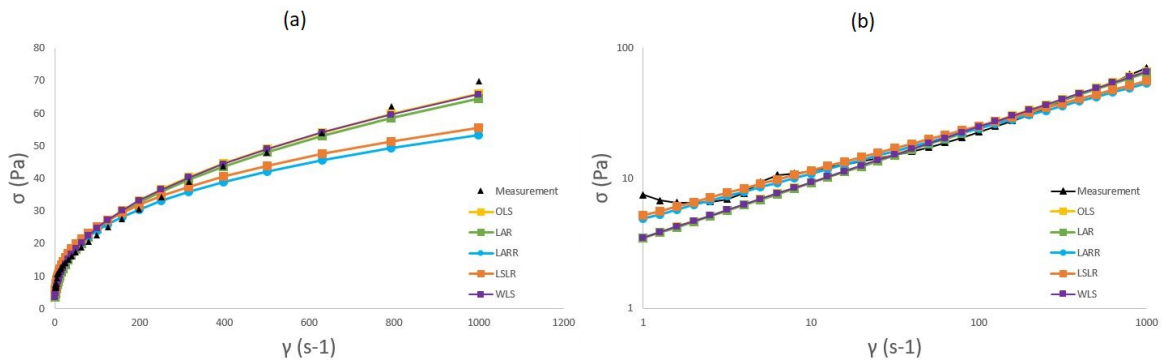


Figure 6.7: The flow curve resulting from the Power law curve fitting using the different regression methods (Naturell)

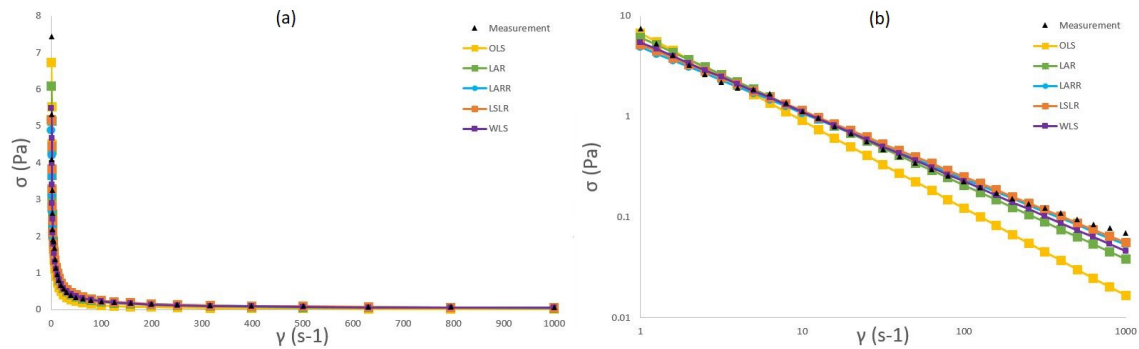


Figure 6.8: The flow curve resulting from the Power law viscosity equation curve fitting using the different regression methods (Naturell)

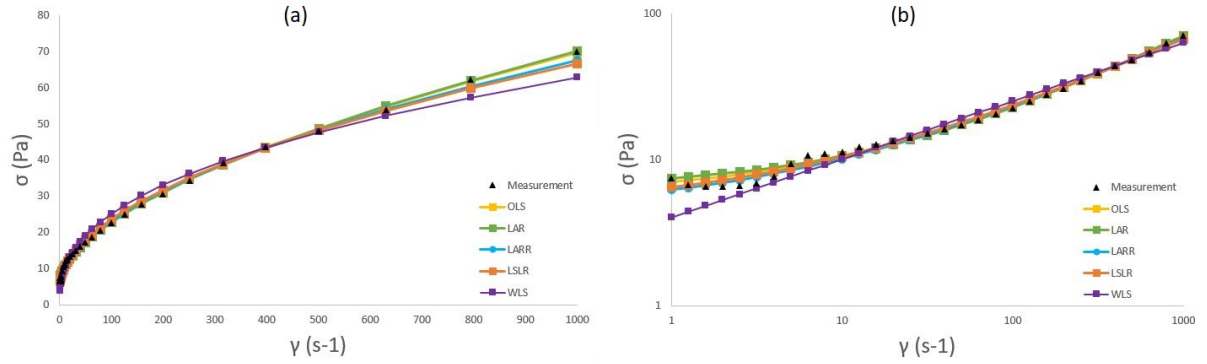


Figure 6.9: The flow curve resulting from the Herschel- Bulkly curve fitting using the different regression methods (Naturell)

Fitted flow curves using different regression methods for Långfil

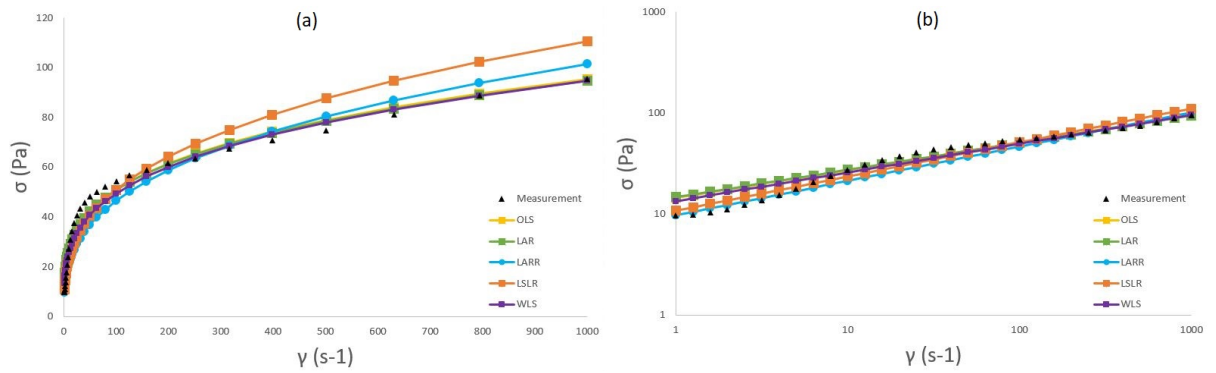


Figure 6.10: The flow curve resulting from the Power law curve fitting using the different regression methods (Långfil)

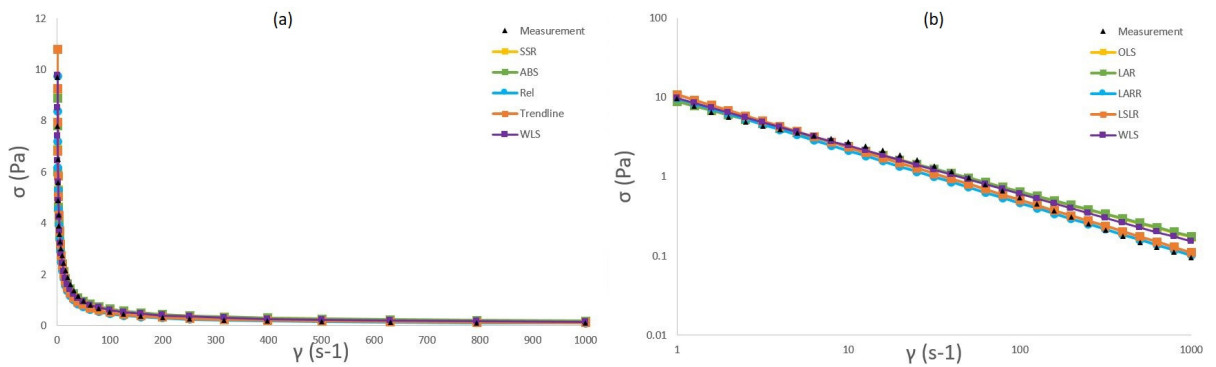


Figure 6.11: The flow curve resulting from the Power law viscosity equation curve fitting using the different regression methods (Långfil)

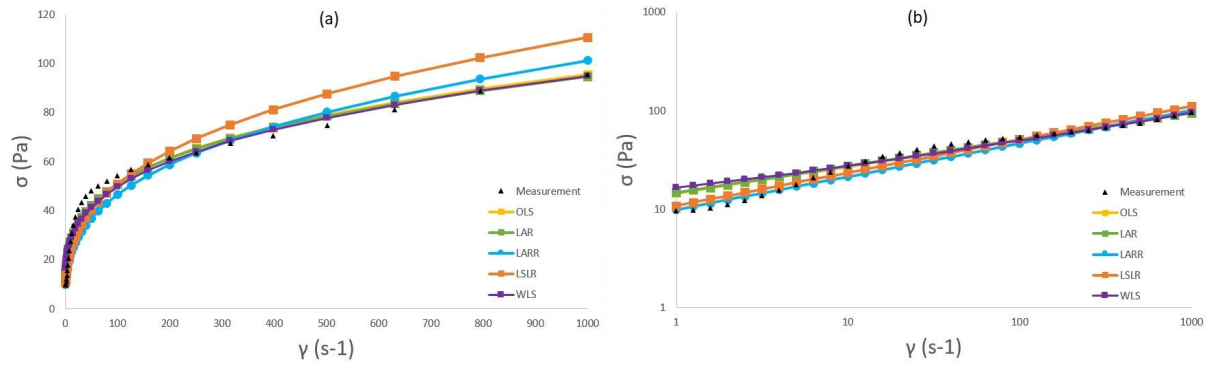


Figure 6.12: The flow curve resulting from the Herchel- Bulkly curve fitting using the different regression methods (Långfil)

6.7. Evaluating the goodness of the fits for Naturell and Långfil

The residuals plots of the different regression methods for Naturell

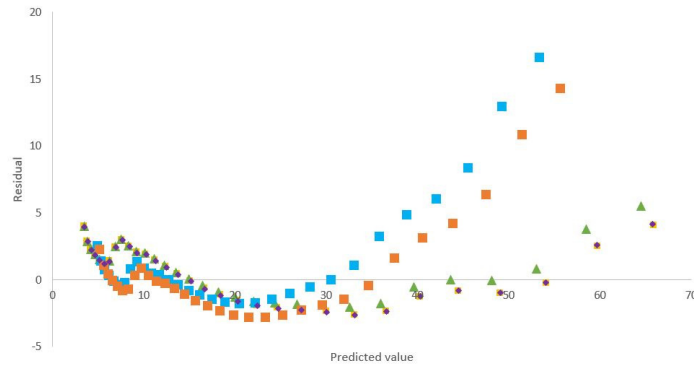


Figure 6.13: The residual plot resulting from the Power law curve fitting using the different regression methods (Naturell)

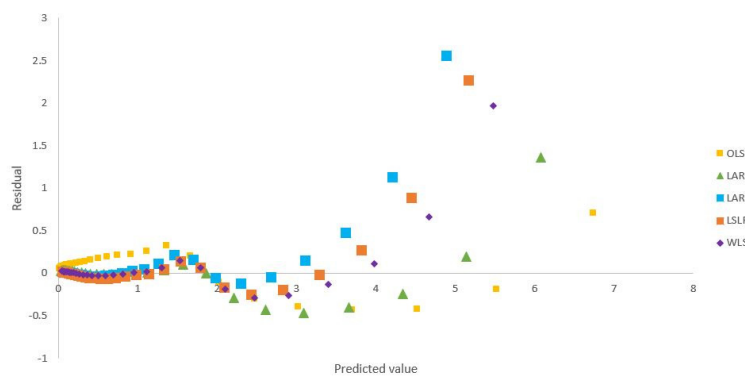


Figure 6.14: The residual plot resulting from the Power law viscosity equation curve fitting using the different regression methods (Naturell)

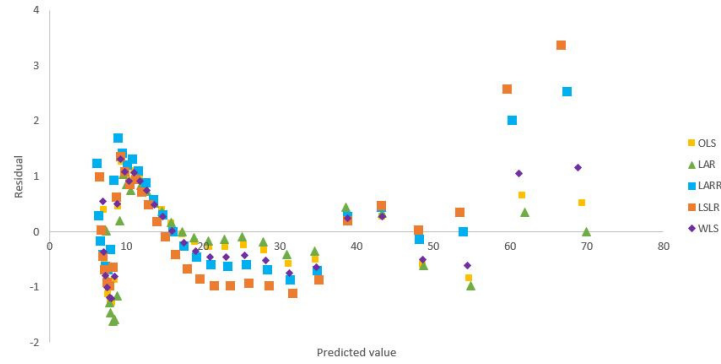


Figure 6.15: The residual plot resulting from the Herchel- Bulky curve fitting using the different regression methods (Naturell)

The residuals plots of the different regression methods for Långfil

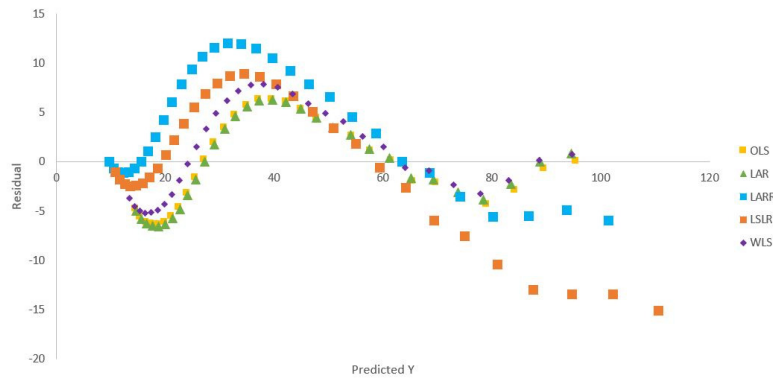


Figure 6.16: The residual plot resulting from the Power law curve fitting using the different regression methods (Långfil)

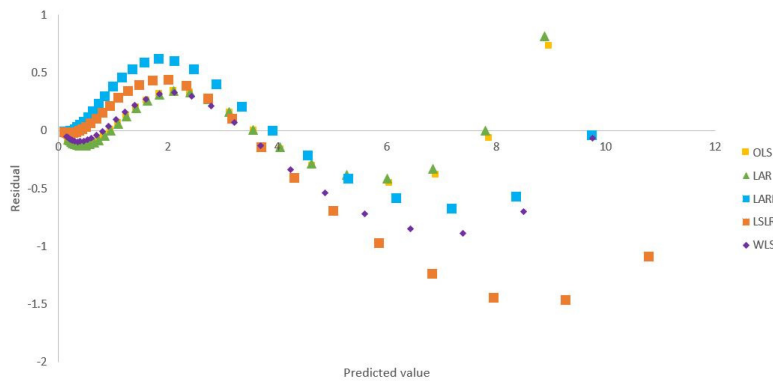


Figure 6.17: The residual plot resulting from the Power law viscosity equation curve fitting using the different regression methods (Långfil)

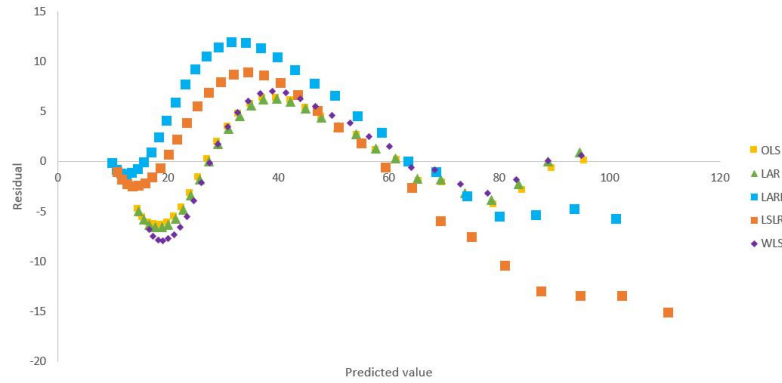


Figure 6.18: The residual plot resulting from the Herchel- Bulkly curve fitting using the different regression methods (Långfil)

6.8. The uncertainty analysis for the Power Law viscosity equation when regressed using different curve fitting methods

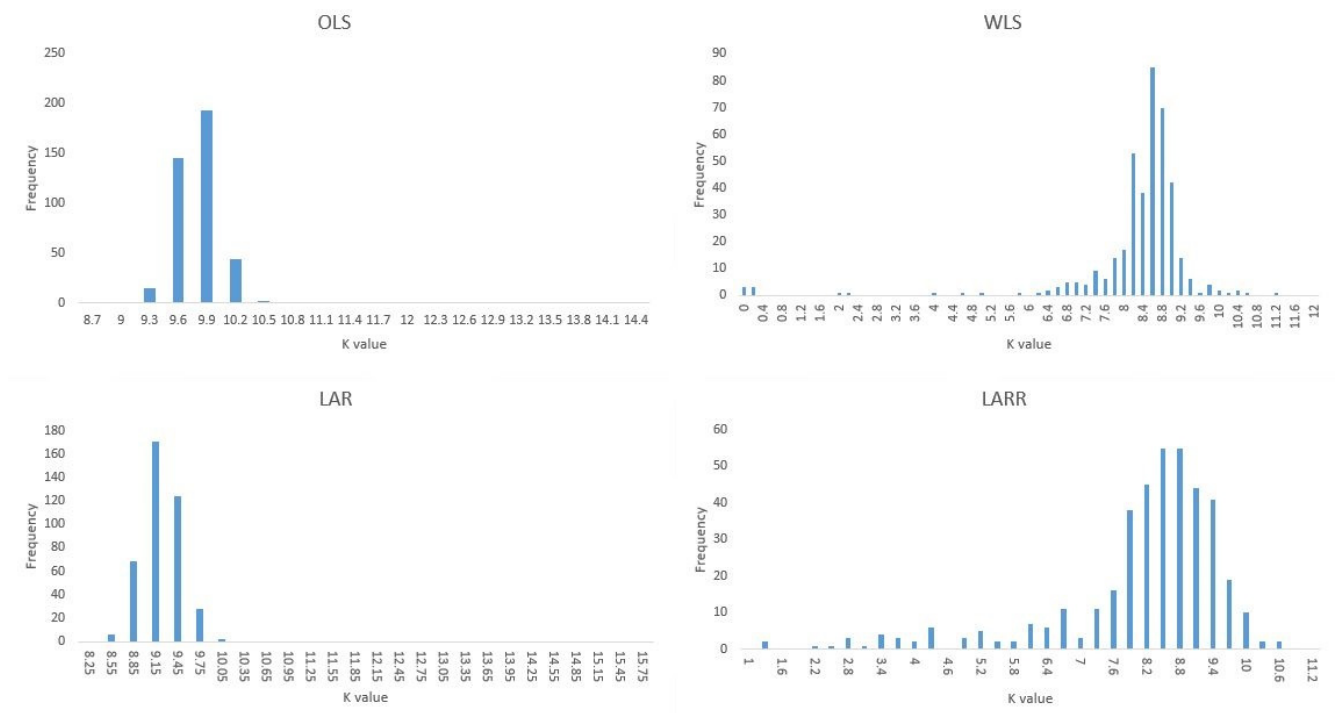


Figure 6.19: The frequency distribution histogram of K, for the Power law viscosity equation curve fitting using different regression methods (Vanilla)

	OLS	WLS	LAR	LARR
	OLS	WLS	LAR	LARR

	OLS		WLS		LAR		LARR	
	CI of mean	CI of value	CI of mean	CI of value	CI of mean	CI of value	CI of mean	CI of value
Upper bound	9.67	10.05	8.35	9.71	9.11	9.58	8.13	9.73
Lower bound	9.63	9.24	8.09	4.94	9.06	8.59	7.82	3.38
Upper- Lower limit	0.04	0.81	0.27	4.77	0.05	1.00	0.30	6.34

Table 6.7: The uncertainty of the K value when using different regression methods to apply the Power law viscosity equation

	OLS		WLS		LAR		LARR	
	CI of mean	CI of value	CI of mean	CI of value	CI of mean	CI of value	CI of mean	CI of value
Upper bound	0.15	0.20	0.29	0.34	0.23	0.29	0.29	0.71
Lower bound	0.14	0.09	0.26	0.15	0.23	0.16	0.25	0.00
Upper- Lower limit	0.01	0.11	0.03	0.19	0.01	0.13	0.04	0.71

Table 6.8: The uncertainty of the n value when using different regression methods to apply the Power law viscosity equation